Title
Lateral Control Of Heavy Duty Vehicles For Automated Highway Systems

Authors
Tai, M.
Wang, J.-y.
Hingwe, P.
et al.

Publication Date
1998

CALIFORNIA PATH PROGRAM
INSTITUTE OF TRANSPORTATION STUDIES
UNIVERSITY OF CALIFORNIA. BERKELEY

Lateral Control of Heavy Duty Vehicles for Automated Highway Systems

Meihua Tai, Jeng-Yu Wang, Pushkar Hingwe, Chieh Chen, Masayoshi Tomizuka
University of California, Berkeley

California PATH Research Report
UCB-ITS-PRR-98-8

This work wasperformed as part of the California PATH Program of the University of California, in cooperation with the State of California Business, Transportation, and Housing Agency, Department of Transportation; and the United States Department of Transportation, Federal Highway Administration.

Report for MOU 289

February 1998

ISSN 1055- 1425

Lateral Control of Heavy Duty Vehicles for Automated Highway Systems

Meihua Tai

Jeng-Yu Wang

Pushkar Hingwe

Chieh Chen

Masayoshi Tomizuka

Department of Mechanical Engineering

University of California at Berkeley

Berkeley CA 94720

Abstract

Three results pertaining to lateral control of heavy duty vehicles on Automated Highway System are presented. First, a time domain, frequency domain and pole/zero analysis of the linearized model for lateral control of tractor-trailer vehicles is presented. The steering response subject to variation of speed, road adhesion and look-ahead distance is studied. Based on the analysis, a simple baseline controller is designed. The close-loop simulation is conducted to show that the designed controller meets the requirement of the maximum lateral displacement that should not exceed $0.2m$.

Secondly, an offtracking analysis based on the linear model of tractor semitrailer is presented. It is shown that as the longitudinal velocity decreases, the dynamic offtracking converges to the kinematic offracking value.

Finally, a general method of deriving dynamic models for any configuration of heavy duty vehicles is presented. For a heavy duty vehicle with N units, a complex 6N

degree of freedom simulation model is derived. Additionally, a simple (2 + N) degree of freedom model is derived for the purpose of controller design. Constraint forces between adjacent units are obtained. The effects of dolly tire steering angle, front tire steering angles of each unit, if any, and traction and braking torques on each wheel are included in both models. A simplified non-linear analytical model of tractor-semitrailer is presented and compared to the previous model.

keywords: Dynamic Modeling, Advanced Vehicle Control Systems, Lateral Control, Steering Control, Heavy Duty Vehicles.

Executive Summary

This report summarizes the research results on Lateral Control of Heavy Duty Vehicles for Automated Highway Systems (AHS) concluded under MOU 289 for the year 1996-97.

This project is a continuation of the project "Lateral Control of Commercial Heavy Duty Vehicles", MOU 242. Under MOU 242, dynamic model of tractor-semitrailer was developed for control purposes. Several linear and non-linear control algorithms were designed for the lateral guidance of tractor semi-trailer and commuter buses. While the accomplishments of MOU 242 were theoretical, the research in MOU289 has been directed towards performing the closed loop experiments on a tractor-semitrailer.

In consonance with the goal of experimental demonstration of lateral guidance of a tractor-semitrailer, a linearized tractor-semitrailer model has been studied. Frequency and time domain analysis to understand the dependence of dynamic response of the tractor-semitrailer on the cornering stiffness, longitudinal velocity and look-ahead distance were done. Off-tracking, a major consideration for lane following control algorithms had been studied for tractor-semitrailer and single unit vehicles with long wheel-bases. Whereas the emphasis of this project is experimental demonstration of the lateral guidance of Heavy vehicles, the modeling and analysis of heavy vehicles was continued. Dynamic modeling of general heavy duty vehicles has been done.

The report is divided in five sections. The first section presents the background for the broad abjective: Placing heavy vehicles in the AHS framework. Subsequent sections are concerned with related analysis. The second section describes the linear analysis of tractor-semitrailers. Frequency and time domain analysis is used to study the effect of look-ahead distance and velocity on the steering response of the tractor-semitrailer. It is shown that the variation of vehicle speed and road surface quality have significant influence in system dynamics. It is shown that increasing the look-ahead distance increases the phase lead of system dynamics and increases the damping of zeros of the open-loop system.

The third section reports off-tracking analysis of single-unit and tractor-semitrailer. The dynamical models developed under MOU 242 are used to analyze the steady state

behavior of the vehicles negotiating a curve of constant radius. It is shown that as the longitudinal velocity decreases, the steering angle and off-tracking predicted by the dynamic model approaches the values given by the kinematic model.

The fourth section of this report presents dynamic modeling of generic multi-unit heavy duty vehicle. An arbitray number of connected trailers and all the possible types of combination that are currently in use are considered. In the complex simulation model, translational, bounce, roll, pitch and yaw motion of each unit are incoporated unless contrained by the hitching mechanism. The coupling of roll and pitch motion is investigated and the fifth-wheel dynamics is considered. An analytical simplified model expressed in $2 + N$ dynamic equations is given, where two equations model the system planar translational motion and N equations account for the yaw motions of N units. Conclusions are presented in the last section.

1 Introduction

In the past, the automatic vehicle control research work for AHS has emphasized passenger vehicles (Fenton et al., 1991, Shladover et al., 1991, Peng and Tomizuka, 1993). The study of heavy vehicles for AHS applications has, however, gained interest only recently (Zimmermann et al., 1994, Blosseville et al., 1995, Favre, 1995, Bishel, 1993, Yanakiev et al., 1995, Chen et al., 1995). The study of lateral guidance of heavy vehicles is important because of several reasons. In 1993, the share of the highway miles accounted for by the truck traffic was around 28% (Highway Statistics, 1993). This is a significant percentage of the total highway miles accounted for by all the vehicles in the US. According to Motor Vehicles Facts and Figures (1993), California has largest number of establishments manufacturing truck and truck-trailer combinations in the U.S. In 1991, the total number of the registered heavy vehicles formed approximately 10% of the national figures. In 1991, 34.3% of highway taxes came from heavy vehicles and this figure was above the national average of 30.9%. Also, because of several economic and policy issues, heavy vehicles have the potential of becoming the main beneficiaries of the automated guidance (Kanellakopoulos and Tomizuka, 1996). The main reasons are

- On average, a truck travels six times the miles as compared to a passenger vehicle. Possible reduction in the number of drivers will reduce the operating cost substantially.
- Relative equipment cost for the automation of the heavy vehicles is far less than the cost of automating the passenger vehicles.
- Automation of the heavy vehicles will have a significant impact on the overall safety of the automated highway system. Trucking is a tedious job and the automation will contribute positively to increased safety on highways.

Commercial trucks and buses will gain significant benefit from the AVCS, and may actually get implemented earlier than the passenger vehicles. Various organizations have been involved with automatic guidance of the trucks. Renault and the INRETS in france are involved with the study of AHS application to freight transport in france

and associated issues at various levels (including socio-economic) (Blosseville et al., 1995). In the United States, Ervin (199‘2) tried to identify the domain of research of IVCS which may be of interest to HV manufacturers . The Heavy Vehicle research in PATH from the point of view of lateral guidance and longitudinal control (platooning) has been active since 1993. In the project “Steering and Brake Control of Heavy Vehicles”, a model of tractor-semitrailer was developed. Several control algorithms based on linear and nonlinear control methodologies were developed (Chen, 1996). For details on the accomplishments of this project, refer to MOU 242 final report (Chen, 1997). The work done in this project was mainly theoretical. Some scaled down experiments were, however, done on the pontiac 6000 (Hingwe, 1996).

The success of the San-Diego Demonstration of the AHS by NAHSC provided another thrust to emphasize the development of generated AHS technologies for heavy vehicles. The current project “Lateral Control of Commercial Heavy Vehicles” is aimed at experimental feasibility analysis of the lateral guidance for heavy vehicles. To this end, a class 8 truck has been obtained from Freightliner for conducting closed loop studies. While the instrumentation of the experimental vehicle is in progress, the research was continued in three related areas during 1996-97.

First, a linear analysis similar to the one done for passenger vehicles (Patwardhan et al., 1997) was done for tractor-semitrailers. Even though advanced control algorithms were studied for the lateral guidance of tractor-semitrailer models, the motivation for the linear analysis came from the need to design a simple controller to be potentially implemented on the tractor-semitrailer as the first cut. The tractor-semitrailer dynamics are heavily dependent on the longitudinal speed, road adhesion and look ahead distance. To quantify these dependencies, frequency domain, time domain and complex analysis was done. Based on this analysis, a simple lead compensator has been designed in the output feedback control system. Closed loop simulations were done with the designed controller. The simulations show that the lateral displacement at CG and the trailer end meets the requirement of the maximum allowable lateral displacement.

Secondly, based on the linear model, off-tracking analysis for single unit as well as tractor-semitrailer has also been accomplished. It is also shown that the dynamic

model of both the single unit heavy vehicle and a tractor-semitrailer has a kinematic component embedded in it. As the longitudinal velocity of the vehicle goes to zero, the steering angle required by the dynamic model for negotiating a curve of constant radius matches the angle required by the kinematic model.

Finally, the modeling and analysis of the heavy vehicles was another accomplishment of the project. This part of the report presents a method of deriving both complex simulation model and simplified control model for the general type of multi-unit Heavy Duty Vehicle system. In the complex model, all the units are three dimesional free body and allowed translational motion and three rotational motions except as contrained by different types of hitching mechanisms. In the simple model, only the translational motion and the yaw motions of each unit are considered. Considering the tasks of these models, the scope of information expected from each model, range of dynamic characteristics taken into account and the ease of derivations, we applied different methods to derive each model. Newtonian method is applied to the derivation of complex model. All the constraint forces and constraint moments are also obtained. In the derivation of simple control model, we applied Newtonian method to the translational motion of the whole system and Lagrangian method to the yaw motion of each unit. In both cases, the interal constraint forces do not appear explicitly in the dynamic equations thus allowing an analytical expressions of model equations to be used in controller design.

The organization of this report is as follows. The linear analysis for the tractor-semitrailer is presented in section 2. Section 3 presents the off-tracking analysis. The derivation of the dynamics model of a general Heavy Duty vehicle is presented in section 4. The report is summarized in section 5.

2 Linear Analysis of Tractor Semitrailers*

2.1 Introduction

Automatic Highway System (AHS) technologies have attracted growing attention among researchers throughout the world in the past several years. In contrast to light passenger vehicles, less attention has been paid to control issues of commercial heavy vehicles for AHS. For a comprehensive study of the automation in heavy vehicles, readers is referred to Bishel(1993), Chen(1995), Favre(1995),Kanellakopoulos(1996), Yanakiev(1995), Zimmermann(1994).

Two types of dynamic models are generally used in the study of lateral control of heavy-duty vehicles in AHS (Chen, 1995, Chen 1996). The complex simulation model considers the lateral, yaw and roll motion and the simplified control design model considers the lateral and yaw motion only. Whereas the complex model is significant for studying characteristic like roll over (which is a dominant concern in heavy vehicles), the controller design is usually based on the simplified model. In Chen (1996) a nonlinear simplified model of tractor-semitrailer vehicle was derived and controllers based on LQ and backstepping approaches were designed. The treatment of lateral control of tractor-semitrailer vehicle in Chen (1996) was largely nonlinear. In this section, a linear analysis of the tractor-semitrailer model motivated by Guldner (1997) is presented. In Guldner (1997) it was shown that for a passenger vehicle, a successful design of the lateral controller has to consider the system dynamics subject to variation of vehicle speed, road adhesion and look-ahead distance. In this report, we present the time domain, frequency domain and pole/zero analysis of the linearized tractor-semitrailer vehicle model (based on the nonlinear steering control model derived in Chen (1996) to examine the system dynamics along similar lines. Following the analysis, a linear controller is designed. The linear controller is simpler than nonlinear controllers studied in Chen (1996) though its performance is limited. Because of simplicity, it becomes a good candidate to be implemented in the experimental demonstration using an actual tractor-semitrailer vehicle. It may also set a performance standard for the nonlinear

*Graduate Student Researcher Jeng-Yu Wang is the principle author of this section

controllers. The remainder of this report is organized as follows. In section 2.2 we present the problem description that will include the derivation of the linearized model for steering control and performance specifications. A detailed analysis of system dynamics with varying speed, road adhesion and look ahead distance will be generated in section 2.3, which will be followed by linear controller design in section 2.4. The close-loop simulation results will be shown in section 2.5. Conclusions will be presented in section 5.

2.2 Lateral Control of Tractor-Semitrailer Vehicles

Lateral control of vehicles for AHS consists of lane following and lane changing maneuvers. Emphasis in this report is lane following based on linear control. The controller must generate a desired steering action based on the tracking error signal obtained by the road reference/sensing system, which consist of magnet buried in the road and on-board magnetometers. Linearized model derived in section 2.2.1 is used through out this study. The performance, robustness, ride comfort requirement and practical constraints are described in section 2.2.2 and 2.2.3.

2.2.1 Linearized Vehicle Model

The simplified nonlinear control model for tractor-semitrailer vehicles with front wheel steer in Chen (1996) is based on the following assumptions:

- The roll motion is negligible.
- The longitudinal acceleration $\ddot{x}_r$ is small.
- The relative yaw angle ϵ_r of the tractor with respect to the road center line is small.
- The relative yaw angle ϵ_f between the tractor and semitrailer is small.
- Tire slip angles of the left and the right wheels are the same.
- Tire longitudinal and lateral forces are represented by the linearized tire model

Based on these assumptions, the following simplified model is obtained in Chen (1996)

$$M\ddot{q} + C(q, \dot{q}) + D\dot{q} + Kq = F\delta_f \tag{1}$$

where

$$q = \begin{pmatrix} y_u & \epsilon_1 & \epsilon_f \end{pmatrix}^T \tag{2}$$

is the generalized coordinate vector,

$$M = \begin{pmatrix} m_1 + m_2 & -m_2(d_1 + d_3\cos\epsilon_f) & -m_2 d_3\cos\epsilon_f \\ -m_2(d_1 + d_3\cos\epsilon_f) & I_{z1} + I_{z2} + m_2(d_1^2 + d_3^2) + 2m_2 d_1 d_3\cos\epsilon_f & I_{z2} + m_2 d_3^2 + m_2 d_1 d_3 \\ -m_2 d_3\cos\epsilon_f & I_{z2} + m_2 d_3^2 + m_2 d_1 d_3\cos\epsilon_f & I_{z2} + m_2 d_3^2 \end{pmatrix} \tag{3}$$

is the inertia matrix,

$$C(q, \dot{q}) = \begin{pmatrix} (\mathrm{ml} + m_2)\dot{x}_u\dot{\epsilon}_1 + m_2 d_3 \sin\epsilon_f(\dot{\epsilon}_1 + \dot{\epsilon}_f)^2 \\ -m_2(d_1 + d_3\cos\epsilon_f)\dot{x}_u\dot{\epsilon}_1 - m_2 d_3\sin\epsilon_f\dot{y}_u\dot{\epsilon}_1 - 2m_2 d_1 d_3\sin\epsilon_f\dot{\epsilon}_1\dot{\epsilon}_f - m_2 d_1 d_3\sin\epsilon_f\dot{\epsilon}_1^2 \\ -m_2 d_3\sin\epsilon_f\dot{y}_u\dot{\epsilon}_1 - m_2 d_3\cos\epsilon_f\dot{x}_u\dot{\epsilon}_1 + m_2 d_1 d_3\sin\epsilon_f\dot{\epsilon}_1^2 \end{pmatrix} \tag{4}$$

is the vector of the Coriolis and Centrifugal forces,

$$D = \frac{2}{\dot{x}}\begin{pmatrix} C_{\alpha_f} + C_{\alpha_r} + C_{\alpha_t} & l_1 C_{\alpha_f} - l_2 C_{\alpha_r} - (l_3 + d_1)C_{\alpha_t} & -l_3 C_{\alpha_t} \\ l_1 C_{\alpha_f} - l_2 C_{\alpha_r} - (l_3 + d_1)C_{\alpha_t} & l_1^2 C_{\alpha_f} + l_2^2 C_{\alpha_r} + (l_3 + d_1)^2 C_{\alpha_t} & l_3(l_3 + d_1)C_{\alpha_t} \\ -l_3 C_{\alpha_t} & l_3(l_3 + d_1)C_{\alpha_t} & l_3^2 C_{\alpha_t} \end{pmatrix} \tag{5}$$

is the damping matrix,

$$K = \begin{pmatrix} 0 & 0 & -2C_{\alpha_t} \\ \mathrm{C}\ 1 & 0 & 2(l_3 + d_1)C_{\alpha_t} \\ 0 & 0 & 2l_3 C_{\alpha_t} \end{pmatrix} \tag{6}$$

s the potential matrix, and the vector $F \in R^{3\times 1}$ is

$$F = 2C_{\alpha_f}\begin{pmatrix} 1 & l_1 & 0 \end{pmatrix}^T \tag{7}$$

Parameters in the model are defined in Table (1). Notice that this simplified model is nonlinear. The model can be further linearized by utilizing approximation $\cos\epsilon_f \approx 1$, $\sin\epsilon_f \approx \epsilon_f$ and neglecting the higher order terms: i.e.

$$M \simeq \begin{pmatrix} m_1 + m_2 & -m_2(d_1 + d_3) & -m_2 d_3 \\ -m_2(d_1 + d_3) & I_{z1} + I_{z2} + m_2(d_1^2 + d_3^2) + 2m_2 d_1 d_3 & I_{z2} + m_2 d_3^2 + m_2 d_1 d_3 \\ -m_2 d_3 & I_{z2} + m_2 d_3^2 + m_2 d_1 d_3 & I_{z2} + m_2 d_3^2 \end{pmatrix} \tag{8}$$

Symbols	Definitions (Simulation Value)
y_u	lateral displacement of tractor center of gravity (C.G.) with respect to unsprung mass coordinate
ϵ_1	yaw angle of the tractor w.r.t. inertia frame
ϵ_f	relative yaw angle between the tractor and the semitrailer
m_1	tractor mass $(8440Kg)$
m_2	semitrailer mass $(23472Kg)$
d_1, d_2	relative position between tractor's C.G. to fifth wheel $(3.06m, 0.60m)$
d_3, d_4	relative position between semitrailer's C.G. to fifth wheel $(4.20m, 1.20m)$
I_{z1}	tractor moment of inertia $(65734.6Kgm^2)$
I_{z2}	semitrailer moment of inertia ($181565.5Kgm^2$)
l_1	distance between tractor C.G. and front wheel axle $(2.59m)$
l_2	distance between tractor C.G. and rear wheel axle $(3.29m)$
l_3	distance between joint (fifth wheel) and semitrailer wheel axle $(9.65m)$
$C_{\alpha f}$	cornering stiffness of tractor front wheel $(143330.0N/rad)$
$C_{\alpha r}$	cornering stiffness of tractor rear wheel (143330.0 x $4N/rad$)
Cat	cornering stiffness of semitrailer rear wheel (80312.0 x $4N/rad$)

Table 1: Nomenclature of the control model

$$C(q,\dot{q}) \approx \begin{pmatrix} (m_1+m_2)\dot{x}_u\dot{\epsilon}_1 \\ -m_2(d_1+d_3)\dot{x}_u\dot{\epsilon}_1 \\ -m_2 d_3\dot{x}_u\dot{\epsilon}_1 \end{pmatrix} \tag{9}$$

$$= \begin{pmatrix} (m_1+m_2)\dot{x}_u \\ -m_2(d_1+d_3)\dot{x}_u \\ -m_2 d_3\dot{x}_u \end{pmatrix} \begin{pmatrix} 0 & 1 & 0 \end{pmatrix} \dot{q} \tag{10}$$

$$= \begin{pmatrix} 0 & (m_1+m_2)\dot{x}_u & 0 \\ 0 & -m_2(d_1+d_3)\dot{x}_u & 0 \\ 0 & -m_2 d_3\dot{x}_u & 0 \end{pmatrix} \dot{q} \tag{11}$$

$$= C_1\dot{q} \tag{12}$$

Note that approximations are not required for other matrices, K, D, and F.

If we choose the state variables as

$$X = \begin{pmatrix} y_u & \epsilon_1 & \epsilon_f & \dot{y}_u & \dot{\epsilon}_1 & \dot{\epsilon}_f \end{pmatrix}^T \tag{13}$$

, the linearized state-space equations becomes:

$$\frac{d}{dt}X \quad \begin{pmatrix} 0 & I \\ M^{-1}K & -M^{-1}(D+C_1) \end{pmatrix} X + \begin{pmatrix} 0 \\ M^{-1}F \end{pmatrix} \tag{14}$$

$$= A_u X + B_u \delta_f \tag{15}$$

This representation will be need for analysis in the following section.

2.2.2 Performance Requirement

The total width of the heavy-duty vehicles including side-mirrors may vary within 2m$\sim$2.8m (AASHTO, 1995). US highway lanes have a width of 3.6m, leaving a worst-case margin of 0.4m on each side for lane keeping error. Because of the Jacknifing problem for heavy-duty vehicles, the worst lateral displacement from the road center line whether in the front or tail of the truck should not exceed this value. Thus a maximum error of 0.2m appears reasonable. This error is further subdivided into nominal

operation and an extreme situations, which include significant simultaneous changes of road adhesion μ and concurrent strong braking/acceleration. Hence a nominal maximum error of O.lm and an extreme maximum error of 0.2m are used as performance requirements in this study.

The time derivative of the acceleration, called jerk, effects the comfort level of riders. A continuous steady state acceleration up to $0.3\sim0.4g$ can be comfortably counteracted by humans. Also, accelerations in the 5-10 Hz frequency range can excite the human's internal body resonances. Excitation of these resonances makes the rider uncomfortable. Hence the accelerations in this frequency range should be attenuated.

2.2.3 Practical Constraints

A practical constraint relating to both the tracking performance and the rider comfort is due to random inputs. Randomness may be introduced by system noise. So the white sensor noise, no frequency above approximate $0.1\sim0.5$ Hz should be amplified extraordinarily in the path to lateral acceleration at sensor $\ddot{y}_s$. The road adhesion μ is assumed unknown within its range of uncertainty. The physical upper bound is $\mu = 1$ for dry road with a good surface and empirical data of various studies suggests $\mu \approx 0.5$ for wet (slippery) road. Hence a set of "normal" road is defined for this study as $0.5 \leq \mu \leq 1$ for wet and better road.

The steering actuator dynamics is another implementational design constrains. Implementation without major constructional modification of currently used steering mechanisms limits the available actuator bandwidth. The actuator bandwidth is also subject to uncertainty due to variant operation conditions like temperature and command amplitude. Compared with a human driver (below 1Hz) and the car dynamics (about 1Hz), the bandwidth limitations constitute a serious factor which may limit the performance of the controller. With the above performance criteria in mind, analysis of the tractor-semitrailer vehicle is presented in the next subsection.

2.3 Analysis of the Linearized Vehicle Model

In this section, we choose various linear analysis methods to examine the system (vehicles) dynamics. These include time domain analysis, frequency domain analysis and pole-zero analysis. Based on these analysis, a linear controller will be designed.

2.3.1 Converting State Space to Transfer Functions

Recall equation (15) and consider the following decomposition :

$$A, = \left(\begin{array}{c|c} A_{11} & A_{12} \\ \hline A_{21} & A_{22} \end{array}\right) \tag{16}$$

and

$$B_u = \left(\begin{array}{c} B_1 \\ \hline B_2 \end{array}\right) \tag{17}$$

where A_{11}, A_{12}, A_{21}, A_{22} are 2 x 2, 2 x 4, 4 x 2, 4 x 4 matrices respectively and B_1, B_2 are 2 x 1, 4 x 1 matrices. The state equation (15) can be divided into two subsystems:

$$\frac{d}{dt} \begin{matrix} \text{YU} \\ \theta \ \epsilon_1 \end{matrix} = A_{11} \begin{pmatrix} y_u \\ \epsilon_1 \end{pmatrix} + A_{12} \begin{pmatrix} \epsilon_f \\ \dot{y}_u \\ \dot{\epsilon}_1 \\ \dot{\epsilon}_f \end{pmatrix} + B_1 \delta_f \tag{18}$$

$$\frac{d}{dt} \begin{pmatrix} \epsilon_f \\ \dot{y}_u \\ \dot{\epsilon}_1 \\ \dot{\epsilon}_f \end{pmatrix} = A_{21} \begin{pmatrix} y_u \\ \epsilon_1 \end{pmatrix} + \text{-422} \begin{pmatrix} \epsilon_f \\ \dot{y}_u \\ \dot{\epsilon}_1 \\ \dot{\epsilon}_f \end{pmatrix} + B_2 \delta_f \tag{19}$$

Further, because the first two columns of K are zeros, $A_{11} = 0^{2\times 2}$ and $A_{21} = 0^{4\times 2}$. This implies

$$\frac{d}{dt}\begin{pmatrix} \epsilon_f \\ \dot{y}_u \\ \dot{\epsilon}_1 \\ \dot{\epsilon}_f \end{pmatrix} = A_{22}\begin{pmatrix} \epsilon_f \\ \dot{y}_u \\ \dot{\epsilon}_1 \\ \dot{\epsilon}_f \end{pmatrix} + B_2\delta_f \tag{20}$$

$$= \begin{pmatrix} A_{22}(1) \\ A_{22}(2) \\ A_{22}(3) \\ A_{22}(4) \end{pmatrix}\begin{pmatrix} \epsilon_f \\ \dot{y}_u \\ \dot{\epsilon}_1 \\ \dot{\epsilon}_f \end{pmatrix} + \begin{vmatrix} B_2(1) \\ B_2(2) \\ B_2(3) \\ B_2\ (4) \end{vmatrix}\delta_f \tag{21}$$

Therefore, the transfer function from δ_f to $\ddot{y}_u$ is

$$V_u(s) = A_{22}(2)(sI - A_{22})^{-1}B_2 + B_2(2) \tag{22}$$

If we define

$$C_1 = \begin{pmatrix} 0 & 1 & 0 \end{pmatrix} \tag{23}$$

the transfer function from δ_f to $\dot{\epsilon}_1$ can be obtained as follows :

$$W_1(s) = C_1(sI - A_{22})^{-1}B_2 \tag{24}$$

And the transfer function from δ_f to $\ddot{\epsilon}_1$ is

$$W(s) = A_{22}(3)(sI - A_{22})^{-1}B_2 + B_2(3) \tag{25}$$

Note

$$\mathbf{v_{CG}} = \dot{x}_u\mathbf{i_u} + \dot{y}_u\mathbf{j_u} \tag{26}$$

$$\Longrightarrow \mathbf{a_{CG}} = (\ddot{x}_u - \dot{y}_u\dot{\epsilon}_1)\mathbf{i_u} + (\ddot{y}_u + \dot{x}_u\dot{\epsilon}_1)\mathbf{j_u} \tag{27}$$

where $\mathbf{i_u}$ and $\mathbf{j_u}$ are unsprung mass coordinates which have same orientation as the tractor. Therefore, the lateral acceleration at CG is

$$\ddot{y}_{CG} = \ddot{y}_u + \dot{x}_u\dot{\epsilon}_1 \tag{28}$$

Denoting $\dot{x}_u$ as v, the transfer function from δ_f to $\ddot{y}_{CG}$ is obtained as :

$$V_{CG}(s) = V_u(s) + vW_1(s) \tag{29}$$

If we consider the sensor location which is ds ahead of CG, the velocity $\mathbf{v_s}$ is given by

$$\mathbf{v_s} = \dot{x}_u \mathbf{i_u} + (\dot{y}_u + d_s\dot{\epsilon}_1)\mathbf{j_u} \tag{30}$$

$$\Longrightarrow \mathbf{a_s} = (\ddot{x}_u - \dot{y}_u\dot{\epsilon}_1 - d_s\dot{\epsilon}_1^2)\mathbf{i_u} + (\ddot{y}_u + \dot{x}_u\dot{\epsilon}_1 + d_s\ddot{\epsilon}_1)\mathbf{j_u} \tag{31}$$

so the lateral acceleration at sensor is given by

$$\ddot{y}_S = \ddot{y}_u + \dot{x}_u\dot{\epsilon}_1 + d_s\ddot{\epsilon}_1 \tag{32}$$

$$= \ddot{y}_{CG} + d_s\ddot{\epsilon}_1 \tag{33}$$

In equation (33), the lateral acceleration $\ddot{y}_s$ comprises lateral acceleration at CG and yaw acceleration $\ddot{\epsilon}_1$ scaled by look-ahead distance d_s. The transfer function from δ_f to $\ddot{y}_s$ is thus

$$V_s(s) = V_{CG}(s) + d_sW(s) \tag{34}$$

2.3.2 Time Domain Analysis

Based on the transfer functions shown in section 2.3.1, a set of illustrative step responses using steering input of δ_f = 0.01 rad with zero initial conditions is shown in Fig. 1. Note that the actuator dynamics have not been included. The upper two plots show the dependency of the lateral acceleration $\ddot{y}_{CG}(t)$ on speed v and road adhesion μ. As we can see, the initial lateral acceleration at CG $(\ddot{y}_{CG}(0))$ is speed independent but varies linearly in road adhesion μ. The steady-state lateral acceleration at CG $(\ddot{y}_{CG}(\infty))$ is both speed and μ dependent. At low speeds $(v < 12m/s)$, the initial lateral acceleration at CG is larger than the steady state lateral acceleration, which features a transient without overshoot and oscillation. On the other hand, for high speeds $(v > 12m/s)$, the initial lateral acceleration at CG is smaller than the steady state lateral acceleration and the transient is subject to increasing overshoot and oscillatory behavior. The lower two plots depict the dependency of yaw rate $\dot{\epsilon}_1(t)$ on speed and road adhesion. Note

steady state yaw rate $\dot{\epsilon}_1(\infty)$ increases significantly from v=10m/s to v=20m/s but only slightly from there on for higher speeds. However it depends almost linearly on road adhesion μ. Also, for increasing speed and degrading road quality, yaw rate step response tends to overshoot and oscillate, even more than lateral acceleration.

2.3.3 Frequency Domain Analysis

In this section, we continue the analysis but using bode diagram (frequency domain analysis). Fig. 2 shows the bode diagrams of the lateral vehicle dynamics $V_{CG}(s)$ in equation (29). The left diagram illustrates the dependency of $V_{CG}(s)$ on driving speed v for the range 10m/s to 40m/s on a dry road with good surface μ = 1. Note the lateral acceleration transfer function $V_{CG}(s)$ have notch characteristics with a distinct natural mode around 0.1~2Hz. At low speed, the steady-state gain $V_{CG}(0)$ is less than high frequency gain $V_{CG}(\infty)$. The overall gain increase from $V\&(0)$ to $V_{CG}(\infty)$ for $v \leq 12m/s$ provides phase lead in the range of the natural mode and leads to the step response with initial values $\ddot{y}_{CG}(0)$ exceeding steady-state $\ddot{y}_{CG}(\infty)$ (Recall Fig. 1). For increasing speed, the steady state gain $V_{CG}(0)$ increases strongly with speed v while high frequency gain $V_{CG}(\infty)$ remains constant. Increasing v higher than 12m/s, the gain drop from $V_{CG}(0)$ to $V_{CG}(\infty)$ results in significant phase lag in the range of 0.01~2Hz. Also note at high speed, the natural modes is accompanied by a gain "undershoot" around 0.5~3Hz (even double for higher speed). This hints a dominant and poorly damped zero-pair. The right diagram depicts variation of road adhesion from wet road μ = 0.5 to dry and good road μ = 1.0 at speed v=40m/s. Note decreasing μ decreases the gain $|V_{CG}(j\omega)|$ for all frequencies (which is visible in the step response in Fig. 1 (upper right plot)) and also decreases the frequency of the natural mode.

A set of bode diagrams for yaw acceleration transfer function W(s) in equation (25) is shown in Fig. 3. Compared with $V_{CG}(s)$, yaw acceleration has differentiating characteristics at low frequency with associated phase lead up to corner frequency w,. The gain in the low frequency region depends linearly on speed v, whereas the high frequency gain is speed independent (left upper plot). The natural mode is less

markable in $W(s)$ than $V_{CG}(s)$, hinting that the zero-pair in lateral acceleration rather than the pole-pair causes the gain undershoot in the $0.5\sim3$Hz rigion of $V_{CG}(s)$ because W(s) and V_{CG}(s) share the same denominator.

If viewed at sensor location S, the lateral vehicle acceleration has an embedded additional yaw acceleration component (recall equation (34)). Figure 4 shows the bode diagrams for the lateral acceleration at sensor $V_s(s)$ for varying speed v and look-ahead distance d_s. Note $V_s(s)$ is linear combination of $V_{CG}(s)$ and W(s) (equation (34)). In the low frequency region, the magnitude of ***V&(s)*** exceeds that of W(s), which leads to dominance of V_{CG} in $V_s(s)$. That explains the similar low frequency gain of $V_s(s)$ (The left diagram) and of V_{CG}. The steady-state gain, $V_s(0)$ is strongly dependent on speed v while the high frequency gain $V_s(\infty)$ is velocity independent. Although the high frequency gain $V_s(\infty)$ is velocity independent, it varies linearly with look-ahead distance d_s (The right diagram). Phase lag in the range of $0.01\sim1$Hz increases for increasing speed with fixed d_s = 2m. Conversely, increasing d_s will decrease phase lag and eventually provide phase lead even at high speed. The phase lag around the natural mode has significant consequence for control design.

2.3.4 Pole-Zero Analysis

The pole-zero analysis of the vehicle dynamics $V_{CG}(s)$ reveals the controller design from a different point of view. The frequency domain analysis in the previous section indicated the gain "undershoot" for $0.5\sim3$Hz hints a dominant and poorly damped zero-pair. This can be studied in more detail in Fig. 5. Increasing speed v, we can see both the poles (the right plot) and zeros (the left plot) approach the imaginary axis, leading to respective poor damping, with the zeros having less damping than the associated pole-pair.

Figure 6 shows pole and zero location of $V_{CG}(s)$ for variation of road adhesion μ. As decreasing μ, poles and zeros further approach the imaginary axis in a uniform manner. This results even lower damping of both the pole-pairs and zero-pairs. It coincides with that to control orientation of the car in slip road is difficult. The description of damping associated with the zero and pole pairs of $V_{CG}(s)$ is emphasized in Fig. 7.

Damping D_p of the pole-pairs (upper two plots) is contrasted with damping D_z of the zero-pairs (lower two plots). Apparently, the zero-pair damping D_z is smaller than the pole-pair damping D_p. The zero-pair damping D_z decreases sharply with increasing speed to value as low as 0.4 for $v = 20m/s$ and further to 0.23 for $v = 40m/s$ on any road surface. Damping of the poles, on the other hand, drops steadily with speed v. Deteriorating road adhesion μ further decreases D_p for any speed. Note in a close loop system, the pole-pair is inevitably attracted to the zero-pair which leads to even more poor damping. Since these poles dominate other vehicle transfer function (like $V_s(s)$ and vehicle yaw rate $W_1(s)$), poor comfort results. However, damping associated with the zero-pairs of the lateral acceleration transfer function V_s at sensor location S increases with look-ahead distance d_s. Figure 8 shows an example at high speed v=30m/s on a good road. The damping increases dramatically with increases of d_s up to about 8m. For even larger d_s, the further damping increase is less significant. As we can see, the poor damping of zero-pairs of V_s for look-down reference system is one of the major obstacles towards automatic steering control.

2.4 Controller Design

This subsection is devoted to the investigation of a possible PID controller design. The block diagram in Fig. 9 shows the double integrator is to be controlled via the lateral acceleration $\ddot{y}_s$, based on displacement measurement Δy_s, and with input $\ddot{y}_{ref}$. The open loop characteristic G(s), obtained by combining controller C(s) and vehicle lateral acceleration $V_s(s)$ (here again, the actuator dynamics are neglected) is written as

$$G(s) = C(s)V_s(s) \tag{35}$$

and constitutes the "control" for the "plant"($). The closed loop input-output relationship between road curvature ρ_{ref} and lateral displacement Δy_s is :

$$\Delta y_s = \frac{v^2}{s^2 + G(s)}\rho_{ref} \tag{36}$$

$$= H(s)\rho_{ref} \tag{37}$$

Instead of isolated design of the controller C(s), the vehicle dynamic $V_s(s)$ is now included in the design of G(s) to control the double integer. Here we use the dual-role

concept in Guldner (1997). First, an appropriate G(s) is designed, taking in account all practical requirements and constraints on closed-loop H(s). Then G(s) is realized via concurrent design of vehicle dynamics $V_s(s)$ and controller C(s). In the second step, ***V,(s)*** and C(s) play complementary roles and may be regarded dual to each other. The combined "controller" G(s) should be designed for closed-loop H(s) to fulfill the performance requirement discussed in subsection 2.2.2, in particular with respect to maximum lateral displacement, damping for ride comfort, and robustness with respect to road adhesion μ. Furthermore, controller roll-off to prevent excitation of actuator dynamics is required.

Note that there exists several constraints to the design of the controller. First, the controller C(s) should avoid excessive phase lead in the vicinity of actuator dynamics since this could cause the actuator to saturate, with consequent harmful and possibly unstable limit cycles. Second, higher controller gain at high frequencies are extremely undesirable because it amplifies the noise in measurement Δy_s, leading to poor comfort and also to high wear of mechanical parts in the steering mechanism. Third, the phase lead region of the controller has to sustain for a significant frequency range since the nature mode changes with variation of μ. And this will deprive the necessary room for designing a robust controller C(s).

The double integrator has to be stabilized by G(s) via lead compensator with approximately 50" phase lead at cross-over for appropriate damping. The simplest linear solution is a PIDT structure for G(s). The proportional gain P is the essential part to meet the design requirement. The integral I-term might be necessary to meet steady-state requirement but should not introduce excessive phase lag in the vicinity of cross-over. The differential term D is a lead compensator to provide sufficient phase margin. And T is the low-pass filter for roll-off. In addition to vehicle dynamics $V_s(s)$, controller C(s) may also provide phase lead for stabilization. The interchangeability of the roles of $V_s(s)$ and C(s) in G(s) is discussed in two cases:

- Case A: Choose look-ahead distance d_s such that $V_s(s)$ contributes sufficient phase lead of G(s) for the range $0.5 \leq \mu \leq 1$. Then C(s) is chosen with P-type to match the phase lead region of $V_s(s)$ with the cross-over region for the plant.

- Case B: Look-ahead distance d_s is chosen such that $V_s(S)$ contributes no or little overall phase lag/lead to G(s) and is approximately P-type transfer function for the range $0.5 \leq \mu \leq 1$. C(s) is then chosen with a lead compensator to provide sufficient phase lead to G(s) for stabilization of $(1/s^2)$, according to the performance requirements.

Intermediate solutions can include sharing phase lead requirements between ***V,(s)*** and C(s).

Case A using "natural" phase lead in $V_s(s)$ by appropriate selection of d_s offers straight forward control design at the price of a pre-determined cross-over frequency and hence pre-determined system bandwidth and also generally leads to a higher noise level in the lateral displacement measurement Δy_s. Only two control parameters, d_s and P-gain, have to be selected for robustness with respect to the range $0.5 \leq \mu \leq 1$, possibly gain scheduled with velocity v. Case B, on the other hand, provides flexibility in choosing cross-over, but requires more involved higher order control design which may require excessive actuator bandwidth.

For studying the respective merits of the different approaches, see the bode diagram in Fig. 10. The left diagram (case A) shows an example for $v=40\text{m/s}, d_s = 16\text{m}$ (resulting in a minimum phase lead of 30^o), μ_1 = 1 (solid line), μ_2 = 0.5 (dashed line), with P-control $C(s)=0.08$. Inherent "almost" satisfaction of performance and robustness requirement are attributed to the steering designed to accommodate human driving behavior. In fact it can be argued that case A resembles the steering characteristics of a concentrated human driver. The right diagram (case B) shows similar situation as above with $d_s = 8m$ and C(s) = $0.08\frac{0.853s+1}{0.147s+1}$ where C(s) is a lead compensator providing 50^o to 60^o phase lead consistently over the necessary frequency range. The above analysis points out the crucial trade-off in automatic steering control design (large look-ahead with large measurement error or look-down system with higher order controller design).

2.5 Simulation Results

In this subsection, we choose case B as our designed controller. the simulation scenario is shown in Fig. 11. The tractor-semitrailer vehicle travels along a straight roadway with zero initial displacement and enters a curved section with a radius of curvature of 800m at time $t=5\,\text{sec}$ and leave at $t=12$ sec. The closed-loop response, shown in Fig. 12, is of using the lead compensator C(s) = $0.08\frac{0.853s+1}{0.147s+1}$. The solid line shows test constant velocity 28m/s which is maximum allowed speed in the Highway. The dashed line is test for low speed 10m/s. Apparently the low test speed has smooth steering angle, less lateral displacement at sensor and CG, but comparatively larger lateral displacement at the trailer end than at high speed. Also at low speed the response shows that the yaw angle relative to the road is larger. Now increase the gain of the controller to 0.2. The closed-loop response is shown in Fig. 13. Note there are some fluctuation of steering angle when the vehicle enters and leaves the curve road. The lateral displacement at CG and sensor are proportionally decreased while it doesn't change much of the lateral displacement of the trailer and the relative yaw angle. The articulation angle are almost the same as the one using lower gain controller.

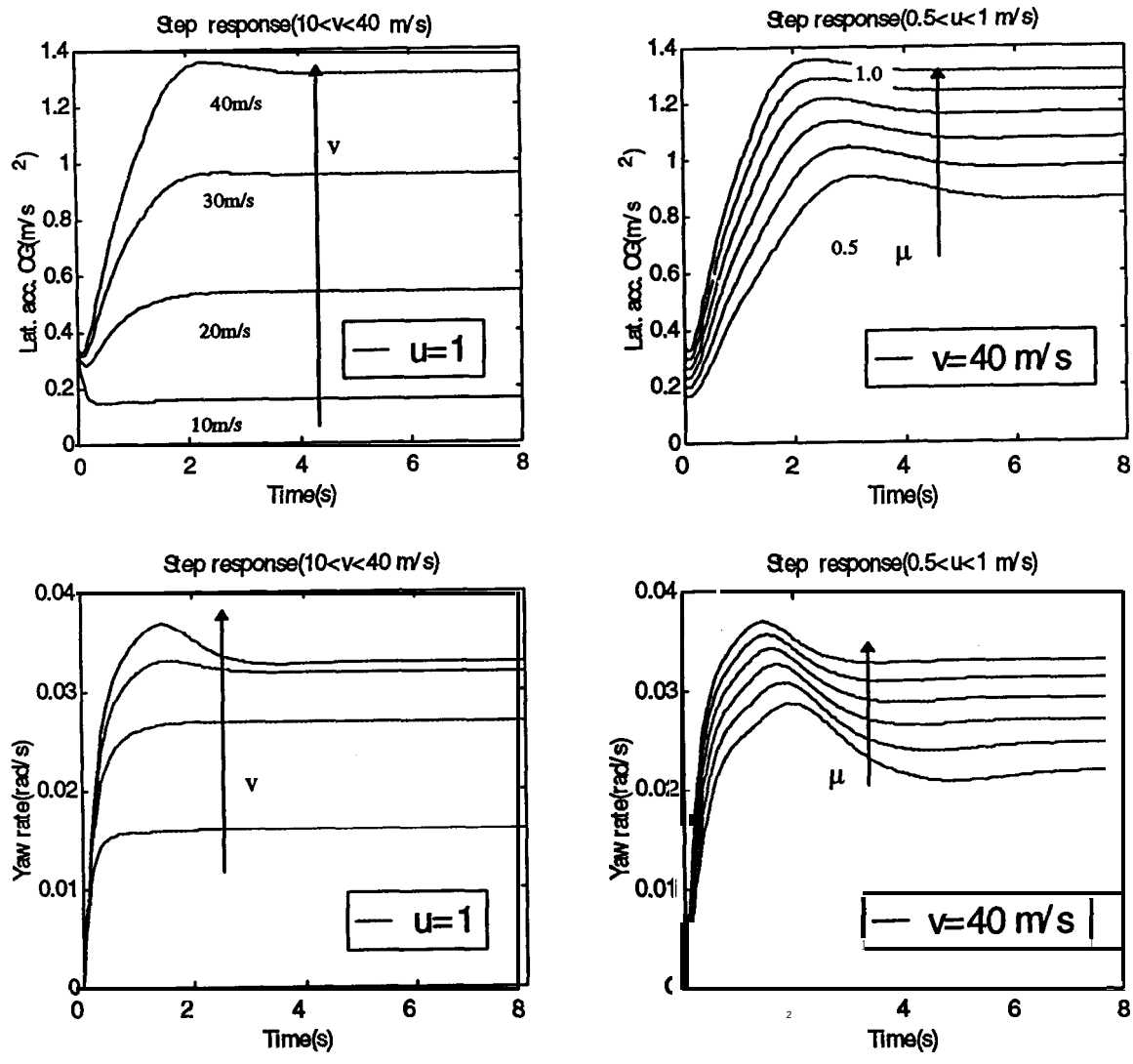

Fig. 1: Step response of $\ddot{y}_{CG}(t)$ and yaw rate $\dot{\varepsilon}_1(t)$ for varying v and μ

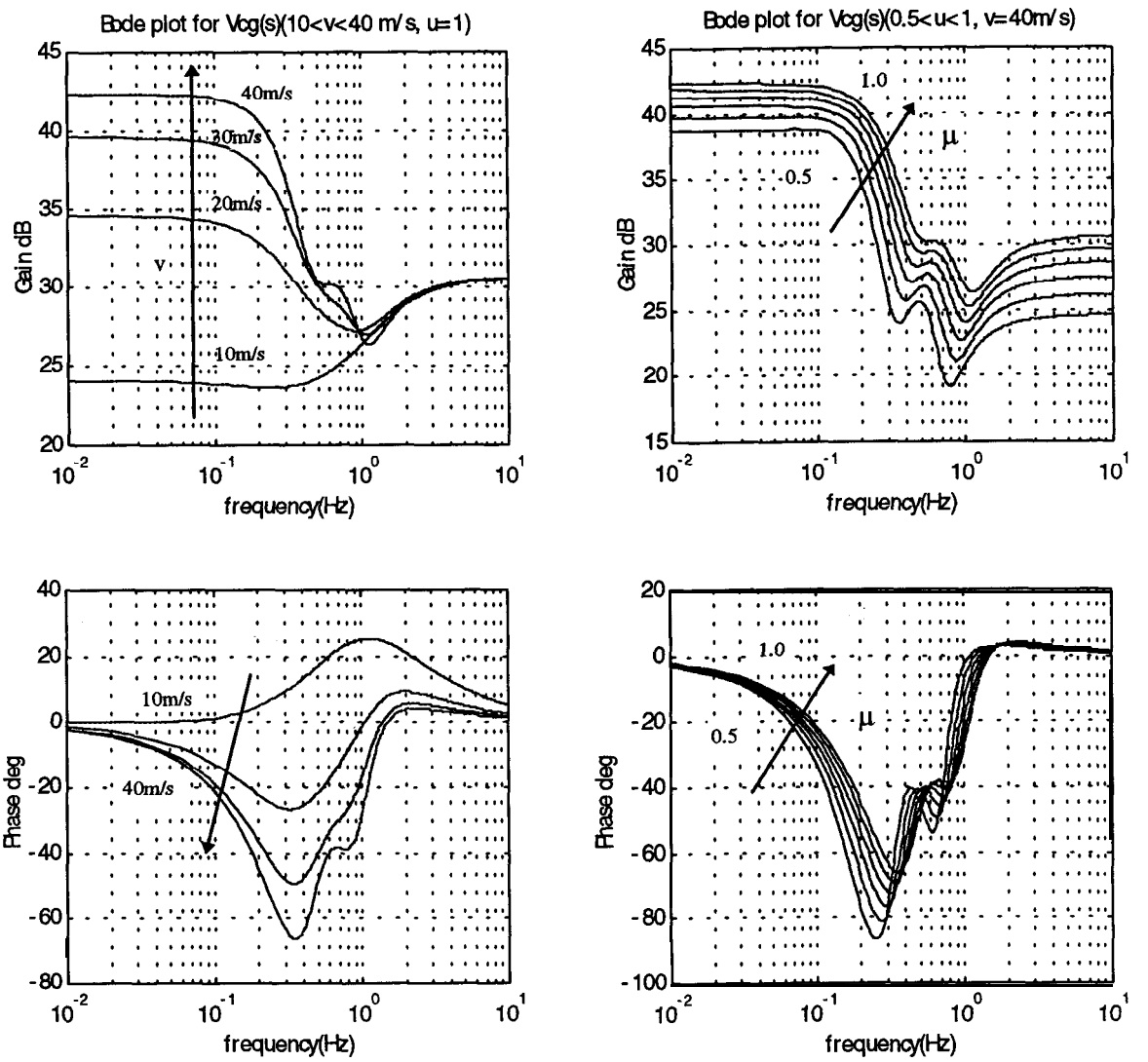

Fig. 2: Bode plot for lateral acceleration dynamics $V_{cg}(s)$ for varying speed v and road adhesion μ

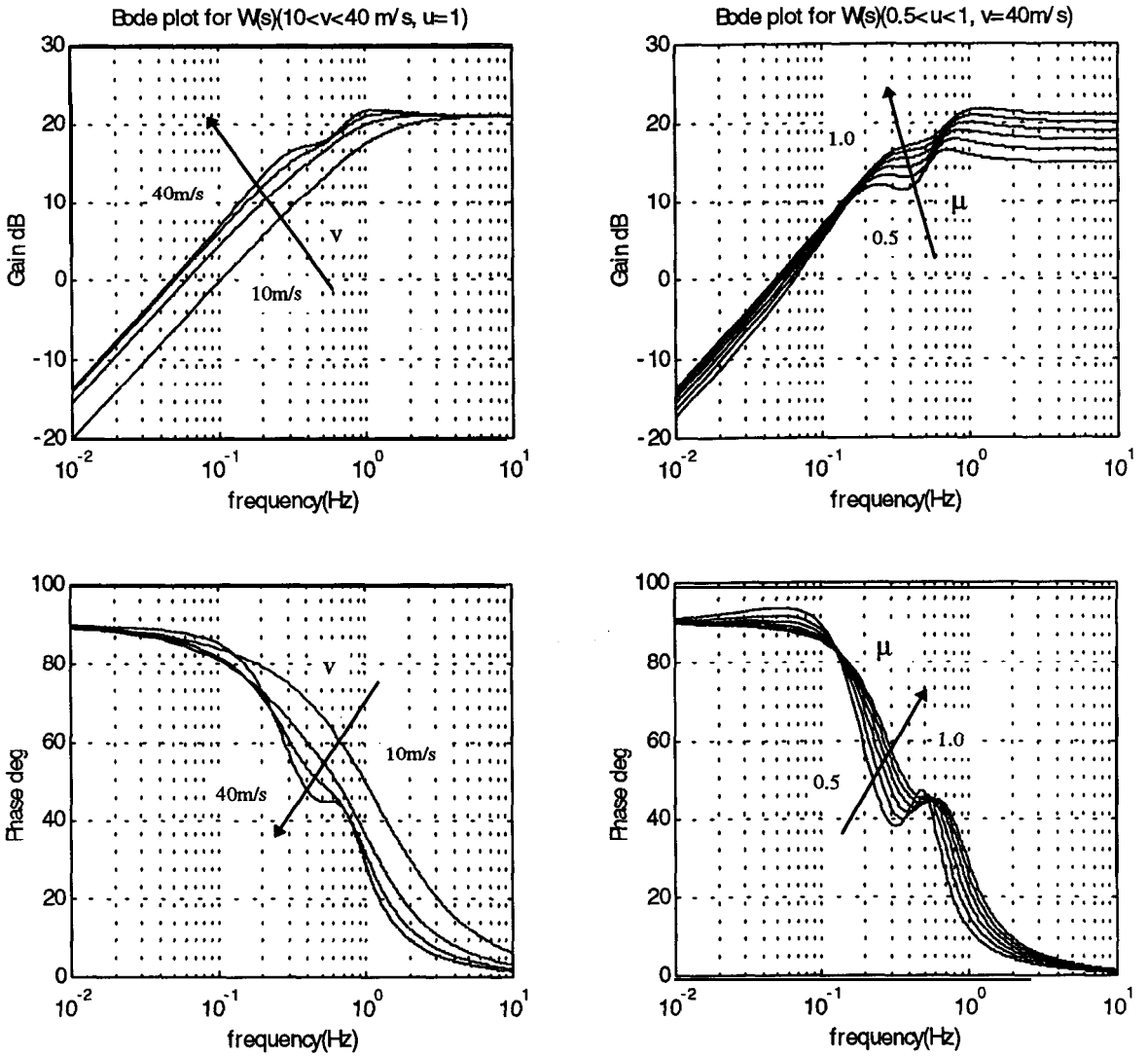

Fig. 3: Bode plot for yaw acceleration dynamics **W(s)** for varying speed v and road adhesion μ

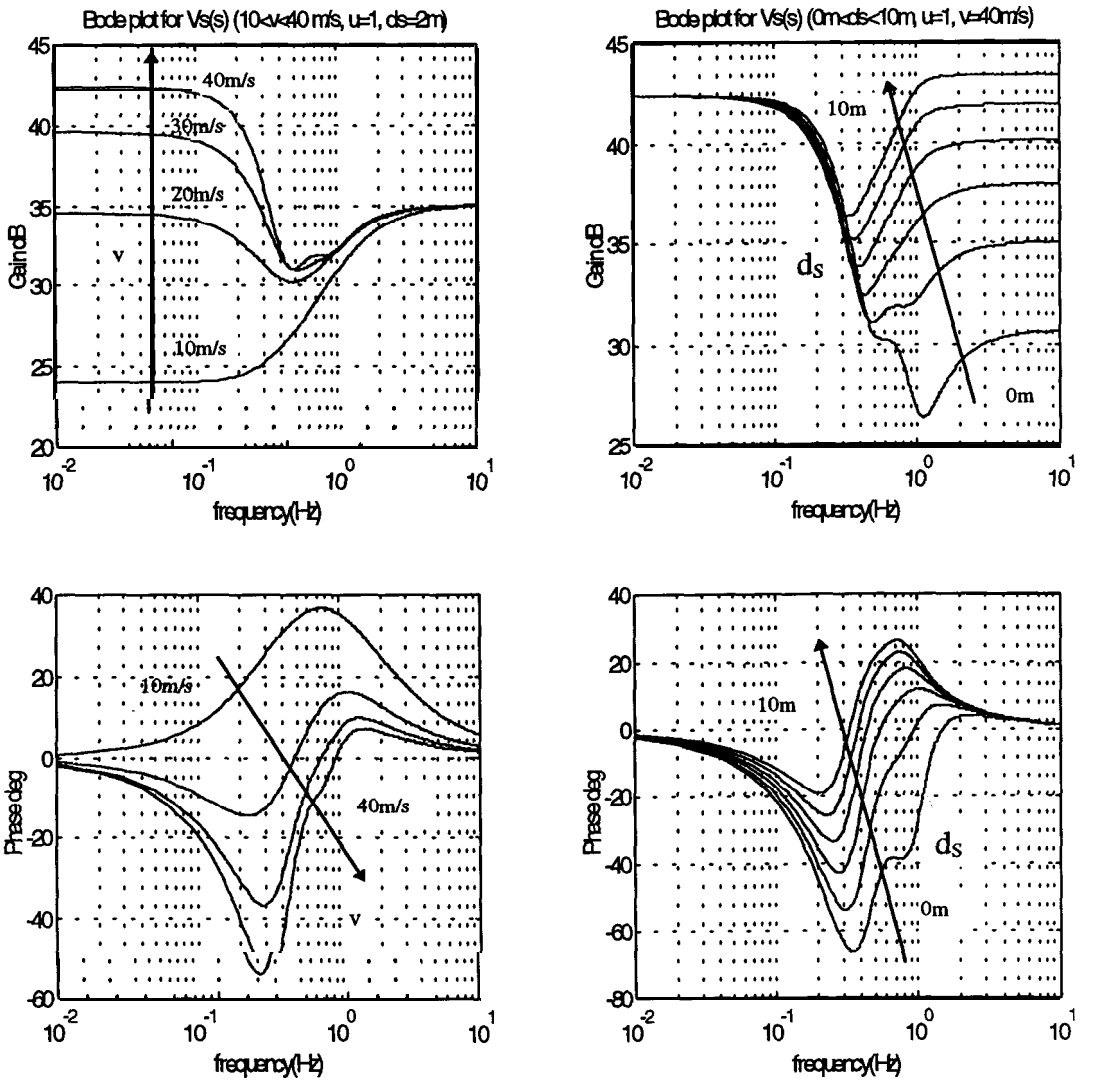

Fig. 4: Bode plot for lateral acceleration dynamics $V_s(s)$ for varying speed v and look-ahead distance ds.

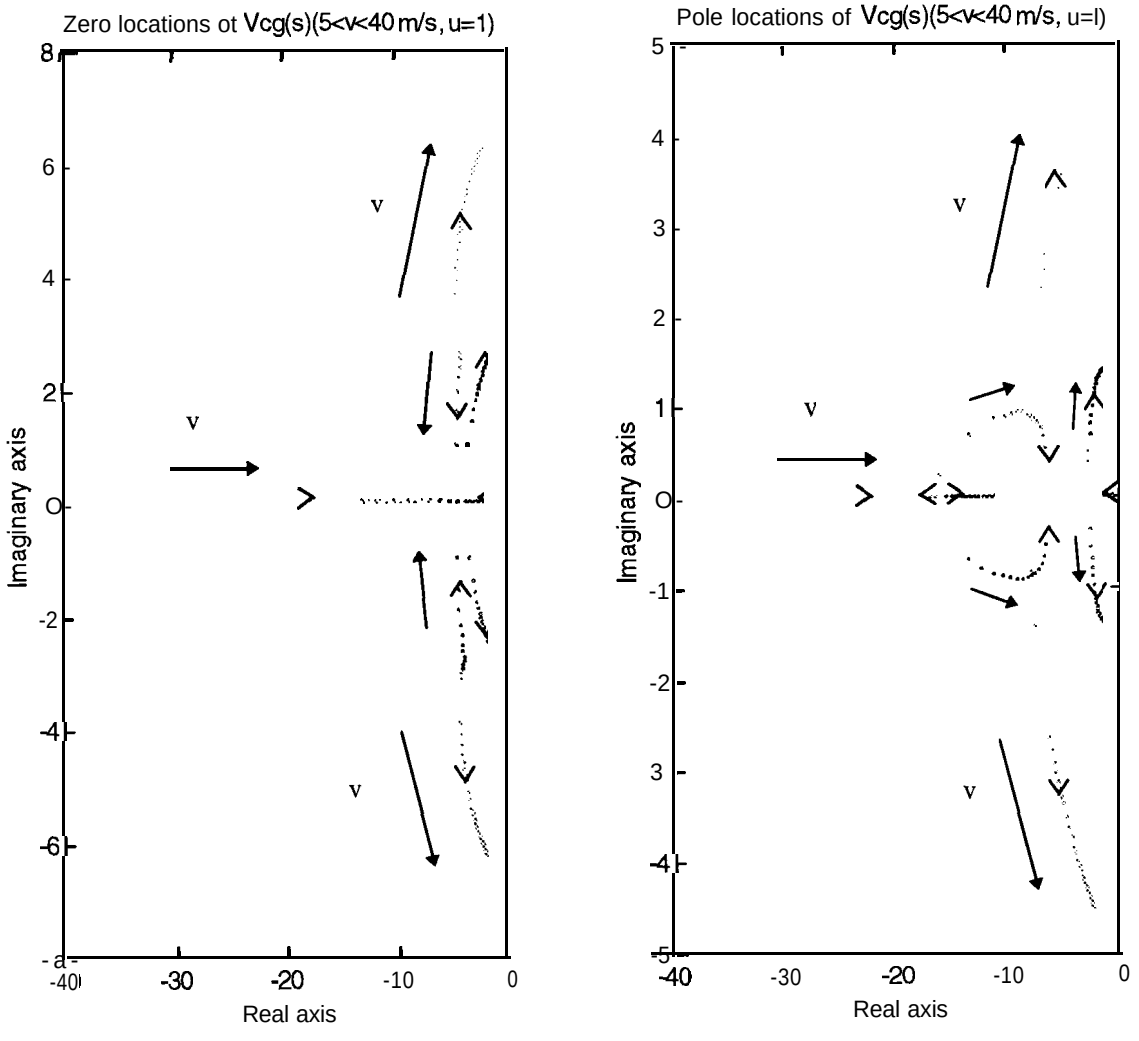

Fig. 5: Pole and zero location of $V_{CG}(s)$ for variation of speed v (arrow indicates the direction of increasing speed)

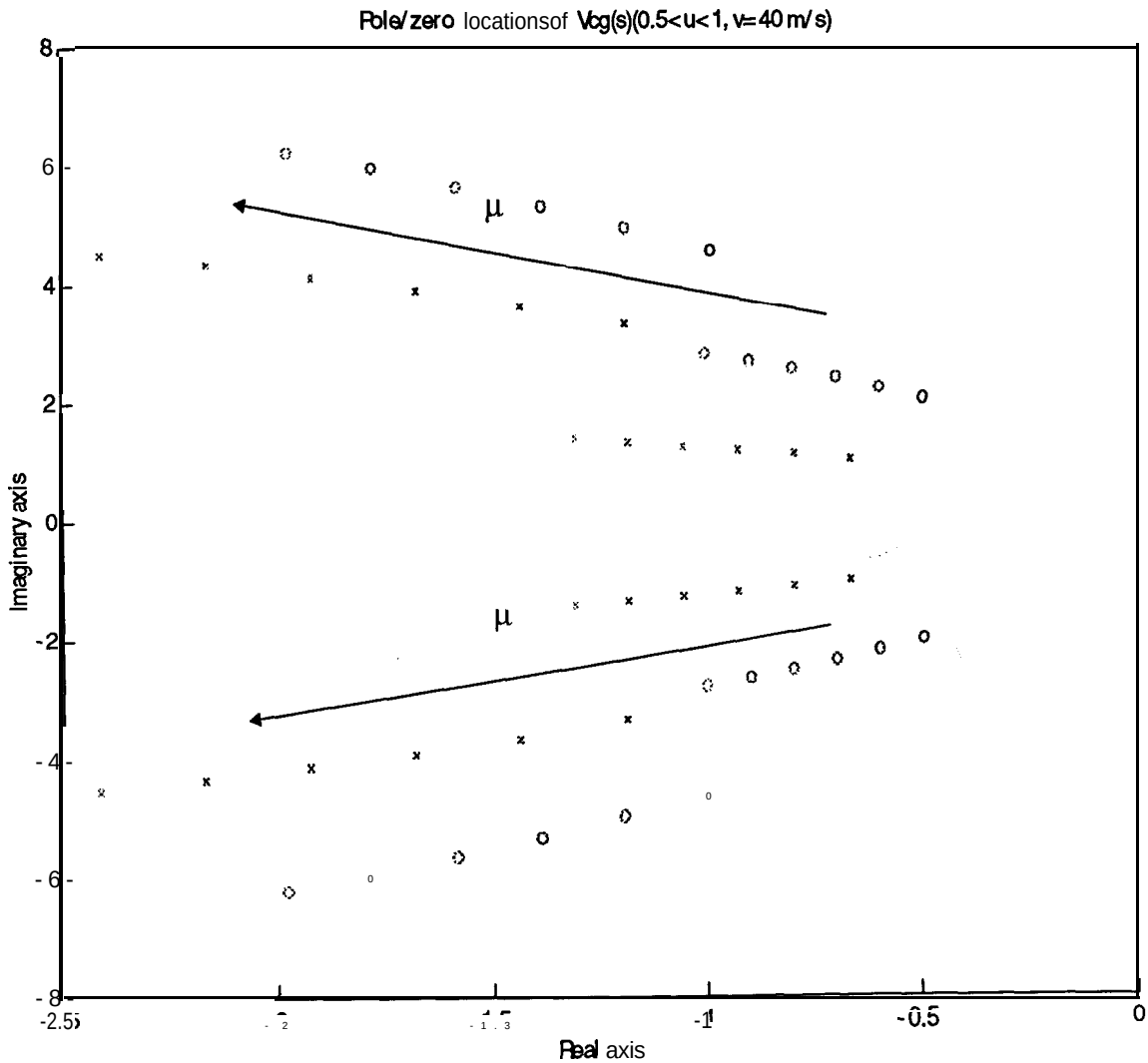

Fig. 6: Pole and zero location of $V_{CG}(s)$ for variation of road adhesion μ

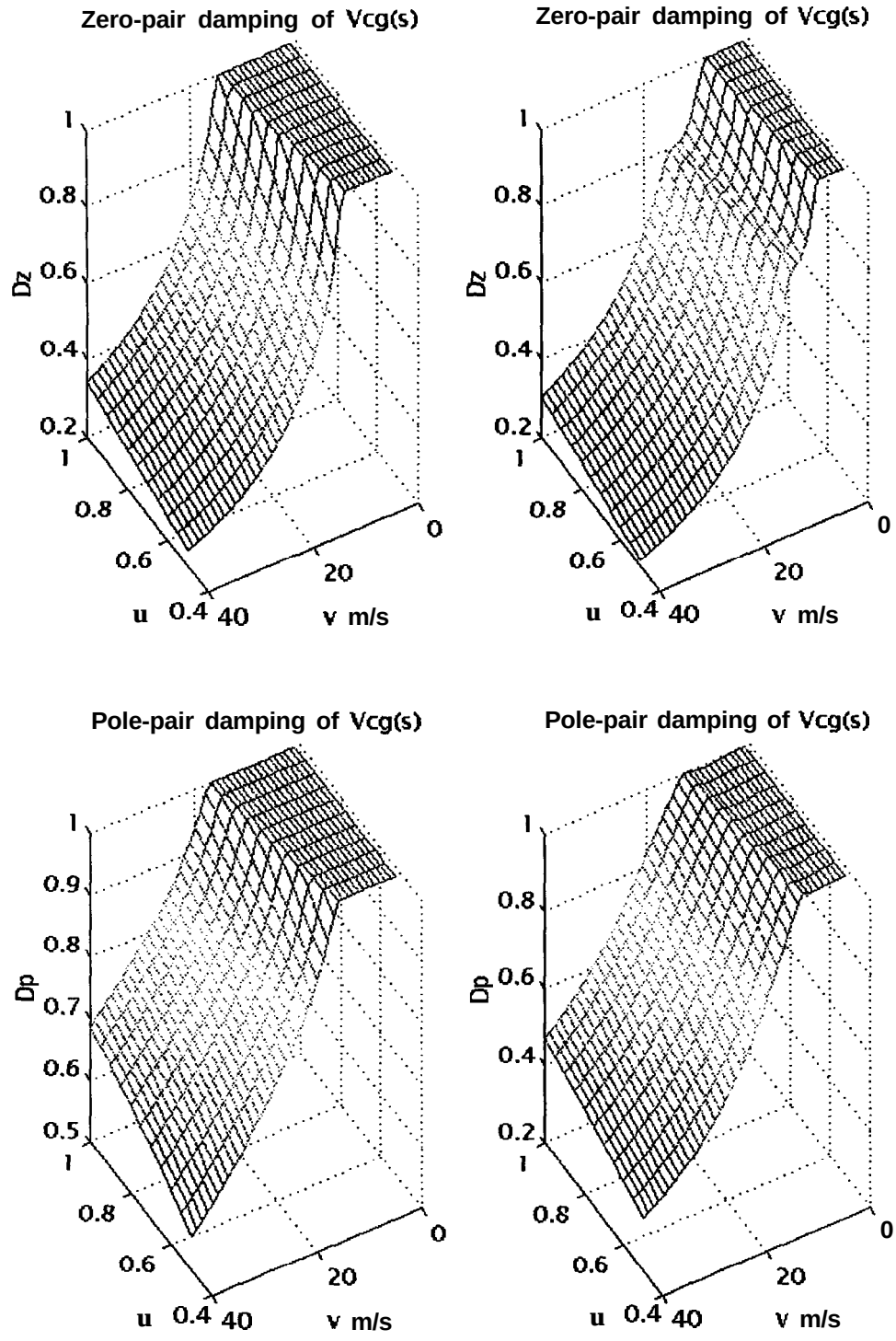

Fig. 7: Damping of the zero-pairs(upper plot) and pole-pairs(lower plot) of the lateral acceleration transfer function $V_{CG}(s)$ for varying speed v and road adhesion μ

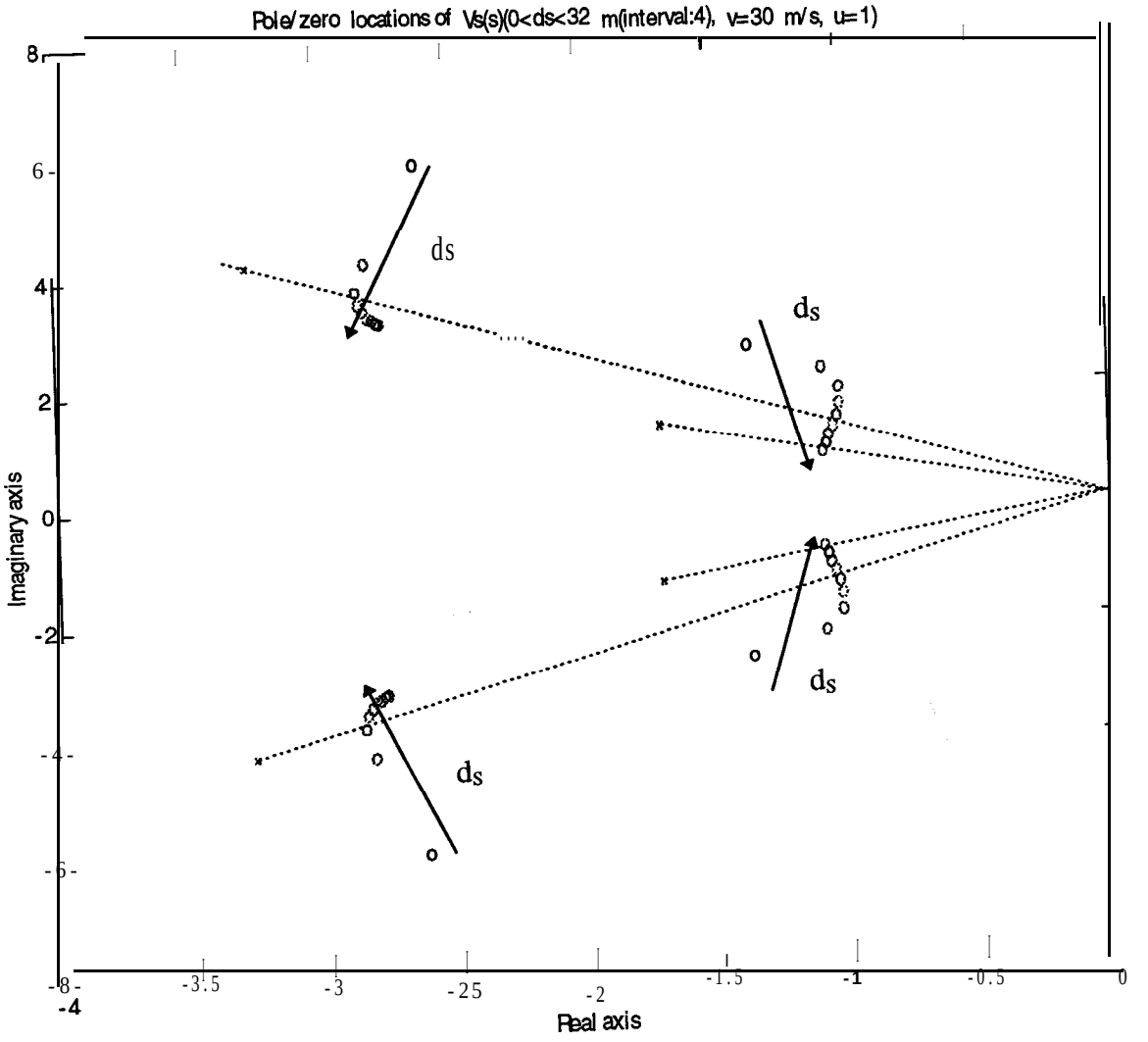

Fig. 8: Zero locations of $V_s(s)$ for variation of look-ahead distance d_s for high speed $v=30m/s$ and on good road with $\mu=1$.

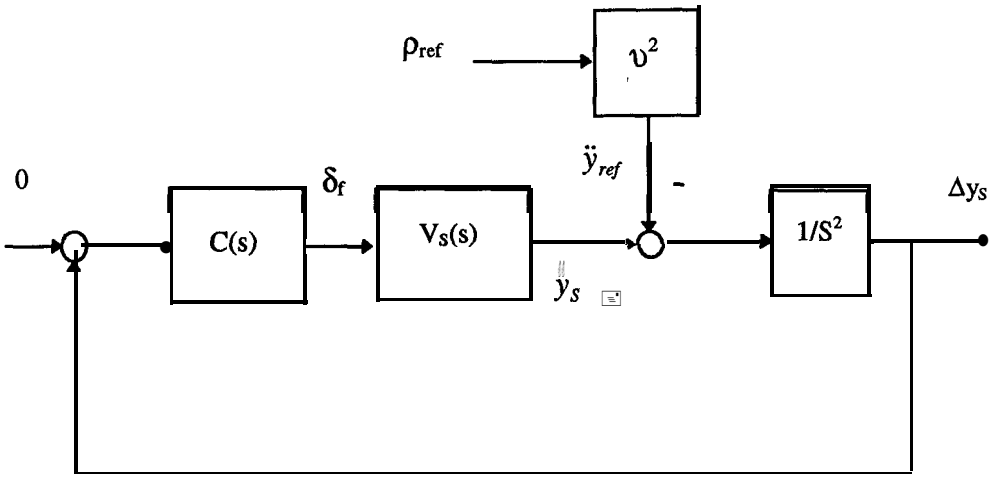

Fig. 9: Block diagram of an output feedback steering control system

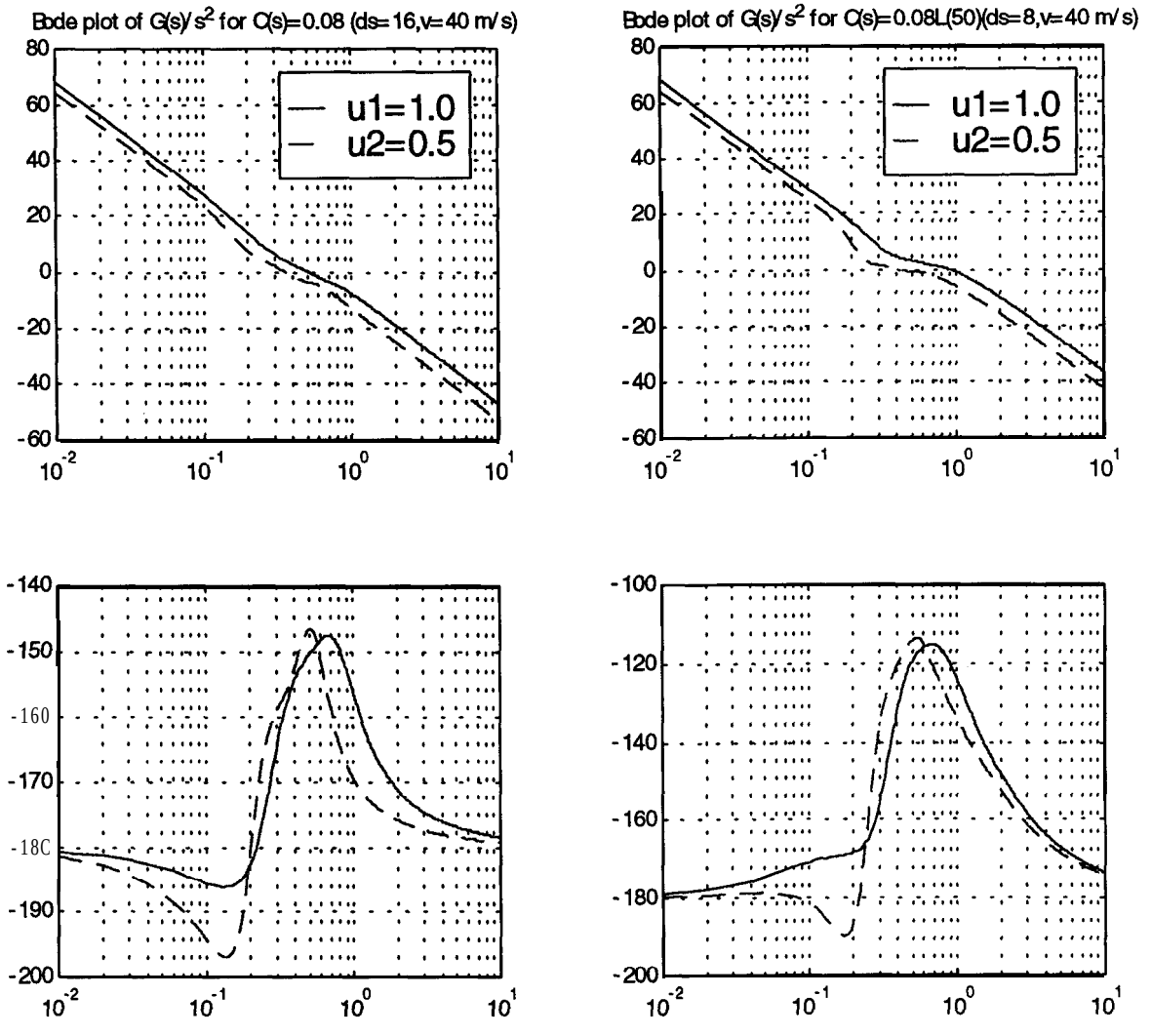

Fig. 10: Robust stabilization by vehicle phase lead with long look-ahead ds (Case I, left bode diagram) is dual to robust stabilization by a lead compensator with small look-ahead ds (Case II, right bode diagram)

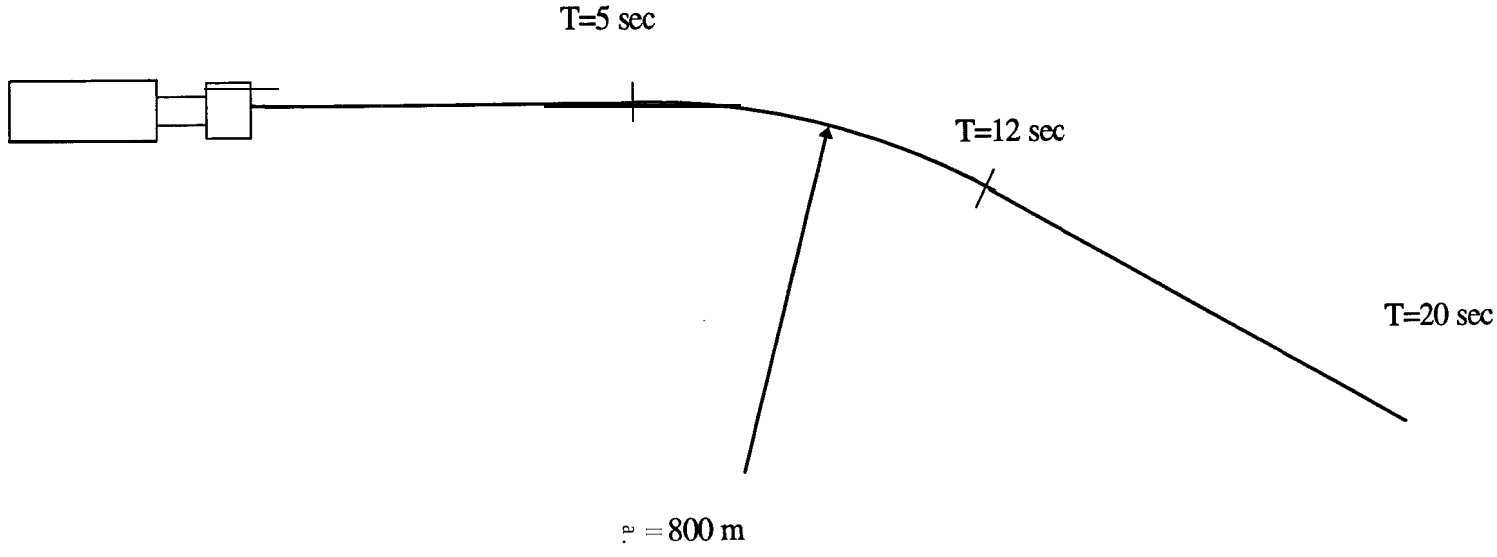

Fig. 11: The simulation scenario

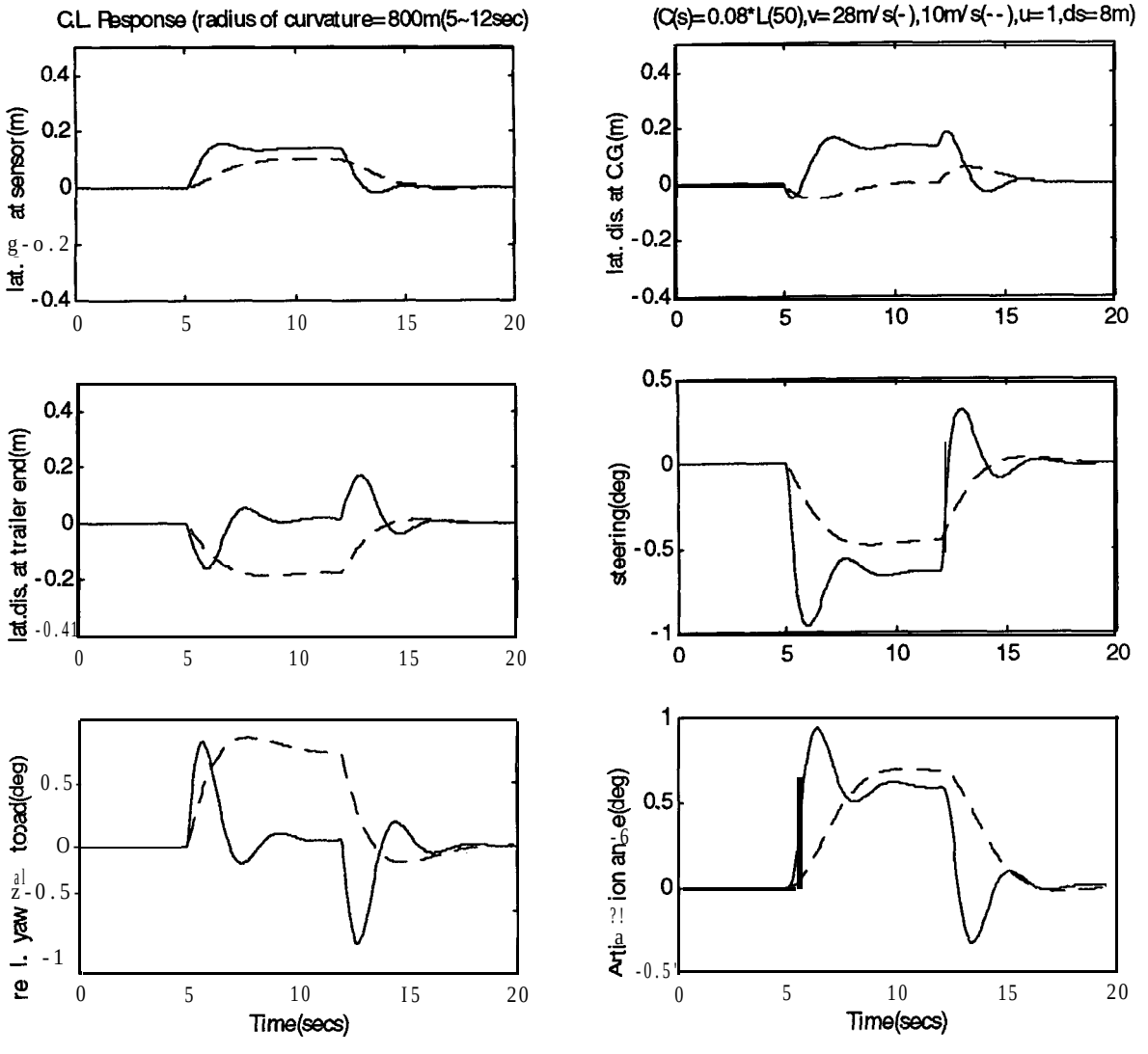

Fig. 12: Close-loop response of using the controller C(s) = $0.08\frac{0.853s + 1}{0.147s + 1}$ for radius of the road curvature **800m between** 5-12 **sec** (solid **line:v=28** m/s, dashed **line:v=10** m/s). In each case μ = 1 and d_s = Sm.

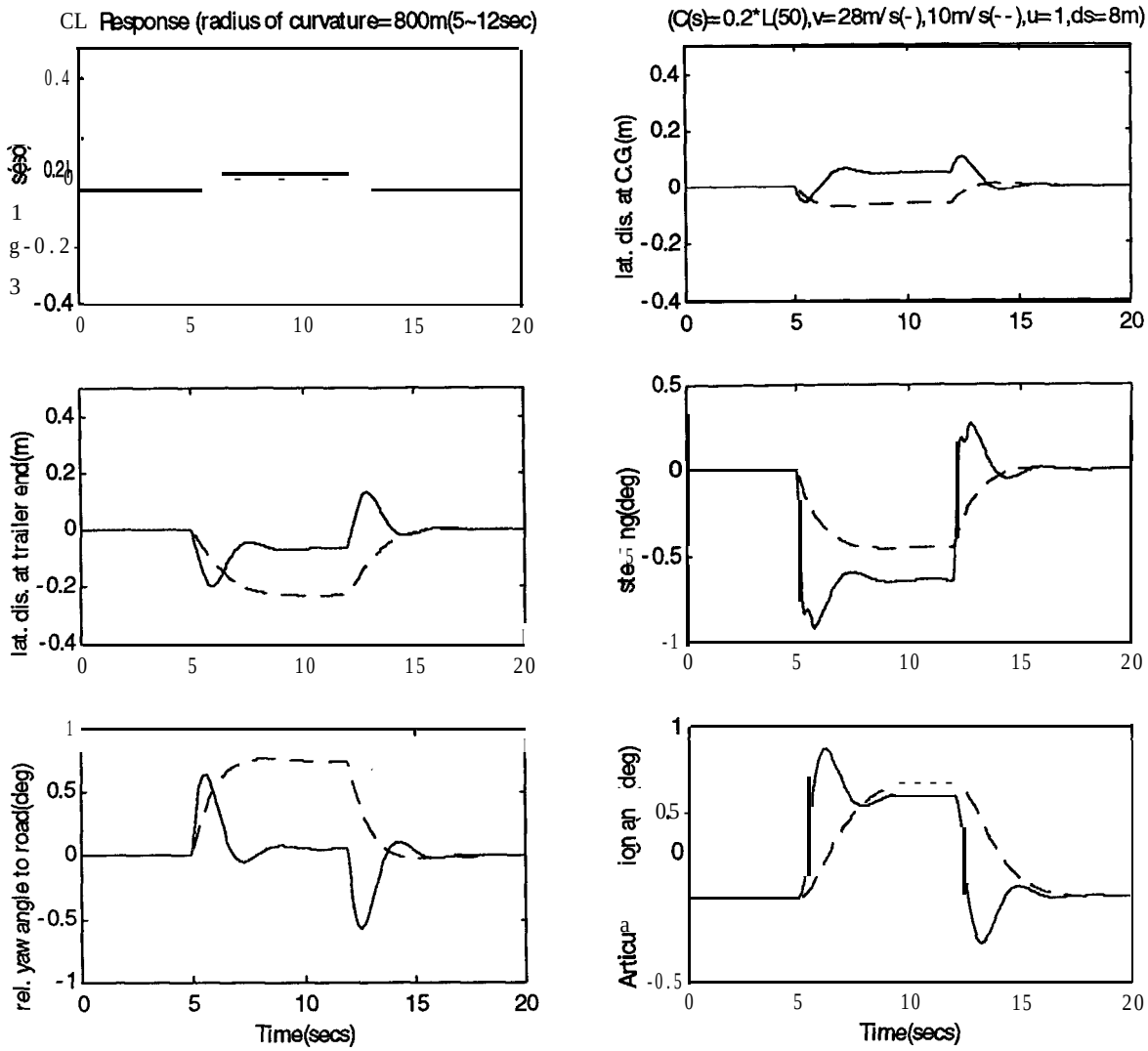

Fig. 13: Close-loop response of using the controller $C(s) = 0.2\frac{0.853s + 1}{0.147s + 1}$ for radius of the road curvature 800m between 5-12' sec (solid line:v=28 m/s, dashed line:v=10 m/s). In each case $\mu = 1$ and d_s = Sm.

3 Off-tracking in Single Unit Heavy Vehicles and Tractor Semitrailers:

3.1 Introduction

Off-tracking is the maximal difference in the trace of the vehicle wheels measured from the center of the turning radius. Off-tracking of articulated and single unit vehicles with long wheel bases have been studied for a long time. Society for Automotive Engineers (SAE) was the first to standardize the off-tracking formula (SAE Handbook, 1964). Western Highway Institute (WHI) presented new formulae for computing off-tracking and were adopted as an industry standard (WHI report, 1970). Much of this analysis was kinematic or empirical. However, off-tracking analysis from the dynamic model of the vehicles was first presented by Bernard and Vanderploeg (1984). In this report, the off-tracking is analyzed along similar lines. The dynamic model of the single unit derived in Hingwe and Tomizuka (1997) is used for off-tracking in single unit vehicles with long wheel base. Also, the dynamic model derived in Chen (1996) is used to derive the off-tracking in tractor-semitrailer vehicles. First, the dynamical equations of the linearized (simplified) model are presented. Then, a steady state constraint is imposed on this model. The relative yaw between the vehicle and the road given by imposing this constraint gives the value of off-tracking.

The rest of the report is derived in two subsections. In the first subsection the dynamic model and the steady state analysis for a single unit vehicle is presented. In the second subsection, the results are extended to tractor semitrailers.

[‡]Graduate Student Researcher Pushkar Hingwe is the principle author of this section.

3.2 Dynamic Model of Single Unit Vehicles

The dynamical equations of the single unit vehicle are given by

$$\ddot{y}_s = -\frac{(\phi_1+\phi_2)}{\dot{x}}\dot{y}_s + (\phi_1+\phi_2)\epsilon_r + \frac{\phi_1(d_s-l_1)+\phi_2(d_s+l_2)}{\dot{x}}\dot{\epsilon}_r + \frac{\phi_2 l_2 - \phi_1 l_1 - \dot{x}^2}{\dot{x}}\dot{\epsilon}_d + \phi_1\delta \tag{38}$$

$$\ddot{\epsilon}_r = -\frac{2(l_1 C_{\alpha_f} - l_2 C_{\alpha_r})}{I_z \dot{x}}\dot{y}_s - \frac{2(l_1 C_{\alpha_f} - l_2 C_{\alpha_r})}{I_z}\epsilon_r - \frac{2(C_{\alpha_f}(l_1{}^2 - l_1 d_s) + C_{\alpha_r}(l_2{}^2 + l_2 d_s))}{I_z \dot{x}}\dot{\epsilon}_r - \frac{2(C_{\alpha_f} l_1^2 + C_{\alpha_r} l_2^2)}{I_z \dot{x}}\dot{\epsilon}_d + \frac{2C_{\alpha_f} l_1}{I_z}\delta \tag{39}$$

where

$y_s =$ distance of the front end of the vehicle from the center of gravity (see Fig.14).

$\epsilon_r =$ the relative orientation of the vehicle with respect to the road.

$\dot{x} =$ Component of the velocity of the center of mass along the longitudinal principle axis m/s,

$l_1 =$ Longitudinal distance of the front axle from the center of gravity in m,

$l_2 =$ Longitudinal distance of the rear axle from the center of gravity in m,

$\delta =$ steering angle in rad.

$C_{\alpha_r} =$ Cornering stiffness of the rear tires in KN/rad,

$C_{\alpha_f} =$ Cornering stiffness of the front tires in KN/rad and

$\phi_1 = 2C_{\alpha_f}(\frac{1}{m} + \frac{l_1 d_s}{I_z})$,

$\phi_2 = 2C_{\alpha_r}(\frac{1}{m} - \frac{l_2 d_s}{I_z})$.

The pictorial representation of this model is shown in Fig. 14.

3.3 Steady operation on a curve

In this section, the steady state steering angle when the vehicle is on a curve of curvature ρ is examined. In the steady state on a curve,

- $\dot{y}_s = 0$.
- $\dot{\epsilon}_r = 0$.

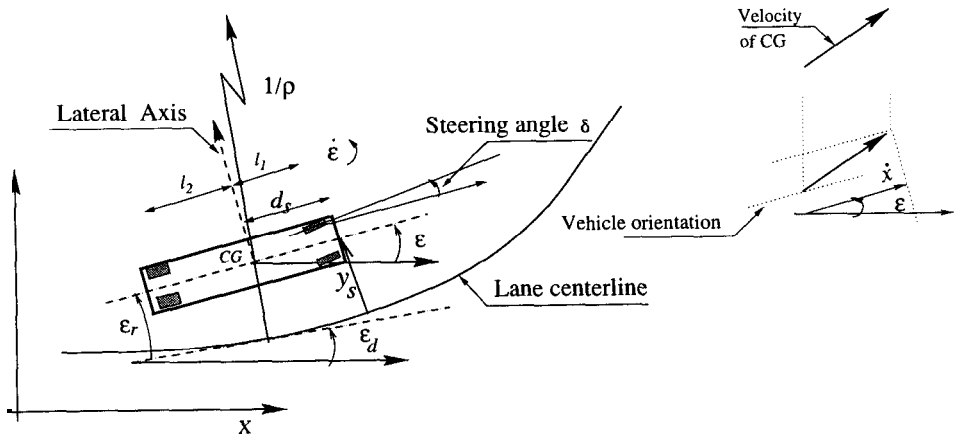

Figure 14: Geometric parameters of the bicycle model

Applying these to equations (38) and (39), we get

$$(\phi_1+\phi_2)\epsilon_r + \frac{\phi_2 l_2 - \phi_1 l_1 - \dot{x}^2}{\dot{x}}\dot{\epsilon_d} + \phi_1\delta = 0 \tag{40}$$

$$\frac{(C_{\alpha_f} l_1 - l_2 C_{\alpha_r})}{I_z}\epsilon_r - \frac{C_{\alpha_f}(l_1^2 + l_2^2 C_{\alpha_r})}{I_z \dot{x}}\dot{\epsilon_d} + \frac{l_1 C_{\alpha_f}}{I_z}\delta = 0 \tag{41}$$

Furthermore, it is assumed that $\dot{\epsilon}_d = \dot{x}\rho$. This assumption reduces equations (40) and (41) to

$$(\phi_1+\phi_2)\epsilon_r + (\phi_2 l_2 - \phi_1 l_1 - \dot{x}^2)\rho + \phi_1\delta = 0 \tag{42}$$

$$\frac{(C_{\alpha_f} l_1 - l_2 C_{\alpha_r})}{I_z}\epsilon_r - \frac{(C_{\alpha_f} l_1^2 + l_2^2 C_{\alpha_r})}{I_z}\rho + \frac{l_1 C_{\alpha_f}}{I_z}\delta = 0 \tag{43}$$

For sufficiently small longitudinal velocity,

$$\dot{x}^2 << |\phi_2 l_2 - \phi_1 l_1|$$

Therefore, the term $\dot{x}^2\rho$ in equation (42) can be neglected. Solving (42) and (43) for δ and ϵ_r, we get the steady state value of δ (given by $\overline{\delta}$) and ϵ_r (given by $\overline{\epsilon_r}$) as

$$\overline{\delta} = (l_1 + l_2)\rho$$

and

$$\overline{\epsilon_r} = -l_2\rho \tag{44}$$

If $\dot{x}$ is not assumed small, the solving equations (42) and (43) for δ and ϵ_r gives the steady state value of $\delta, (\overline{\delta})$ and $\epsilon_r, (\overline{\epsilon_r})$ as

$$\overline{\delta} = (l_1 + l_2)\rho - m\frac{(C_{\alpha_f} l_1 - l_2 C_{\alpha_r})}{C_{\alpha_f} C_{\alpha_r} (l_1 + l_2)}\dot{x}^2 \rho \tag{45}$$

and

$$\overline{\epsilon_r} = -l_2\rho + \frac{m}{C_{\alpha_r}}\frac{l_1}{(l_1 + l_2)}\dot{x}^2\rho \tag{46}$$

It can be seen that the steady state steering angle given by simplified dynamic model is a perturbation on the kinematic steering angle. It is interesting to note that as $\dot{x} \to 0$, the steady state steering angle and the relative yaw reduce to the kinematic value. Therefore it can be said that the dynamic model is a perturbation on the kinematic model. In a kinematic model, if the vehicle is to follow any planar trajectory, then the steering angle required to follow that trajectory is given by the wheel-base, $(l_1 + l_2)$, and the instantaneous curvature, ρ, at the point of interest. In a kinematic model, there are no transients. It is therefore sufficient to compare the dynamic and the kinematic model in steady state to conclude that the kinematic model is embedded in the dynamic model. This has important implication towards the control design. Controllers designed on the dynamic model of the vehicle are therefore valid for all range of the longitudinal velocities. This eliminates the need to design "kinematic controllers" at low speeds. Depending on the value of the term $m\frac{(C_{\alpha_f} l_1 - l_2 C_{\alpha_r})}{C_{\alpha_f} C_{\alpha_r} (l_1 + l_2)}\dot{x}^2$ in (45) as compared to $(l_1 + l_2)$, the dynamic component of the steering may be small or large compared to the kinematic component. In practice, for speeds less than highway speeds, the kinematic component is dominant. If a controller designed on the kinematic model is robust to the dynamic perturbation, then the controller will work for longitudinal velocities which are large.

Another usefulness of this analysis is its application in the calculation of offtracking. The relative yaw angle given by equation (44) can be directly used for this purpose. Off-tracking 0, using equation (44) is given as

$$0 = \overline{\epsilon_r}(l_1 + l_2) \tag{47}$$

For typical values of the parameters in equation (46) (see Table 2) and for the right curve of 800 m radius, Fig. 15 shows the extent of off tracking expected. For velocities

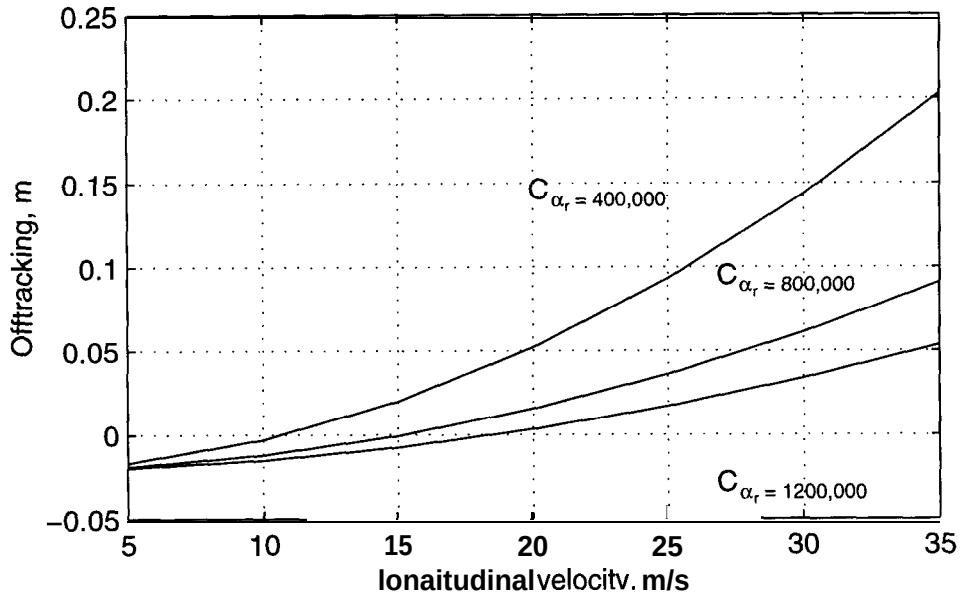

Figure 15: Offtracking value for a typical single unit heavy vehicle

higher than 20 m/s, the offtracking is greater than .5 meters for $C_{\alpha_r} = 400,000 N/rad$. Caution, however, has to be applied while judging this numerical value because it is dependent on the cornering stiffness. For vehicles with more number of tires at the rear axle, the effective cornering stiffness will increase, decreasing the offtracking as shown in Fig. 15

Similar results hold true for the tractor-semitrailer as well. In the next section, the steady state operation of a tractor semi-trailer is examined.

3.4 Dynamic Model of a Tractor-semitrailer

The dynamical equations in this section are borrowed from Chen (1997). Simplifying assumptions are stated in Chen (1997, pp. 146). Under these assumptions, the model is given by

$$M\ddot{q}_r + \Phi(q_r, \dot{q}_r, \dot{\epsilon}_d, \ddot{\epsilon}_d) = F\delta$$

Parameter symbol	Description	Value
m	Mass of the sprung mass	15,000 kg
l_1	distance between the front wheel and the center of gravity of the sprung mass	3.9 m
l_2	distance between the rear wheel and the center of gravity of the sprung mass	2.6 m
c_{α_r}	Cornering stiffness of the rear tires	400,000 to $1200,000 N/rad$
ρ	Curvature of the curve described by the center of gravity of the vehicle	$1/800$ $1/m$

Table 2: Parameters of a commercial bus

where $q_r = [y_r, \epsilon_r, \epsilon_f]^T$ gives the states of the system, $F = C_{\alpha_f}[1, l_1, 0]^T$,

$$M = \begin{bmatrix} m_1 + m_2 & -m_2(d_1 + d_3) & -m_2 d_3 \\ -m_2(d_1 + d_3) & I_{z1} + I_{z2} + m_2(d_1^2 + d_3^2) + 2m_2 d_1 d_3 & I_{z2} + m_2 d_3^2 \\ -m_2 d_3 & I_{z2} + m_2 d_3^2 + m_2 d_1 d_3 & I_{z2} + m_2 d_3^2 \end{bmatrix}$$

$$\Phi_1 = \frac{2}{\dot{x}}((C_{\alpha_f} + C_{\alpha_r} + C_{\alpha_t})(\dot{y}_r - \dot{x}_r \epsilon_r) + (l_1 C_{\alpha_f} - l_2 C_{\alpha_r} - (l_3 + d_1) C_{\alpha_t})(\dot{\epsilon}_r + \dot{\epsilon}_d)$$
$$- 2C_{\alpha_t}\epsilon_f + m_2 d_3 \sin \epsilon_f \text{ (i,. } + \dot{\epsilon}_d + \dot{\epsilon}_f)^2 + (m_1 + m_2)\dot{x}\dot{\epsilon}_d - m_2(d_1 + d_3 \cos \epsilon_f)\ddot{\epsilon}_d$$

$$\Phi_2 = \frac{2}{\dot{x}}((l_1 C_{\alpha_f} - l_2 C_{\alpha_r} - (l_3 + d_1) C_{\alpha_t})(\dot{y}_r - \dot{x}_r \epsilon_r)$$
$$+ (l_1^2 C_{\alpha_f} + l_2^2 C_{\alpha_r} + (l_3 + d_1)^2 C_{\alpha_t})(\dot{\epsilon}_r + \dot{\epsilon}_d)$$
$$+ l_3(l_3 + d_1) C_{\alpha_t}\dot{\epsilon}_f) + 2(l_3 + d_1) C_{\alpha_t}\epsilon_f - m_2 d_3 \sin \epsilon_f (\dot{y}_r - \dot{x}_r \epsilon_r)(\dot{\epsilon}_r + \dot{\epsilon}_d)$$
$$- 2m_2 d_1 d_3 \sin \epsilon_f (\dot{\epsilon}_r + \dot{\epsilon}_d)\dot{\epsilon}_f - m_2 d_1 d_3 \sin \epsilon_f \dot{\epsilon}_f^2 - m_2(d_1 + d_3 \cos \epsilon_f)\dot{x}\dot{\epsilon}_d$$
$$+ (I_{z1} + I_{z2} + m_2 d_1^2 + m_2 d_3^2 + 2m_2 d_1 d_3 \cos \epsilon_f)\ddot{\epsilon}_d$$

$$\Phi_3 = \frac{2}{\dot{x}}(-l_3 C_{\alpha_t}(\dot{y}_r - \dot{x}\epsilon_r) + l_3(l_3 + d_1) C_{\alpha_t}(\dot{\epsilon}_r + id) + l_3^2 C_{\alpha_t}\dot{\epsilon}_f)$$
$$+ m_2 d_3 \sin \epsilon_f (\dot{\epsilon}_r + \dot{\epsilon}_d)^2 + 2l_3 C_{\alpha_t}\epsilon_f - m_2 d_3 \sin \epsilon_f (\dot{y}_r - \dot{x}\epsilon_r)((\dot{\epsilon}_r + id)$$
$$- m_2 d_3 \cos \epsilon_f \dot{x}\dot{\epsilon}_d + (I_{z2} + m_2 d_3^2 + m_2 d_1 d_3 \cos \epsilon_f)\ddot{\epsilon}_d \qquad (48)$$

Various states and parameters associated with the tractor-semitrailer model are given

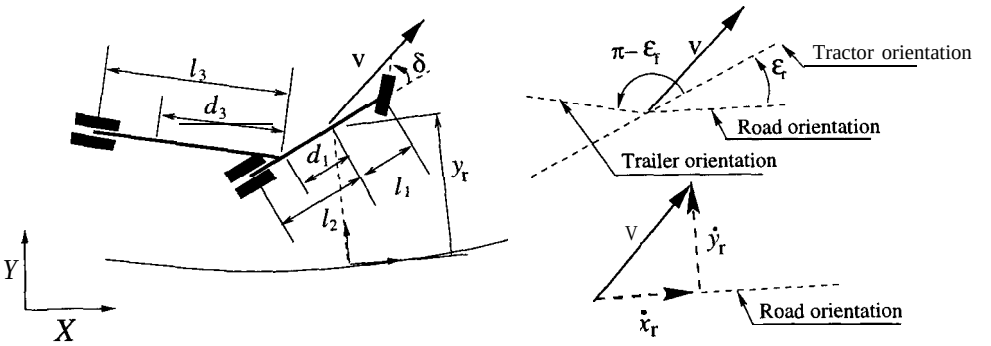

Figure 16: States and geometric parameters of the tractor-semitrailer model

in Fig.16. m_1 and m_2 are the mass of the tractor and the mass of semitrailer respectively. I_{z1} and I_{z2} are the moments of inertia of the tractor and the semitrailer respectively. C_{α_f},C_{α_r} and C_{α_t} are the cornering stiffnesses of the front tires of the tractor, rear tires of the tractor and tires of the trailer respectively. The steady state behavior of this model on a curve of curvature ρ is now examined.

3.5 Steady operation on a curve

In steady state on a curve of curvature p, $\dot{y}_r = 0$, $\dot{\epsilon}_r = 0$, $\dot{\epsilon}_f = 0$ and $\dot{\epsilon}_d \approx \dot{x}_r\rho \approx \dot{x}\rho$. After neglecting higher order terms involving the relative yaw and the square of the road yaw rate, the simplified dynamic model at steady state on a curve is given by

$$\begin{bmatrix} (C_{\alpha_f} + C_{\alpha_r} + C_{\alpha_t}) & C_{\alpha_t} & l_1C_{\alpha_t} \\ (l_1C_{\alpha_f} - l_2C_{\alpha_r} - (l_3 + d_1)C_{\alpha_t}) & -(l_3 + d_1)C_{\alpha_t} & l_1C_{\alpha_t} \\ l_3C_{\alpha_t} & l_3C_{\alpha_t} & 0 \end{bmatrix} \begin{bmatrix} \epsilon_r \\ \epsilon_f \\ \delta \end{bmatrix} = \begin{bmatrix} (l_1C_{\alpha_f} - l_2C_{\alpha_r} - (l_3 + d_1)C_{\alpha_t})\rho + (m_1 + m_2)\dot{x}^2\rho \\ (l_1^2C_{\alpha_f} + l_2^2C_{\alpha_r} + (l_3 + d_1)^2C_{\alpha_t})\rho - m_2(d_1 + d_3)\dot{x}^2\rho \\ -l_3(l_3 + d_1)C_{\alpha_t}\rho + m_2d_3\dot{x}^2\rho \end{bmatrix} \quad (49)$$

The solution to the equation (49) gives the steady state values of ϵ_r,ϵ_f and δ. Let these be represented by $\bar{\epsilon}_r$, $\bar{\epsilon}_f$ and $\bar{\delta}$ respectively. After some algebra, we get

$$\bar{\epsilon}_r = -l_2\rho + \frac{m_1}{C_{\alpha_r}}\frac{l_1}{(l_1 + l_2)}\dot{x}^2\rho \quad (50)$$

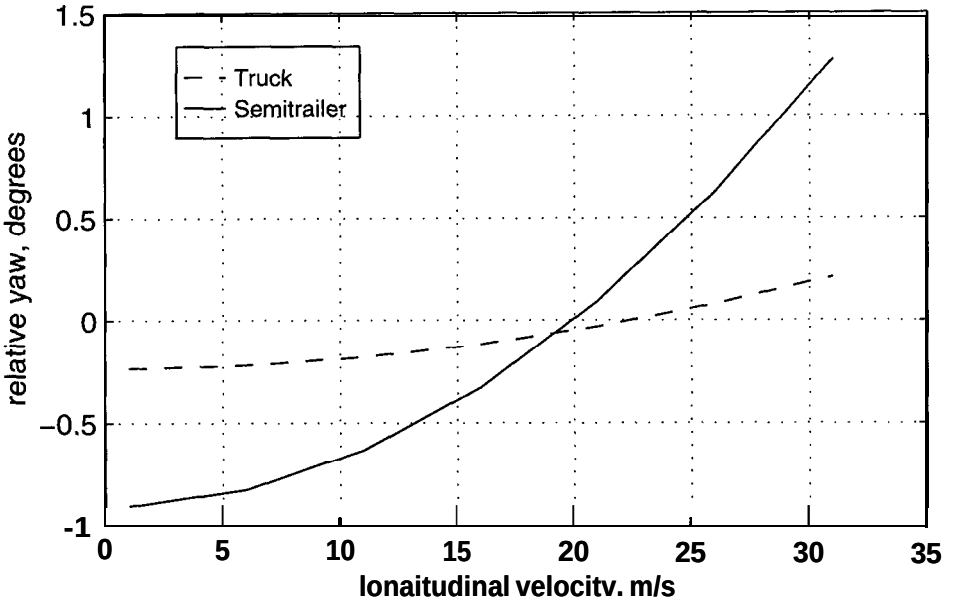

Figure 17: Relative yaw of the tractor and the semitrailer

as the steady steady-state yaw of the tractor relative to the road. The relative yaw of the trailer with respect to the road is given by $\epsilon_r + \epsilon_f$. The steady state value of the yaw of the trailer relative to the road is given by

$$\bar{\epsilon}_r + \bar{\epsilon}_f = -(l_3 + d_1)\rho + \frac{m_2}{C_{\alpha_t}} \frac{d_3}{l_3} \dot{x}^2 p \tag{51}$$

For parameter values of tractor semitrailer given Table 1, Fig. 17 shows the relative yaw of the tractor and the trailer with respective to the road. The curve has a positiveradius of 800 m, i.e., $\dot{\epsilon}_d$ is positive for positive longitudinal velocity $\dot{x}$. Note that for small velocities, the tractor and trailer are inside the curve. For high velocities, however, the tractor and the trailer get flung towards the outside.

The second part of the steady state analysis is the steering angle. The steering angle necessary to achieve steady state on the curve is given by

$$\begin{aligned} \bar{\delta} &= (l_1 + l_2)\rho \\ &+ m_1 \left[\frac{C_{\alpha_r} l_2 - C_{\alpha_f} l_1}{C_{\alpha_f} C_{\alpha_r} (l_1 + l_2)} \right] \dot{x}^2 \rho \\ &+ m_2 \frac{(l_3 - d_3)}{l_3} \left[\frac{C_{\alpha_r} (d_1 + l_2) - C_{\alpha_f} (l_1 - d_1)}{C_{\alpha_r} C_{\alpha_f} (l_1 + l_2)} \right] \dot{x}^2 \rho \end{aligned} \tag{52}$$

From (52), it can be seen that the steering angle required for negotiating a curve of curvature ρ is a sum of a kinematic component $((l_1 + l_2)\rho)$ and a dynamic component (the coefficient of $\dot{x}^2$ in (52)). It is interesting that the kinematic component of the steady state steering angle required by a tractor-semitrailer is the same as the kinematic component of the steady state steering angle required by a single unit vehicle. Moreover, the dynamic perturbation of the steering angle has two separate components. The term $m_1 \left[\frac{C_{\alpha_r} l_2 - C_{\alpha_f} l_1}{C_{\alpha_f} C_{\alpha_r} (l_1+l_2)}\right] \dot{x}^2 \rho$ is a function of the parameters of the tractor and is the same as the dynamic component of the steady state steering angle of a single unit vehicle. The second term $m_2 \frac{(l_3 - d_3)}{l_3} \left[\frac{C_{\alpha_r}(d_1+l_2) - C_{\alpha_f}(l_1-d_1)}{C_{\alpha_r} C_{\alpha_f} (l_1+l_2)}\right] \dot{x}^2 \rho$ is dependent only on the trailer mass and on the tractor and the trailer parameters. The relative yaw of the trailer is similarly dependent only on the trailer parameters. Another interesting observation is that the steady state relative *yaw* of the tractor given by (50) is the same as that of a single unit vehicle. It is not influenced by the presence of the trailer. As in the case of single unit vehicles, in the limit $\dot{x} \to 0$, the steering angle and the relative yaw angles of the tractor and the semitrailer approach the kinematic values.

Off-tracking analysis of the tractor semitrailer utilizes (50) and (51). The off-tracking, O, is given by

$$O = \bar{\epsilon}_r (l_1 + d_1) + (\bar{\epsilon}_r + \bar{\epsilon}_f) l_3 \tag{53}$$

In Fig. 19, this value corresponds to O_f + 0,. It is clear that for long vehicles, this does not give the difference betwen the inner tire trace and the outer tire trace. In such cases the offtracking is given by $Q_f + Q_r$. Because the road geometry is known, this value is computable. The offtracking values for the vehicle parameters given in Chen (1996) are shown in Fig.18

3.6 Summary

In the limit $\dot{x} \to 0$, the steady state value of the steering angle is exactly the same as given by a kinematic model of the vehicle. Thus, we can conclude that the behavior of the dynamical model approaches the kinematic model in the limit $\dot{x} \to 0$. It is, then, of interest to treat the dynamical model as a perturbation on the kinematic model. The

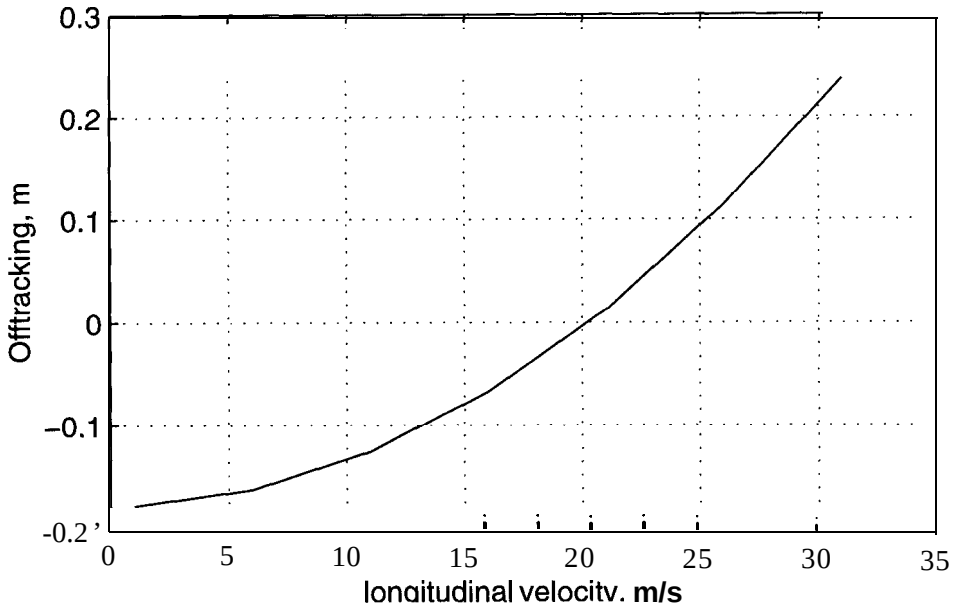

Figure 18: Offtracking value for a tractor semitrailer

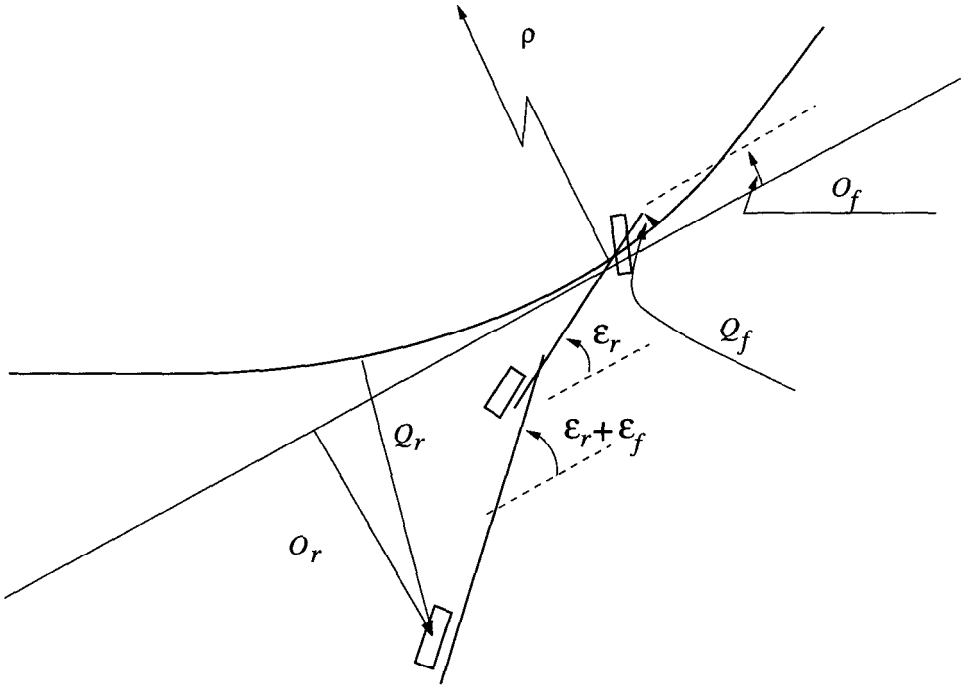

Figure 19: Offtracking scenario for a tractor semitrailer

stability of control algorithms that are designed for a kinematic model can then be verified for robustness to such perturbations. Alternately, the expressions for steady state relative yaw and the steering angle of a single-unit vehicle can be utilized to compensate the steering angle given by a kinematic design for the perturbations due to dynamical terms. Similar conclusion can be made from the analysis of the steady state behavior of the dynamical model of tractor-semitrailer. What is interesting to note is that the tractor's yaw relative to the road is the same as the relative yaw of a single unit vehicle. The steering angle required by the truck-semitrailer differs from the steering angle required by the single-unit vehicle by a term dependent on the mass of the trailer.

The control implications of the steady state results of this report are

- The yaw error E,. is not zero in general while negotiating a curve. Therefore, it will be unrealistic for the controller to demand that the yaw error go to zero.
- Significant portion of the steering effort is kinematic and this term is independent of the cornering stiffness or the vehicle velocity.
- Non zero yaw error is the source of steady state off-tracking. The expressions derived in this report can be used to compensate for the off-tracking.

4 Dynamic Modeling of Multi-Unit Heavy Vehicle†

4.1 Introduction

A commercial heavy duty vehicle combination (road train) is defined as a tractor unit and an arbitrary number of trailers. The most commonly used types of trains are: tractor-semitrailer (two unit), truck-trailer (three units) and tractor-semitrailer-semitrailer (doubles, four units). Economic considerations result in a very wide application of articulated vehicles currently. Considering the ever increasing density of highway traffic and the relatively high average transport velocities, the safety of commercial vehicle combinations should be considered an important subject.

A good deal of the safety of road vehicles depends on their dynamic performance. Vehicle dynamic performance has been investigated taking into consideration the following features: directional performance (Bernard, 1971), roll dynamics (Dugoff et al., 1967, Ervin et al., 1979, Gillespie et al., 1978, Kemp et al., 1978), braking performance and combined directional and braking performance (Adams et al., 1977, Ellis et al. 1976, Lam et al. 1979, North et al., 1967). Some experimental results (Eshleman et al. 1973, Genbom et al., 1977, Winkeler et al., 1978) are also reported.

The lateral dynamics of road trains is more involved than single unit vehicles because of the increased number of interacting units. The resulting mathematical model, simulations and experiments are more complex. For example, road trains exhibit features such as jackknifing (Keller, 1973, Walsh et al., 1973, Susemihl et al. 1974, Mikulcik, 1968), trailer swing and trailer lateral oscillation (Segel, 1958) that are not part of the dynamics of single unit. At high vehicle velocity, articulated vehicles tend to have pronounced yaw causing large amplitudes of trailer oscillations. The truck-trailer combination is more prone to lateral oscillations than is the tractor-semitrailer units.

There are mainly two types of dynamic models associated with Heavy Duty Vehicle (HDV) that appear. Mikulcik (1968), using Newtonian mechanics, derived the most

† Graduate student researcher Meihua Tai is the principle author of this section.

complete complex model for tractor-semitrailer. In his model, the tractor and semitrailer are three dimensional objects and both are allowed to translate, pitch, yaw and roll except as constrained by a fifth-wheel type hitch. A linear model is then derived under small angle assumptions on roll, pitch and yaw motions. On the other hand, Chen (1996), used Lagrangian mechanics to derive a five degree of freedom (translational motion, yaw motions of the tractor and semitrailer, and roll motion of the tractor) complex model for the tractor-semitrailer. The use of Lagrangian method eliminated all holonomic constraint forces between tractor and semitrailer. Furthermore, a linear and nonlinear simplified model is derived by ignoring the tractor roll dynamics and assuming a constant longitudinal velocity.

Recently, X. Tong, B. Tabarrok and M. El-Gindy (1995) derived a computer simulation model for different axel configurations of Canadian logging trucks (tractor-semitrailer type) taking into account the effect of different hitching methods between the leading unit and the trailing unit. The model not only considered the pitch and roll motions of the sprung mass but also the roll and bounce motions of the unsprung mass (wheels and axels). Subhash Rakheha, et al., (1995) studied the infulence of articulation damping on the yaw and lateral dynamics of tractor-semitrailer. A kinematics analysis of the dampers, mounted externally to the articulation mechanisim is performed to derive the lateral damping forces and yaw damping moments acting on the sprung masses. The equations of motion of a tractor-semitrailer model are incorporated with the nonlinear force characteristics of tyres and articulation damper.

Most of the literature in analytical modeling of the road trains has addressed two units vehicles only. Therefore, the development of the dynamic model of a general multi-unit road train becomes important. This part of the report presents a method of deriving complex simulation model and simplified control model of a general class of multi-unit HDV system. In the complex model, all units are three dimensional free bodies and are allowed to have translational motions and three rotational motions except as constrained by different types of hitching mechanisms. In the simple model, only the translational motion and the yaw motions of each unit are considered. Considering the roles of these models, the scope of information expected from each

model, the range of dynamic characteristics taken into account and the relative ease of derivation, we apply different methods to derive part or all of the dynamic equations of each model. A method employing Newtonian mechanics is applied to the derivation of the complex model. All of the constraint forces and constraint moments are obtained. In the derivation of the simplified control model, we apply the Newtonian method to the translational motion of the whole system and the Lagrangian method to the yaw motion of each unit. In both cases, internal constraint forces do not appear in the dynamic equations. The analytical expression of the model thus obtained is directly useful for control design.

4.2 Nomenclature

Note: Superscript of the capital letter means the index of the unit; superscript of the lower case letter indicates the power of the quantity; the index **of** *the* **lower** *case* **letter** *is shown in subscript*

4.2.1 Vehicle Parameters

Vehicle parameters used in this report are defined below. For further clarification, see Fig. 20

M_i: Mass of the i^{th} unit

$I^i_{xx}, I^i_{yy}, I^i_{zz}$: Inertia tensor components of the i^{th} unit

l_{fi}: Distance from the center of gravity of the i^{th} unit to the front wheel of the i^{th} unit; if there is no front wheel, then set to zero

l_{ri}: Distance from the center of gravity to the rear wheel

d_{fi}: Distance from the center of gravity to the front joint; for i = 0 (tractor), set to zero

d_{ri}: Distance from the center of gravity to the rear joint; for $i = N$ (the last unit), set to zero

Z^i_{cg}: Height of the center of gravity from ground

Z^i_f: Height of the front suspension from ground

Z^i_r: Height of the rear suspension from ground

C_f^i: Height of the front articulation joint from ground

C_r^i: Height of the rear articulation joint from ground

T_{wf}^i: Front wheel width

T_{wr}^i: Rear wheel width

p_i: Longitudinal coordinate of the i^{th} unit pitch center from the center of gravity of the i^{th} unit

r_i: Vertical coordinate of the i^{th} unit roll center from the center of gravity of the i^{th} unit

N_f^i: Number of wheels in each side of the front axle

N_r^i: Number of wheels in each side of the rear axle

$K1_f^i, K2_f^i, D1_f^i, D2_f^i, LIM_f^i$: Front suspension coefficients

$K1_r^i, K2_r^i, D1_r^i, D2_r^i, LIM_r^i$: Rear suspension coefficients

I_{wf}^i: Front wheel inertia

I_{wr}^i: Rear wheel inertia

R_{wf}^i: Front wheel radius

R_{wr}^i: Rear wheel radius

K_{zf}^i, K_{zr}^i: Front and rear wheel vertical stiffness coefficients

$MD_f^i, GD_f^i, SN40_f^i$: Front wheel and road interaction coefficients

$MD_r^i, GD_r^i, SN40_r^i$: Rear wheel and road interaction coefficients

$C_{\alpha f}^i, C_{\alpha r}^i$: Front and rear wheel cornering stiffness

C_{sf}^i, C_{sr}^i: Front and rear wheel longitudinal stiffness

α_{if}: Front wheel slip angle

a;,: Rear wheel slip angle

λ_{if}: Front wheel slip ratio

λ_{ir}: Rear wheel slip ratio

K_{yaw}^i: Spring coefficient of the fifth wheel connection between the (i $-1)^{th}$ unit and the i^{th} unit

D_{yaw}^i: Damping coefficient of the fifth wheel connection between the (i $-1)^{th}$ unit and the i^{th} unit

C_{yaw}^i: Coulomb friction coefficient of the fifth wheel connection between the (i $-1)^{th}$

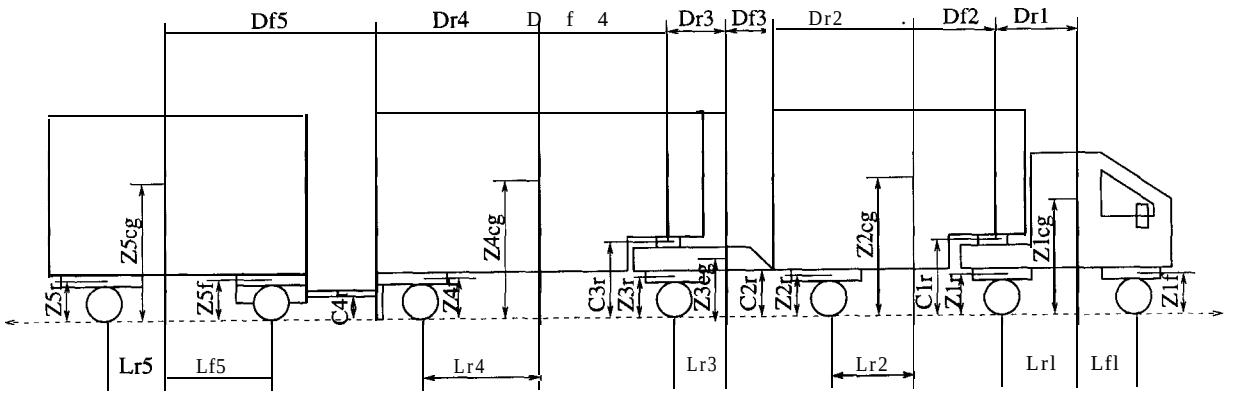

Figure 20: Typical Heavy Duty Vehicle Configuration

unit and the i^{th} unit

4.2.2 Kinematic Quantities

$T_{1\to 2}$: Transformation matrix from coordinate system 1 to coordinate system 2

ϕ_i: Roll angle of the i^{th} unit about the x axis of its sprung mass coordinate system (S_i-frame)

θ_i: Pitch angle of the i^{th} unit about the y axis of its sprung mass coordinate system

ϵ_i: Yaw angle of the i^{th} unit about the z axis of its unsprung mass coordinate system (U_i-frame)

θ_{pi}: Pitch angle of the i^{th} unit about the y axis of its previous unit sprung mass coordinate system (S_{i-1}-frame), it is an actual pitch motion of the fifth wheel connecting the i^{th} unit to the (i $-1)^{th}$ unit

$\dot{\phi}_i, \dot{\theta}_i, \dot{\epsilon}_i, \dot{\theta}_{pi}$: Roll rate, pitch rate, yaw rate and actual pitch rate

$\ddot{\phi}_i, \ddot{\theta}_i, \ddot{\epsilon}_i, \ddot{\theta}_{pi}$: Accelerations of roll, pitch, yaw and actual pitch motions

v_x: Tractor unsprung mass longitudinal velocity in U_1-frame

$\dot{v}_x$: Time derivative of v_x

v_y: Tractor unsprung mass lateral velocity in U_1-frame

$\dot{v}_y$: Time derivative of v_y

x_n, y_n: Tractor unsprung mass displacements in the x and y direction of the fixed in-

ertial coordinate system(n-frame)

$x_n, \dot{y}_n$: Tractor unsprung mass velocities in the x and y direction of the fixed inertial coordinate system

$\ddot{x}_n, \ddot{y}_n$: Tractor unsprung mass accelerations in the x and y direction of the fixed inertial coordinate system

$\vec{v}_{ui}$: Velocity of the U_i-frame

$\vec{a}_{ui}$: Acceleration of the U_i-frame

$\vec{v}_i$: Velocity of the center of mass of the i^{th} unit

$\vec{a}_i$: Acceleration of the center of mass of the i^{th} unit

$\vec{\omega}_{ui}$: Angular velocity vector of the unsprung mass frame of the i^{th} unit

$\dot{\vec{\omega}}_{ui}$: Angular acceleration vector of the unsprung mass frame of the i^{th} unit

$\vec{\omega}_{si}$: Angular velocity vector of sprung mass frame of the i^{th} unit. From the definition of the sprung mass frame, it is the angular velocity of the i^{th} unit

$\dot{\vec{\omega}}_{si}$: Angular acceleration vector of the sprung mass frame of the i^{th} unit. From the definition of the sprung mass frame, it is the angular acceleration of the i^{th} unit

$\vec{\omega}_{si/ui}$: Angular velocity of the sprung mass frame of the i^{th} unit relative to the unsprung mass frame of the i^{th} frame

4.3 Coordinate Systems and Description of the Motion

In order to facilitate the description of the dynamics of heavy duty vehicle systems, several different Cartesian coordinate systems are used in the modeling process. As shown in Fig. 21, we define an unsprung mass coordinate system(U_i-frame) and a sprung mass coordinate system(S;-frame) for each unit. The S_i-frame is attached to and moves with the (i^{th} unit) rigid body. The center of gravity (C.G.) is defined as the origin. The longitudinal, lateral and vertical axes of the body are naturally defined as the x, y and z axes respectively. The positive x axis points towards the front, and the positive y axis to the left, the positive z axis points upward. So, the motion of the S_i frame describes the motion of the i^{th} unit of a HDV system. The U_i-frame is also a moving coordinate system and is defined as the projection of the S_i-frame on the road

surface in its static equilibrium state. The static equilibrium state of the S_i-frame is defined to be the stand still state with no roll, pitch or bounce motion. As defined, the U_i-frame has only planar translational motion and yaw motion about the z axis. Now, we define an inertial coordinate system, n-frame. This frame is fixed with respect to the ground. The yaw angle(ϵ_i) of each unit is measured from the x axis of the n-frame to the x axis of the U_i-frame.

The motion of each unit of a HDV system can be considered to be the addition of the motion of U_i-frame relative to n-frame and the motion of S_i-frame relative to Q-frame. U_i-frame has planar translational motion and yaw motion (ii) relative to n-frame, and S_i-frame has bounce(i), roll($) and pitch$(\dot{\theta})$ motions relative to U_i-frame. Both roll and pitch motions are considered to be small. For the uniformity of the the treatment of each unit and clarity of description, all the above mentioned notational motions are nominal, that is, the rotational angles are measured about the sprung mass or unsprung mass coordinate axes. Due to the holonomic constraints, the actual rotations do not happen about the unsprung mass frame axes or about the sprung mass axes. The relationship between the nominal rotational motions and the actual rotational motions are investigated in section 4.5.

In theory, the dynamic equations can be expressed in any coordinate system and can be transformed into any other coordinate system through coordinate transformations, In practice, there is usually a coordinate system in which the dynamic equations are simple but may have apparently stronger physical interpretation in another coordinate system. Also in some coordiante system, the control design task may be convenient. All these considerations necessitate the utilization of coordinate transformation between two different coordinate systems.

Let T denote 3 x 3 coordinate transformation matrix between two different frames. Then, the coordinate transformations between unsprung mass frame U_i and the inertial

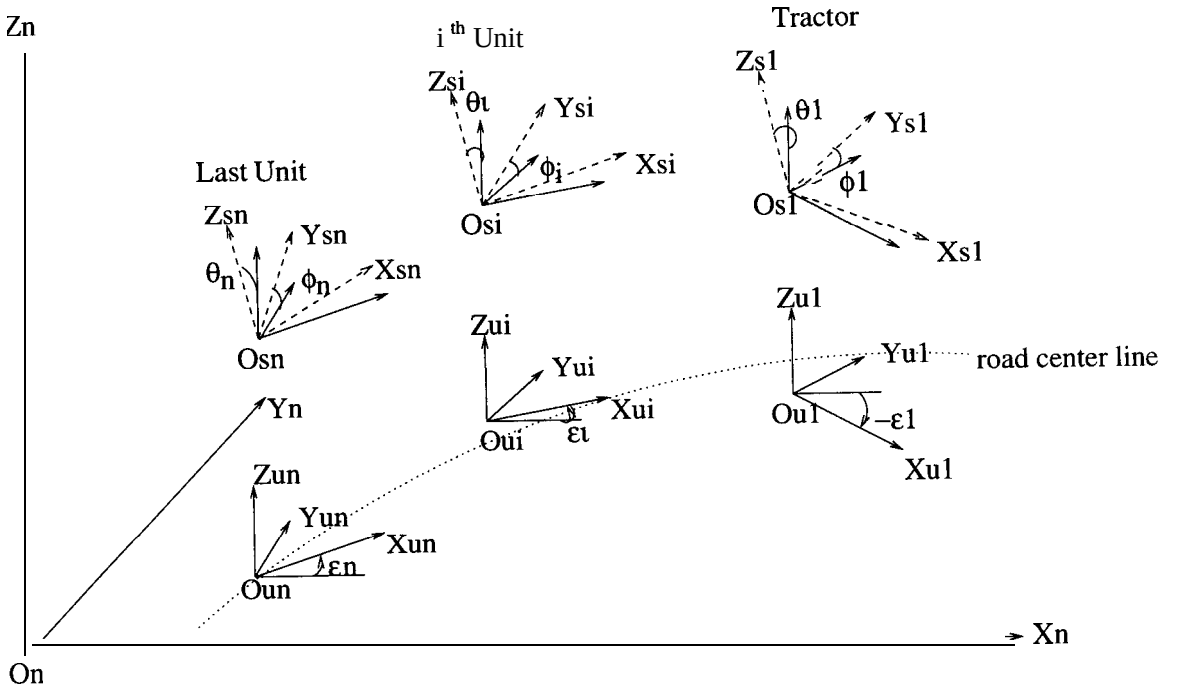

Figure 21: Different Coordinate Frames

n-frame are:

$$T_{n\leftarrow ui} = \begin{bmatrix} \cos\epsilon_i & -\sin\epsilon_i & 0 \\ \sin\epsilon_i & \cos\epsilon_i & 0 \\ 0 & 0 & 1 \end{bmatrix}$$

$$T_{ui\leftarrow n} = \begin{bmatrix} \cos\epsilon_i & \sin\epsilon_i & 0 \\ -\sin\epsilon_i & \cos\epsilon_i & 0 \\ 0 & 0 & 1 \end{bmatrix} \tag{54}$$

The coordinate transformations between two unsprung mass frames, namely U_i-frame

and U_j-frame are:

$$T_{ui\leftarrow uj} = \begin{bmatrix} \cos(\epsilon_{uj} - \epsilon_{ui}) & -\sin(\epsilon_{uj} - \epsilon_{ui}) & 0 \\ \sin(\epsilon_{uj} - \epsilon_{ui}) & \cos(\epsilon_{uj} - \epsilon_{ui}) & 0 \\ 0 & 0 & 1 \end{bmatrix}$$

$$T_{uj\leftarrow ui} = \begin{bmatrix} \cos(\epsilon_{uj} - \epsilon_{ui}) & \sin(\epsilon_{uj} - \epsilon_{ui}) & 0 \\ -\sin(\epsilon_{uj} - \epsilon_{ui}) & \cos(\epsilon_{uj} - \epsilon_{ui}) & 0 \\ 0 & 0 & 1 \end{bmatrix} \tag{55}$$

The coordinate transformations between the sprung mass frame and unsprung mass frame of the same unit, under small roll and pitch motion assumptions, are:

$$T_{si\leftarrow ui} = \begin{bmatrix} 1 & 0 & -\theta_i \\ 0 & 1 & \phi_i \\ \theta_i & -\phi_i & 1 \end{bmatrix}$$

$$T_{ui\leftarrow si} = \begin{bmatrix} 1 & 0 & \theta_i \\ 0 & 1 & -\phi_i \\ -\theta_i & \phi_i & 1 \end{bmatrix} \tag{56}$$

4.4 Kinematics of the Heavy Duty Vehicle

In this section, the expressions of the kinematic quantities such as translational velocities, angular velocities, translational accelerations and angular accelerations of both U_i and S_i-frame are given in different coordinate systems. Because of the constraints between units, the relative motion of the i^{th} U-frame to the $(i-1)^{th}$ U-frame is defined by the relative yaw angle, e.g., $\epsilon_i - \epsilon_{i-1}$. The relative translational motions are confined. Inductively, the absolute motion (motion relative to the inertial n-frame) of the U_i-frame is a function of the motion of tractor unsprung mass frame, the yaw motions of all the previous units and yaw motion of the current unit only. This is an importance feature, we will make extensive use of this characteristics in the derivation of both complex model and simple model.

4.4.1 Tractor Unsprung Mass Dynamics

In the inertial coordinate system, position vector of the C.G. of tractor is defined as:

$$[\vec{r}_1]_n = \begin{bmatrix} x_n \\ y_n \\ z_n \end{bmatrix}_n \tag{57}$$

From the definition of the unsprung mass frames, the position of the origin of U_1-frame in the inertial coordinate system is given by:

$$[\vec{r}_{u1}]_n = \begin{bmatrix} x_n \\ y_n \\ 0 \end{bmatrix}_n \tag{58}$$

The velocity and the acceleration of U_1-frame in terms of time derivatives of x_n and y_n are:

$$[\vec{v}_{u1}]_n = \begin{bmatrix} \dot{x}_n \\ \dot{y}_n \\ 0 \end{bmatrix}_n , \qquad [\vec{a}_{u1}]_n = \begin{bmatrix} \ddot{x}_n \\ \ddot{y}_n \\ 0 \end{bmatrix}_n \tag{59}$$

The U_1-frame velocity in U_1-frame is obtained by coordinate transformation given in equation (54) of section 4.3:

$$[\vec{v}_{u1}]_{u1} = T_{u1 \leftarrow n}[\vec{v}_{u1}]_n = \begin{bmatrix} \dot{x}_n \cos \epsilon_1 + \dot{y}_n \sin \epsilon_1 \\ -\dot{x}_n \sin \epsilon_1 + \dot{y}_n \cos \epsilon_1 \\ 0 \end{bmatrix}_{u1} \tag{60}$$

In control applications, the traveling velocity and deviation rate of the vehicle from the desired path are of interest. We define the longitudinal velocity and the lateral velocity of the tractor, v_x and v_y respectively as,

$$\begin{bmatrix} v_x \\ v_y \\ 0 \end{bmatrix}_{u1} = [\vec{v}_{u1}]_{u1} \tag{61}$$

From equation (60) and equation (61), we have the following relations:

$$\begin{aligned} v_x &= \dot{x}_n \cos \epsilon_1 + \dot{y}_n \sin \epsilon_1 \\ v_y &= -\dot{x}_n \sin \epsilon_1 + \dot{y}_n \cos \epsilon_1 \end{aligned} \tag{62}$$

and,

$$\begin{aligned} \dot{x}_n &= v_x \cos \epsilon_1 - v_y \sin \epsilon_1 \\ \dot{y}_n &= v_x \sin \epsilon_1 + v_y \cos \epsilon_1 \end{aligned} \tag{63}$$

By taking time derivative of equation (61), the acceleration of tractor is obtained in terms of v_x and v_y and their derivatives.

$$\begin{aligned} [\vec{a}_{u1}]_{u1} &= \tfrac{d}{dt}[\vec{v}_{u1}]_{u1} \\ &= \left[\tfrac{d}{dt}\vec{v}_{u1}\right]_{u1} + [\vec{\omega}_{u1}]_{u1} \times \left[\tfrac{d}{dt}\vec{v}_{u1}\right]_{u1} \\ &= \begin{bmatrix} \dot{v}_x - \dot{\epsilon}_1 v_y \\ \dot{v}_y + \dot{\epsilon}_1 v_x \\ 0 \end{bmatrix}_{U1} \end{aligned} \tag{64}$$

where, $[\vec{\omega}_{u1}]_{u1}$ is the angular velocity of U_1-frame. It is equal to $[0 \quad 0 \quad \dot{\epsilon}_1]^T_{u1}$.

By applying coordinate transformation to $\vec{a}_{u1}$, the acceleration of the U_1-frame is obtained in terms of n-frame variables.

$$[\vec{a}_{u1}]_{u1} = T_{u1 \leftarrow n}[\vec{a}_{u1}]_n = \begin{bmatrix} \ddot{x}_n \cos \epsilon_1 + \&\sin \epsilon_1 \\ -\ddot{x}_n \sin \epsilon_1 + \ddot{y}_n \cos \epsilon_1 \\ 0 \end{bmatrix}_{u1} \tag{65}$$

From equation (64) and equation (65), we have the following relations:

$$\begin{aligned} v_x - \dot{\epsilon}_1 v_y &= \ddot{x}_n \cos \epsilon_1 + \ddot{y}_n \sin \epsilon_1 \\ \dot{v}_y + \dot{\epsilon}_1 v_x &= -\ddot{x}_n \sin \epsilon_1 + \ddot{y}_n \cos \epsilon_1 \end{aligned} \tag{66}$$

The complex model is derived in U_i-frame and the simple model is derived in U_1-frame. By utilizing the coordinate transformations given in section 4.3, the tractor

velocity in U_k coordinate system in terms of v_x and v_y is obtained as:

$$[\vec{v}_{u1}]_{uk} = \begin{bmatrix} v_x \cos(\epsilon_k - \epsilon_1) + v_y \sin(\epsilon_k - \epsilon_1) \\ -v_x \sin(\epsilon_k - \epsilon_1) + v_y \cos(\epsilon_k - \epsilon_1) \\ 0 \end{bmatrix}_{uk} \tag{67}$$

The acceleration of tractor in U_k coordinate system in terms of $v_x, v_y, \dot{v}_x$ and $\dot{v}_y$ is obtained as:

$$\begin{aligned} [\vec{a}_{u1}]_{uk} &= \begin{bmatrix} \dot{v}_x \cos(\epsilon_k - \epsilon_1) + \dot{v}_y \sin(\epsilon_k - \epsilon_1) \\ -\dot{v}_x \sin(\epsilon_k - \epsilon_1) + \dot{v}_y \cos(\epsilon_k - \epsilon_1) \\ 0 \end{bmatrix}_{uk} \\ &+ \begin{bmatrix} -v_y \cos(\epsilon_k - \epsilon_1) + v_x \sin(\epsilon_k - \epsilon_1) \\ v_y \sin(\epsilon_k - \epsilon_1) + v_x \cos(\epsilon_k - \epsilon_1) \\ 0 \end{bmatrix}_{uk} \dot{\epsilon}_1 \end{aligned} \tag{68}$$

In the following sections, we will use $v_x, v_y, \dot{v}_x$ and $\dot{v}_y$ to describe the dynamics of semi-trailers, dollies and trailers. If one need to express the dynamic equations in terms of $\dot{x}_n, \dot{y}_n, \ddot{x}_n$ and $\ddot{y}_n$, equations(62) and (63) can be used to fulfill the task.

4.4.2 Velocities of the U_i-frame

Once the tractor velocity is defined, from the kinematics, the velocities of the following units are obtained inductively. See Figure 26.

The velocity of the second unit$(i = 2)$ is given by:

$$\vec{v}_{u2} = \begin{bmatrix} \vec{v}_{u1} - d_{r1}\dot{\epsilon}_1 \\ 0 \end{bmatrix}_{u1} - \begin{bmatrix} 0 \\ d_{f2}\dot{\epsilon}_2 \\ 0 \end{bmatrix}_{u2} \tag{69}$$

and.

$$\vec{v}_{ui} = \vec{v}_{u1} - \begin{bmatrix} 0 \\ d_{r1}\dot{\epsilon}_1 \\ 0 \end{bmatrix}_{u1} - \sum_{j=2}^{i-1} \begin{bmatrix} 0 \\ (d_{fj} + d_{rj})\dot{\epsilon}_j \\ 0 \end{bmatrix}_{uj} - \begin{bmatrix} 0 \\ d_{fi}\dot{\epsilon}_i \\ 0 \end{bmatrix}_{ui} \tag{70}$$

for all units with $i > 2$.

These velocities can be expressed in terms of v_x and v_y in U_k coordinate system by applying appropriate coordinate transformations. For completeness, we also give the velocity of the tractor. The velocities of the tractor and trailing units are :
for the tractor, $i = 1$,

$$[\vec{v}_{u1}]_{uk} = \begin{bmatrix} v_x \cos(\epsilon_k - \epsilon_1) + v_y \sin(\epsilon_k - \epsilon_1) \\ -v_x \sin(\epsilon_k - \epsilon_1) + v_y \cos(\epsilon_k - \epsilon_1) \\ 0 \end{bmatrix}_{uk} \tag{71}$$

for the second unit, $i = 2$,

$$\begin{aligned} [\vec{v}_{u2}]_{uk} &= \begin{bmatrix} v_x \cos(\epsilon_k - \epsilon_1) + v_y \sin(\epsilon_k - \epsilon_1) \\ -v_x \sin(\epsilon_k - \epsilon_1) + v_y \cos(\epsilon_k - \epsilon_1) \\ 0 \end{bmatrix}_{uk} \\ &\quad - \begin{bmatrix} \sin(\epsilon_k - \epsilon_1) \\ \cos(\epsilon_k - \epsilon_1) \\ 0 \end{bmatrix}_{uk} d_{r1}\dot{\epsilon}_1 - \begin{bmatrix} \sin(\epsilon_k - \epsilon_2) \\ \cos(\epsilon_k - \epsilon_2) \\ 0 \end{bmatrix}_{uk} d_{f2}\dot{\epsilon}_2 \end{aligned} \tag{72}$$

for i > 2,

$$\begin{aligned} [\vec{v}_{ui}]_{uk} &= \begin{bmatrix} v_x \cos(\epsilon_k - \epsilon_1) + v_y \sin(\epsilon_k - \epsilon_1) \\ -v_x \sin(\epsilon_k - \epsilon_1) + v_y \cos(\epsilon_k - \epsilon_1) \\ 0 \end{bmatrix}_{uk} - \begin{bmatrix} \sin(\epsilon_k - \epsilon_1) \\ \cos(\epsilon_k - \epsilon_1) \\ 0 \end{bmatrix}_{uk} d_{r1}\dot{\epsilon}_1 \\ &\quad - \sum_{j=2}^{i-1} \begin{vmatrix} \sin(\epsilon_k - \epsilon_j) \\ \cos(\epsilon_k - \epsilon_j) \\ 0 \end{vmatrix}_{uk} (d_{fj} + d_{rj})\dot{\epsilon}_j - \begin{bmatrix} \sin(\epsilon_k - \epsilon_i) \\ \cos(\epsilon_k - \epsilon_i) \\ 0 \end{bmatrix}_{uk} d_{fi}\dot{\epsilon}_i \end{aligned} \tag{73}$$

4.4.3 Angular Velocities and Angular Accelerations of the U_i and S_i Frames

The unsprung mass frame rotates only about its z axis ϵ_i radians relative to the inertial n-frame. Therefore the angular velocity of U_i-frame is:

$$[\vec{\omega}_{ui}]_{ui} = \begin{bmatrix} 0 \\ 0 \\ \dot{\epsilon}_i \end{bmatrix}_{\text{ui}} \tag{74}$$

The sprung mass frame has roll(ϕ_i) and pitch(θ_i) motion relative to unsprung mass frame. The relative angular velocity of the S_i-frame to the U_i-frame is:

$$\left[\vec{\omega}_{si/ui}\right]_{Isi} = \begin{bmatrix} \dot{\phi}_i \\ \dot{\theta}_i \\ 0 \end{bmatrix}_{si} \tag{75}$$

Then the angular velocity of S_i-frame relative to inertial n-frame is given by:

$$\vec{\omega}_{si} = \vec{\omega}_{ui} + \vec{\omega}_{si/ui} \tag{76}$$

in U_i coordinate system, it can be expressed as:

$$[\vec{\omega}_{si}]_{ui} = [\vec{\omega}_{ui}]_{ui} + T_{ui \leftarrow si}\left[\vec{\omega}_{si/ui}\right]_{si} = \begin{bmatrix} \dot{\phi}_i \\ \dot{\theta}_i \\ \dot{\epsilon}_i - \dot{\phi}_i\theta_i + \dot{\theta}_i\phi_i \end{bmatrix}_{ui} \tag{77}$$

and in S_i coordinate system, it can be expressed as:

$$[\vec{\omega}_{si}]_{si} = T_{si \leftarrow ui}\,[\vec{\omega}_{ui}]_{ui} + \left[\vec{\omega}_{si/ui}\right]_{si} = \begin{bmatrix} \dot{\phi}_i - \theta_i\dot{\epsilon}_i \\ \dot{\theta}_i + \phi_i\dot{\epsilon}_i \\ \dot{\epsilon}_i \end{bmatrix}_{si} \tag{78}$$

The rate of change of angular velocity of S_i-frame in S_i coordinate system is:

$$\left[\dot{\vec{\omega}}_{si}\right]_{\text{I si}} = \begin{bmatrix} \ddot{\phi}_i - \theta_i\ddot{\epsilon}_i - \dot{\theta}_i\dot{\epsilon}_i \\ \ddot{\theta}_i + \phi_i\ddot{\epsilon}_i + \dot{\phi}_i\dot{\epsilon}_i \\ \ddot{\epsilon}_i \end{bmatrix}_{\text{Si}} \tag{79}$$

4.4.4 Accelerations of U_i-frame

Now that we know the translational velocity and angular velocity of the U_i-frame, we can obtain the translational acceleration by taking the time derivative of the velocity.

$$[\vec{a}_{ui}]_{ui} = \frac{d}{dt}[\vec{v}_{ui}]_{ui} \tag{80}$$

or,

$$[\vec{a}_{ui}]_{ui} = \left[\frac{d}{dt}\vec{v}_{ui}\right]_{ui} + [\vec{\omega}_{ui}]_{ui} \times [\vec{v}_{ui}]_{ui} \tag{81}$$

From equation(73) for the case of $k = i$ and equation(74), we have the accelerations of the U_i-frames in terms of $v_x, v_y, \dot{v}_x$ and $\dot{v}_y$ expressed in U_i-frame as follows:
for tractor, i = 1,

$$[\vec{a}_{u1}]_{u1} = \begin{bmatrix} \dot{v}_x - \dot{\epsilon}_1 v_y \\ \dot{v}_y + \dot{\epsilon}_1 v_x \\ 0 \end{bmatrix}_{u1} \tag{82}$$

for the second unit, $i = 2$,

$$\begin{aligned}[\vec{a}_{u2}]_{u2} = & \begin{bmatrix} \dot{v}_x \cos(\epsilon_2 - \epsilon_1) + \dot{v}_y \sin(\epsilon_2 - \epsilon_1) \\ -\dot{v}_x \sin(\epsilon_2 - \epsilon_1) + \dot{v}_y \cos(\epsilon_2 - \epsilon_1) \\ 0 \end{bmatrix}_{u2} + \begin{bmatrix} -v_y \cos(\epsilon_2 - \epsilon_1) + v_x \sin(\epsilon_2 - \epsilon_1) \\ v_y \sin(\epsilon_2 - \epsilon_1) + v_x \cos(\epsilon_2 - \epsilon_1) \\ 0 \end{bmatrix}_{u2} \dot{\epsilon}_1 \\ & + \begin{bmatrix} -\ddot{\epsilon}_1 \sin(\epsilon_2 - \epsilon_1) + \dot{\epsilon}_1^2 \cos(\epsilon_2 - \epsilon_1) \\ -\ddot{\epsilon}_1 \cos(\epsilon_2 - \epsilon_1) - \dot{\epsilon}_1^2 \sin(\epsilon_2 - \epsilon_1) \\ 0 \end{bmatrix}_{u2} d_{r1} + \begin{bmatrix} \dot{\epsilon}_2^2 \\ -\ddot{\epsilon}_2 \\ 0 \end{bmatrix}_{u2} d_{f2}\end{aligned} \tag{83}$$

for $i > 2$,

$$
\begin{aligned}
[\vec{a}_{ui}]_{ui} \;=\; & \begin{bmatrix} \dot{v}_x \cos(\epsilon_i - \epsilon_1) + \dot{v}_y \sin(\epsilon_i - \epsilon_1) \\ -\dot{v}_x \sin(\epsilon_i - \epsilon_1) + \dot{v}_y \cos(\epsilon_i - \epsilon_1) \\ 0 \end{bmatrix}_{ui} \\
& + \begin{bmatrix} -v_y \cos(\epsilon_i - \epsilon_1) + v_x \sin(\epsilon_i - \epsilon_1) \\ v_y \sin(\epsilon_i - \epsilon_1) + v_x \cos(\epsilon_i - \epsilon_1) \\ 0 \end{bmatrix}_{ui} \dot{\epsilon}_1 \\
& + \begin{bmatrix} -\ddot{\epsilon}_1 \sin(\epsilon_i - \epsilon_1) + \dot{\epsilon}_1^2 \cos(\epsilon_i - \epsilon_1) \\ -\ddot{\epsilon}_1 \cos(\epsilon_i - \epsilon_1) - \dot{\epsilon}_1^2 \sin(\epsilon_i - \epsilon_1) \\ 0 \end{bmatrix}_{ui} d_{r1} \\
& + \sum_{j=2}^{i-1} \begin{bmatrix} -\ddot{\epsilon}_j \sin(\epsilon_i - \epsilon_j) + \dot{\epsilon}_j^2 \cos(\epsilon_i - \epsilon_j) \\ -\ddot{\epsilon}_j \cos(\epsilon_i - \epsilon_j) - \dot{\epsilon}_j^2 \sin(\epsilon_i - \epsilon_j) \\ 0 \end{bmatrix}_{ui} (d_{fj} + d_{rj}) + \begin{bmatrix} \dot{\epsilon}_i^2 \\ -\ddot{\epsilon}_i \\ 0 \end{bmatrix}_{ui} d_{fi}
\end{aligned}
\tag{84}
$$

The acceleration expressions in U_i-frame are used in the complex model. In deriving the simple model, the acceleration expressions in U_1-frame are needed. By applying coordinate transformations $T_{u1 \leftarrow ui}$, such that,

$$
[\vec{a}_{ui}]_{u1} = T_{u1 \leftarrow ui} [\vec{a}_{ui}]_{ui}, \qquad i = 2, 3, \ldots, N \tag{85}
$$

we have:

for the second unit, (i = 2)

$$
\begin{aligned}
[\vec{a}_{u2}]_{u1} \;=\; & \begin{bmatrix} \dot{v}_x - \dot{\epsilon}_1 v_y \\ \dot{v}_y + \dot{\epsilon}_1 v_x \\ 0 \end{bmatrix}_{u1} + \begin{bmatrix} \dot{\epsilon}_1^2 \\ -\ddot{\epsilon}_1 \\ 0 \end{bmatrix}_{u1} d_{r1} \\
& + \begin{bmatrix} -\ddot{\epsilon}_2 \sin(\epsilon_1 - \epsilon_2) + \dot{\epsilon}_1^2 \cos(\epsilon_1 - \epsilon_2) \\ -\ddot{\epsilon}_2 \cos(\epsilon_1 - \epsilon_2) - \dot{\epsilon}_2^2 \sin(\epsilon_1 - \epsilon_2) \\ 0 \end{bmatrix}_{u1} d_{f2}
\end{aligned}
\tag{86}
$$

and for $i > 2$,

$$
\begin{aligned}
[\vec{a}_{ui}]_{u1} &= \begin{bmatrix} \dot{v}_x - \dot{\epsilon}_1 v_y \\ \dot{v}_y + \dot{\epsilon}_1 v_x \\ 0 \end{bmatrix}_{u1} + \begin{bmatrix} \dot{\epsilon}_1^2 \\ -\ddot{\epsilon}_1 \\ 0 \end{bmatrix}_{u1} d_{r1} \\
&+ \sum_{j=2}^{i-1} \begin{bmatrix} -\ddot{\epsilon}_j \sin(\epsilon_1 - \epsilon_j) + \dot{\epsilon}_j^2 \cos(\epsilon_1 - \epsilon_j) \\ -\ddot{\epsilon}_j \cos(\epsilon_1 - \epsilon_j) - \dot{\epsilon}_j^2 \sin(\epsilon_1 - \epsilon_j) \\ 0 \end{bmatrix}_{U1} (d_{fj} + d_{rj}) \\
&+ \begin{bmatrix} -\ddot{\epsilon}_i \sin(\epsilon_1 - \epsilon_i) + \dot{\epsilon}_i^2 \cos(\epsilon_1 - \epsilon_i) \\ -\ddot{\epsilon}_i \cos(\epsilon_1 - \epsilon_i) - \dot{\epsilon}_i^2 \sin(\epsilon_1 - \epsilon_i) \\ 0 \end{bmatrix}_{u1} d_{fi}
\end{aligned} \tag{87}
$$

4.4.5 Translational Velocity and Acceleration of S_i-frame

The motion of the S_i-frame relative to the inertial n-frame is the addition of the motion of U_i-frame relative to inertial n-frame, the bouncing motion of U_i-frame relative to n-frame and the motion of S_i-frame relative to U_i-frame. Therefore the velocity is given by:

$$
\begin{aligned}
[\vec{v}_i]_{ui} &= [\vec{v}_{ui}]_{ui} + \begin{bmatrix} 0 \\ 0 \\ \dot{z}_{p1} + vv_{zi} \end{bmatrix}_{ui} - T_{ui \leftarrow si} \left(\left[\vec{\omega}^i_{si/ui} \right]_{si} \times \begin{bmatrix} p_i \\ 0 \\ r_i \end{bmatrix} \right) \\
&= [\vec{v}_{ui}]_{ui} + \begin{bmatrix} -r_i \dot{\theta}_i + p_i \theta_i \dot{\theta}_i \\ r_i \dot{\phi}_i - p_i \phi_i \dot{\theta}_i \\ \dot{z}_{p1} + vv_{zi} + p_i \dot{\theta}_i + r_i (\theta_i \dot{\theta}_i + \phi_i \dot{\phi}_i) \end{bmatrix}_{ui}
\end{aligned} \tag{88}
$$

where, vv_{zi}s are the bouncing motion propagation terms and $\dot{z}_{p1}$ is the velocity of the tractor pitch center in the z_{u1} direction (See Fig. 22) and is given by,

$$
\dot{z}_{p1} = \dot{z}_n - p_1 \dot{\theta}_1 \tag{89}
$$

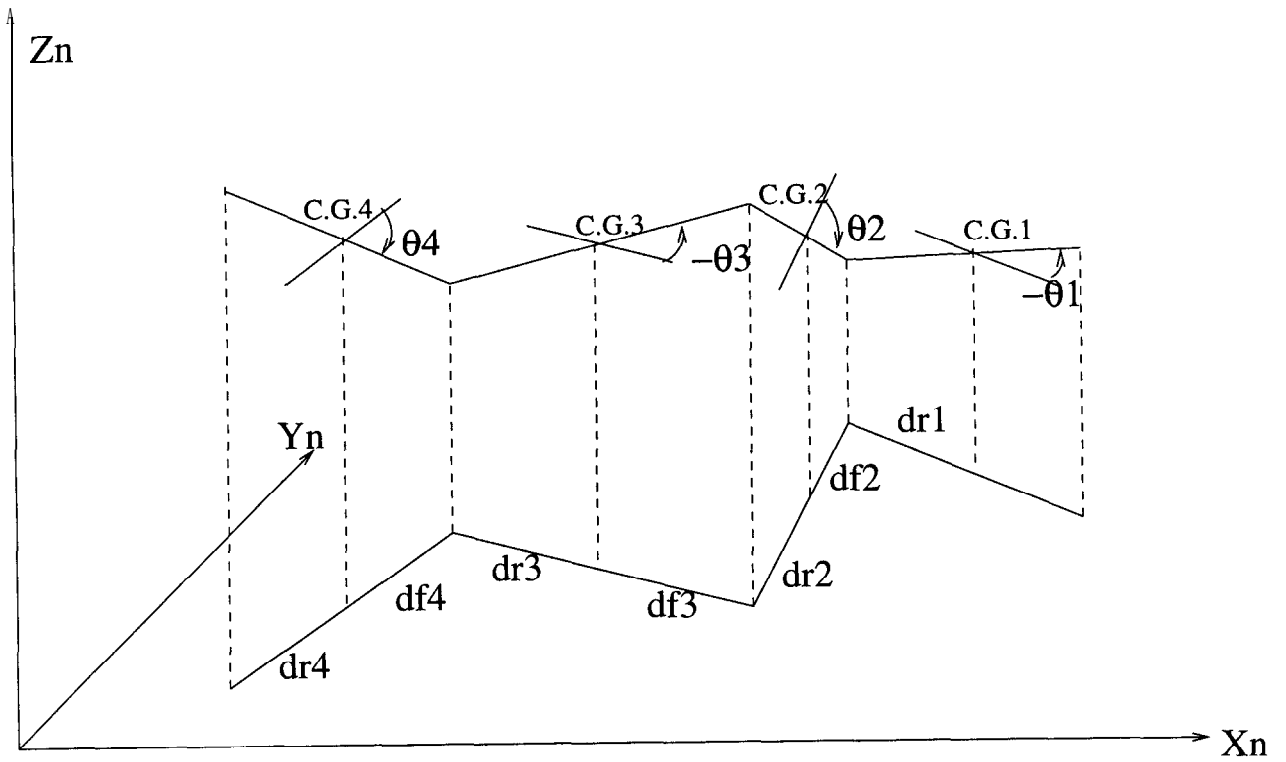

Figure 22: Bouncing Motion of the Units

The bouncing velocity propagation terms are

$$\begin{aligned} vv_{z1} &= 0 \\ vv_{z2} &= p_1\dot{\theta}_1 + d_{r1}\dot{\theta}_1 \\ vv_{zi} &= p_1\dot{\theta}_1 + d_{r1}\dot{\theta}_1 + \textstyle\sum_{j=2}^{i-1}(d_{fj} + d_{rj})\dot{\theta}_j \end{aligned} \tag{90}$$

The roll and pitch motions are usually very small, the second and higher order terms can be assumed negligible. By setting the second order terms in equation (88) to zero, the velocity of the C.G. of the i^{th} unit is obtained as:

$$[\vec{v}_i]_{ui} = [\vec{v}_{ui}]_{ui} + \begin{bmatrix} -r_i\dot{\theta}_i \\ r_i\dot{\phi}_i \\ \dot{z}_{p1} + vv_{zi} + p_i\dot{\theta}_i \end{bmatrix}_{ui} \tag{91}$$

The acceleration is obtained by taking time derivative of the S-frame velocity given by equation (91).

$$[\vec{a}_i]_{ui} = \frac{d}{dt}[\vec{v}_i]_{ui} \tag{92}$$

or,

$$[\vec{a}_i]_{ui} = \left[\frac{d}{dt}\vec{v}_i\right]_{ui} + [\vec{\omega}_i]_{ui} \times [\vec{v}_i]_{ui} \tag{93}$$

Applying the above formula to the velocity expressions given in equation (91) , we get:

$$[\vec{a}_i]_{ui} = [\vec{a}_{ui}]_{ui} + \begin{bmatrix} -r_i\ddot{\theta}_i \\ r_i\ddot{\phi}_i \\ \ddot{z}_{p1} + aa_{zi} + p_i\ddot{\theta}_i \end{bmatrix}_{ui} + \begin{bmatrix} -r_i\dot{\epsilon}_i\dot{\phi}_i \\ -r_i\dot{\epsilon}_i\dot{\theta}_i \\ 0 \end{bmatrix}_{ui} \tag{94}$$

where,

$$aa_{z1} = 0$$

$$aa_{z2} = p_1\ddot{\theta}_1 + d_{r1}\ddot{\theta}_1$$

$$aa_{zi} = p_1\ddot{\theta}_1 + d_{r1}\ddot{\theta}_1 + \sum_{j=2}^{i-1}(d_{fj} + drj)\ddot{\theta}_j$$

Conventions: Right arrow at the top of a character indicates that the character is a vector, e.g. $\vec{v}$. *If a vector is embraced in a pair of square brackets, it means the vector is expressed in a coordinate system designated by the subscript o f the bracket, e.g.* $[\vec{v}]_n$. *The arabic numbers or the character i in subscript denotes the index of the unit that the character represent, i.e.* $\vec{v}_i$ *and* $\vec{a}_1$. *The subscripts x, y and z indicates the directional component of the quantity, e.g.* v_x, v_y *and v,.*

4.5 Propagation of Roll and Pitch Motion

From the roll stability point of view, the hitching mechanisms between tractor and trailer or between trailers are all designed to restrict the relative roll motion of the two

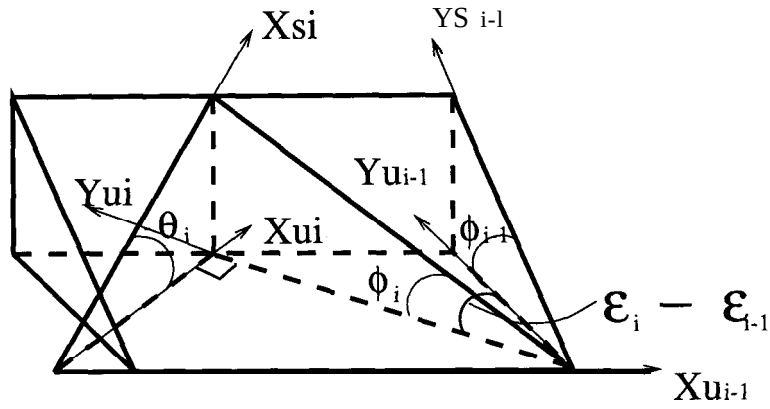

Figure 23: Roll Motion Coupling

connected units. In the fifth wheel connection, considering the pitch motion, the unit rotates about an axis which passes through the connecting point and parallel to the y axis of the previous unit. We define the actual rotating angle of the i^{th} unit relative to the $(i-1)^{th}$ unit as θ_{pi}. Then the nominal roll(&) and pitch(θ_i) angles and all of their derivatives($\dot{\phi}_i, \dot{\theta}_i, \ddot{\phi}_i, \ddot{\phi}_i$) are functions of the roll motion of the previous unit,ϕ_{i-1}, the physical pitch angle, θ_{pi}, and the relative yaw angle, $(\epsilon_i - \epsilon_{i-1})$. For example, if the relative yaw angle, i.e. $\epsilon_i - \epsilon_{i-1} = 0$, is zero, then, $\phi_i = \phi_{i-1}$ and $\theta_i = \theta_{pi}$. If the relative yaw angle, i.e. $\epsilon_i - \epsilon_{i-1} = 90$ deg, then, $\phi_i = \theta_{pi}$ and $\theta_i = \phi_{i-1}$. We assume that the pitch and roll motions are small. Under this assumption, the superposition principle can be applied as follows:

First assume, $\theta_{pi} = 0$. From the geometry in Fig. 23, we have,

$$\begin{aligned} \tan\phi_i &= \tan\phi_{i-1}\cos(\epsilon_i - \epsilon_{i-1}) \\ \tan\theta_i &= -\tan\phi_{i-1}\sin(\epsilon_i - \epsilon_{i-1}) \end{aligned} \tag{95}$$

If $\phi_{i-1} = 0$, then from Fig. 24, we have,

$$\begin{aligned} \tan\theta_i &= \tan\theta_{pi}\cos(\epsilon_i - \epsilon_{i-1}) \\ \tan\phi_i &= \tan\theta_{pi}\sin(\epsilon_i - \epsilon_{i-1}) \end{aligned} \tag{96}$$

Applying the small angle superposition principle, the roll and pitch motion of the i^{th} unit are the joint effect of the $(i-1)^{th}$ unit roll motion and the physical relative pitch

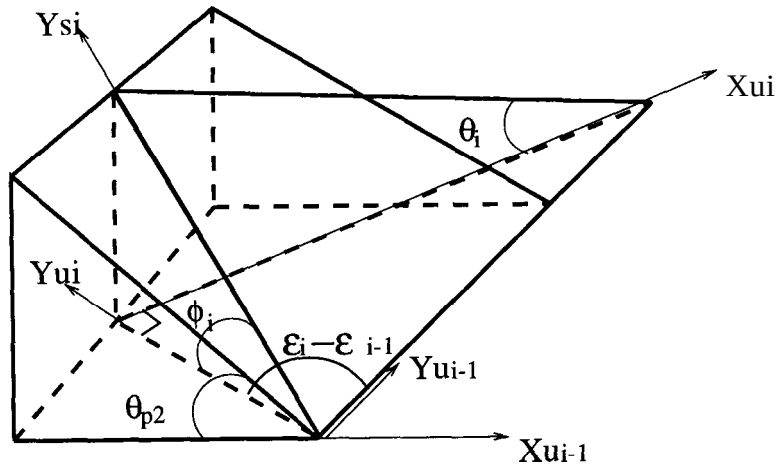

Figure 24: Pitch Motion Coupling

motion: i.e.

$$\begin{aligned}\phi_i &= \arctan(\tan\ \phi_{i-1}\cos(\epsilon_i-\epsilon_{i-1})) + \arctan(\tan\ \theta_{pi}\sin(\epsilon_i-\epsilon_{i-1}))\\ \theta_i &= -\arctan(\tan\ \phi_{i-1}\sin(\epsilon_i-\epsilon_{i-1})) + \arctan(\tan\ \theta_{pi}\cos(\epsilon_i-\epsilon_{i-1}))\end{aligned} \tag{97}$$

In exploring the relationships of the rates of rotational motions, we assume that the yaw motion of U_i-frame relative to U_{i-1}-frame is approximately the same as the yaw motion of S_i-frame relative to S_{i-1}-frame. The angular velocity of S_i-frame in terms of ϕ_{i-1} and θ_{pi} is:

$$\begin{bmatrix} \dot{\phi}_{i-1} \\ \dot{\theta}_{pi} \\ * \end{bmatrix}_{s(i-1)} \tag{98}$$

If the coordinate transformation from S_{i-1}-frame to S_i-frame is approximated as:

$$T_{si\leftarrow s(i-1)} = \begin{bmatrix} \cos(\epsilon_i-\epsilon_{i-1}) & \sin(\epsilon_i-\epsilon_{i-1}) & 0 \\ -\sin(\epsilon_i-\epsilon_{i-1}) & \cos(\epsilon_i-\epsilon_{i-1}) & 0 \\ 0 & 0 & 1 \end{bmatrix} \tag{99}$$

the nominal roll and pitch rates of S_i-frame are

$$\begin{bmatrix} \dot{\phi}_i \\ \dot{\theta}_i \\ * \end{bmatrix}_{si} := T_{si \leftarrow s(i-1)} \begin{bmatrix} \dot{\phi}_{i-1} \\ \dot{\theta}_{pi} \\ * \end{bmatrix}_{s(i-1)} \tag{100}$$

i.e.

$$\begin{aligned} \dot{\phi}_i &= \dot{\phi}_{i-1}\cos(\epsilon_i - \epsilon_{i-1}) + \dot{\theta}_{pi}\sin(\epsilon_i - \epsilon_{i-1}) \\ \dot{\theta}_i &= -\dot{\phi}_{i-1}\sin(\epsilon_i - \epsilon_{i-1}) + \dot{\theta}_{pi}\cos(\epsilon_i - \epsilon_{i-1}) \end{aligned} \tag{101}$$

The rates of change of the roll and pitch angles are:

$$\begin{aligned} \ddot{\phi}_i &= \ddot{\phi}_{i-1}\cos(\epsilon_i - \epsilon_{i-1}) + \ddot{\theta}_{pi}\sin(\epsilon_i - \epsilon_{i-1}) + (\dot{\epsilon}_i - \dot{\epsilon}_{i-1})\dot{\theta}_i \\ \ddot{\theta}_i &= -\ddot{\phi}_{i-1}\sin(\epsilon_i - \epsilon_{i-1}) + \ddot{\theta}_{pi}\cos(\epsilon_i - \epsilon_{i-1}) - (\text{ii} - \dot{\epsilon}_{i-1})\dot{\phi}_i \end{aligned} \tag{102}$$

As we can see, $\ddot{\phi}_i$ and $\ddot{\theta}_i$ are functions of $\ddot{\phi}_1$, and $\ddot{\theta}_{pj}$s for all $2 \leq j \leq i$. For compactness, we define the following quantities:

$$\begin{aligned} A_i &= \cos(\epsilon_i - \epsilon_{i-1}) \\ B_i &= \sin(\epsilon_i - \epsilon_{i-1}) \\ C_i &= (\dot{\epsilon}_i - \dot{\epsilon}_{i-1})\theta_i \\ D_i &= -\sin(\epsilon_i - \epsilon_{i-1}) \\ E_i &= \cos(\epsilon_i - \epsilon_{i-1}) \\ F_i &= -(\dot{\epsilon}_i - \dot{\epsilon}_{i-1})\dot{\phi}_i \end{aligned} \tag{103}$$

The angular acceleration equations can then be rewritten as:

$$\begin{aligned} \ddot{\phi}_i &= A_i\ddot{\phi}_{i-1} + B_i\ddot{\theta}_{pi} + C_i \\ \ddot{\theta}_i &= D_i\ddot{\phi}_{i-1} + E_i\ddot{\theta}_{pi} + F_i \end{aligned} \tag{104}$$

By reapplying formula (104) to all the intermediate roll accelerations, we get the following equations:

$$\begin{aligned} \ddot{\phi}_i &= \left(\prod_{j=2}^{i} A_j\right)\ddot{\phi}_1 + \sum_{k=2}^{i}\left(\prod_{j=k+1}^{i} A_j\right)B_k\ddot{\theta}_{pk} + \sum_{k=2}^{i}\left(\prod_{j=k+1}^{i} A_j\right)C_k \\ \ddot{\theta}_i &= D_i\left(\prod_{j=2}^{i-1} A_j\right)\ddot{\phi}_1 + D_i\sum_{k=2}^{i-1}\left(\prod_{j=k+1}^{i-1} A_j\right)B_k\ddot{\theta}_{pk} \\ &\quad + E_i\ddot{\theta}_{pi} + D_i\sum_{k=2}^{i-1}\left(\prod_{j=k+1}^{i-1} A_j\right)C_k + F_i \end{aligned} \tag{105}$$

4.6 Complex Simulation Model

from the advanced dynamics theory, a dynamic system is defined as a collection of elements which interact with each other and is subject to external forces. In the case that the elements are 3D objects, the elements are called free bodies. For each free body we can write down 6 differential equations, i.e. three translational motion equations and three rotational equations. So, for a system which consists of N free bodies, we have 6N differential equations. This means that we have 6N unknowns to solve for. The external forces are known functions of time and the system states, where the system states refer to the positions and velocities. Some interacting forces are known functions of time and system states, and some are not. The latter is usually referred to as the constraint forces. The nature of constraint forces is that they eliminate the degrees of freedom at the cost of introducing constraint forces which can only be solved from the dynamic equations.

By selecting the states (generalized coordinates) carefully, as we have shown in section 4.4, the translational accelerations and rotational accelerations for each body can be easily expressed in terms of the states only. Furthermore, the sum of the number of general coordinates and the number of constraint forces are always 6 x N, where N is the number of units of the system. Then, for each unit we can apply Newton's equations and Euler's equations of motion, Fig. 25 is a freebody diagram for the i^{th} unit of a truck. Newton's Equations for the i^{th} unit are:

$$M_i \vec{a}_i = \vec{F}_s^i \tag{106}$$

where, $\vec{F}^i$ is a total force vector acting on the i^{th} unit. As shown in Fig. 25, it is the sum of the tire forces of four wheels and constraint forces of both front and rear constraints. The front constraint force $(\tilde{F}_f^i)$ components are defined along the directions of unsprung mass frame of the previous unit. Similarly the rear constraint force(F_r^i) components are defined along the directions of unsprung mass frame of the unit. The directions of all the tire forces are the same as the unsprung mass frame directions of the unit that the wheels are attached to. Therefore, the front constraint

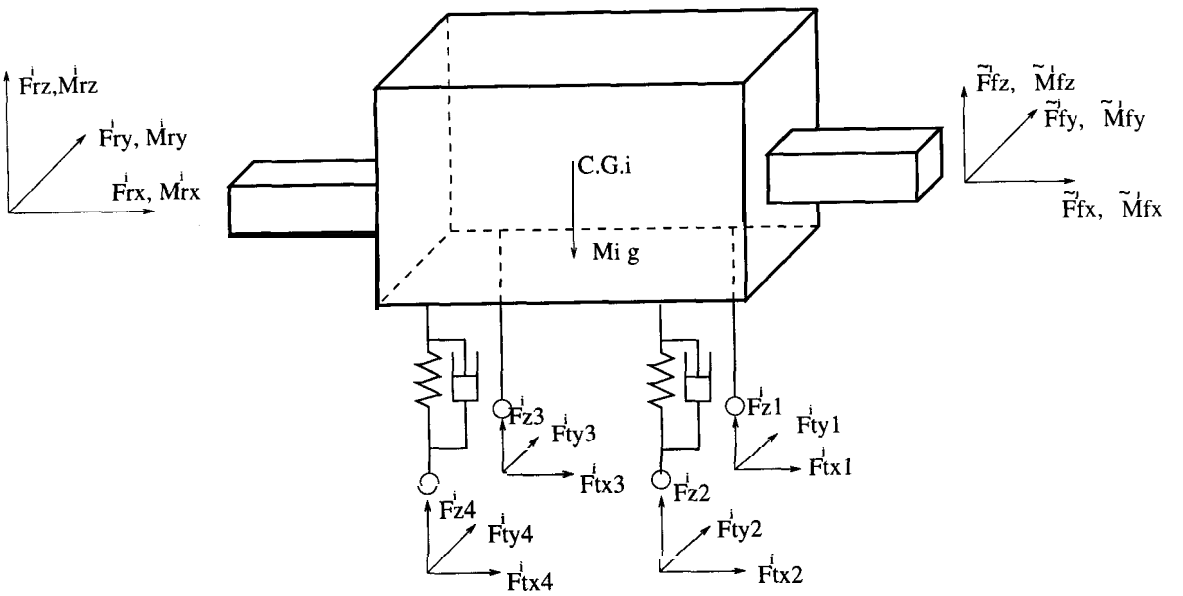

Figure 25: Free-body Diagram of the Truck Unit

forces are given by:

$$\left[\tilde{F}^i_f\right]_{ui} = -T_{ui\leftarrow u(i-1)} \left[F^{i-1}_r\right]_{u(i-1)} \tag{107}$$

By expanding the above expression into its component forms in U_i-frame, we have,

$$\begin{aligned}
\tilde{F}^i_{fx} &= -F^{i-1}_{rx}\cos(\epsilon_i - \epsilon_{i-1}) - F^{i-1}_{ry}\sin(\epsilon_i - \epsilon_{i-1}) \\
\tilde{F}^i_{fy} &= F^{i-1}_{rx}\sin(\epsilon_i - \epsilon_{i-1}) - F^{i-1}_{ry}\cos(\epsilon_i - \epsilon_{i-1}) \\
\tilde{F}^i_{fz} &= -F^{i-1}_{rz}
\end{aligned} \tag{108}$$

The total force $(\vec{F}^i_s = [FL,, F^i_{sy}, F^i_{sz}]^T)$ is given by:

$$\begin{aligned}
F^i_{sx} &= F^i_{t1x} + F^i_{t2x} + F^i_{t3x} + F^i_{t4x} + \tilde{F}^i_{fx} + F^i_{rx} \\
F^i_{sy} &= F^i_{t1y} + F^i_{t2y} + F^i_{t3y} + F^i_{t4y} + \tilde{F}^i_{fy} + F^i_{ry} \\
F^i_{sz} &= F^i_{z1} + F^i_{z2} + F^i_{z3} + F^i_{z4} + \tilde{F}^i_{fz} + F^i_{rz}
\end{aligned} \tag{109}$$

Euler's Equation for the i^{th} Unit is:

$$\begin{aligned} I^i_{xx}\dot{\omega}_{six} - (I^i_{yy} - I^i_{zz})\omega_{siy}\omega_{siz} &= M^i_{sx} \\ I^i_{yy}\dot{\omega}_{siy} - (I^i_{zz} - I^i_{xx})\omega_{siz}\omega_{six} &= M^i_{sy} \\ I^i_{zz}\dot{\omega}_{siz} - (I^i_{xx} - I^i_{yy})\omega_{six}\omega_{siy} &= M^i_{sz} \end{aligned} \tag{110}$$

where, $M\dot{M}^i_{sy}$ and M^i_{sz} are the componets of total moment $\vec{M}^i_s$ in the S-frame. However, it is much easier to calculate the moments in U_i-frame.

$$M^i_u = \tilde{M}^i_u + \vec{R}_{cf} \times \begin{bmatrix} \tilde{F}^i_{fx} \\ \tilde{F}^i_{fy} \\ \tilde{F}^i_{fz} \end{bmatrix}_{ui} + \vec{R}_{cr} \times \begin{bmatrix} F^i_{rx} \\ F^i_{ry} \\ F^i_{rz} \end{bmatrix}_{ui} + \tilde{M}^i_f + M^i_r \tag{111}$$

where, $\tilde{M}^i_u$ is a moment term which comes from the tire forces,

$$\tilde{M}^i_u = \vec{R}^i_1 \times \begin{bmatrix} F^i_{t1x} \\ F^i_{t1y} \\ F^i_{z1} \end{bmatrix}_{ui} + \vec{R}^i_2 \times \begin{bmatrix} F^i_{t2x} \\ F^i_{t2y} \\ F^i_{z2} \end{bmatrix}_{ui} + \vec{R}^i_3 \times \begin{bmatrix} F^i_{t3x} \\ F^i_{t3y} \\ F^i_{z3} \end{bmatrix}_{ui} + \vec{R}^i_4 \times \begin{bmatrix} F^i_{t4x} \\ F^i_{t4y} \\ F^i_{z4} \end{bmatrix}_{ui} \tag{112}$$

and $\vec{M}^i_r$ is a rear constraint moment. $\tilde{M}^i_f$ is the reaction moment acting on the front constraint point. The front constraint reaction moment can be calculated from the rear constraint moment of the previous unit as follows,

$$\left[\tilde{M}^i_f\right]_{ui} = -T_{ui \leftarrow u(i-1)} \left[M^{i-1}_r\right]_{u(i-1)} \tag{113}$$

that is,

$$\begin{aligned} \tilde{M}^i_{fx} &= -M^{i-1}_{rx}\cos(\epsilon_i - \epsilon_{i-1}) - M^{i-1}_{ry}\sin(\epsilon_i - \epsilon_{i-1}) \\ \tilde{M}^i_{fy} &= M^{i-1}_{rx}\sin(\epsilon_i - \epsilon_{i-1}) - M^{i-1}_{ry}\cos(\epsilon_i - \epsilon_{i-1}) \\ \tilde{M}^i_{fz} &= -M^{i-1}_{rz} \end{aligned} \tag{114}$$

In the above equations the wheel position vectors $\vec{R}_1^i, \vec{R}_2^i, \vec{R}_3^i$ and $\vec{R}_4^i$ are given by,

$$\vec{R}_1^i = \begin{bmatrix} l_{fi} \\ \frac{T_{wf}^i}{2} \\ -Z_{CG}^i \end{bmatrix}_{ui} \qquad \vec{R}_2^i = \begin{bmatrix} l_i \\ -\frac{T_{wf}^i}{2} \\ -Z_{CG}^i \end{bmatrix}_{ui}$$

$$\vec{R}_3^i = \begin{bmatrix} -l_{ri} \\ \frac{T_{wr}^i}{2} \\ -Z_{CG}^i \end{bmatrix}_{ui} \qquad \vec{R}_4^i = \begin{bmatrix} -l_{ri} \\ -\frac{T_{wr}^i}{2} \\ -Z_{CG}^i \end{bmatrix}_{ui} \tag{115}$$

The constraint position vectors $\vec{R}_{fc}^i$ and $\vec{R}_{rc}^i$ are given by,

$$\vec{R}_{cf}^i = \begin{bmatrix} d_{fi} \\ 0 \\ C_f^i - Z_{CG}^i \end{bmatrix}_{ui} \qquad \vec{R}_{cr}^i = \begin{bmatrix} -d_{ri} \\ 0 \\ C_r^i - Z_{CG}^i \end{bmatrix}_{ui} \tag{116}$$

The moments in S_i-frame are obtained by the coordinate transformation:

$$\vec{M}_s^i = T_{si \leftarrow ui}^i \vec{M}_u^i \tag{117}$$

that is,

$$\vec{M}_s^i = \begin{bmatrix} M_{ux}^i - \theta_i M_{uz}^i \\ M_{uy}^i - \phi_i M_{uz}^i \\ M_{uz}^i + \theta_i M_{ux}^i - \phi_i M_{uy}^i \end{bmatrix}_{ui} \tag{118}$$

For the sake of convenience, we also define,

$$\tilde{M}_s^i = T_{si \leftarrow ui}^i \tilde{M}_u^i$$

$$\tilde{M}_s^i = \begin{bmatrix} \tilde{M}_{ux}^i - \theta_i \tilde{M}_{uz} \\ \tilde{M}_{uy} + \phi_i \tilde{M}_{uz} \\ \tilde{M}_{uz} + \theta_i \tilde{M}_{ux} - \phi_i \tilde{M}_{uy} \end{bmatrix}_{ui} \tag{119}$$

and,

$$\begin{aligned} \epsilon_f &:= \epsilon_i - \epsilon_{i-1} \\ C^i_{fz} &:= C^i_f - Z^i_{CG} \\ C^i_{rz} &:= C^i_r - Z^i_{CG} \end{aligned} \tag{120}$$

Finally we have the total moment expression in component form of S_i-frame as follows:

$$\begin{aligned} M^i_{sx} &= (-C^i_{fz} - \theta_i d_{fi}) \sin\epsilon_f F^{i-1}_{rx} + (C^i_{fz} + \theta_i d_{fi}) \cos\epsilon_f F^{i-1}_{ry} \\ &\quad + (-C^i_{rz} + \theta_i d_{ri}) F^i_{ry} \\ &\quad - \cos\epsilon_f M^{i-1}_{rx} - \sin\epsilon_f M^{i-1}_{ry} + \theta_i M^{i-1}_{rz} \\ &\quad + M^i_{rx} - \theta_i M^i_{rz} + \tilde{M}^i_{sx} \end{aligned}$$

$$\begin{aligned} M^i_{sy} &= (-C^i_{fz}\cos\epsilon_f + \phi_i d_{fi}\sin\epsilon_f) F^{i-1}_{rx} + (-C^i_{fz}\sin\epsilon_f - \phi_i d_{fi}\cos\epsilon_f) F^{i-1}_{ry} + d_{fi} F^{i-1}_{rz} \\ &\quad + C^i_{rz} F^i_{rx} - \phi_i d^i_r F^i_{ry} + d_{ri} F^i_{rz} \\ &\quad + \sin\epsilon_f M^{i-1}_{rx} - \cos\epsilon_f M^{i-1}_{ry} - \phi_i M^{i-1}_{rz} \\ &\quad + M^i_{ry} + \phi_i M^i_{rz} + \tilde{M}^i_{sy} \end{aligned} \tag{121}$$

$$\begin{aligned} M^i_{sz} &= (d_{fi}\sin\epsilon_f - \theta_i C^i_{fz}\sin\epsilon_f + \phi_i C^i_{fz}\cos\epsilon_f) F^{i-1}_{rx} \\ &\quad + (-d_{fi}\cos\epsilon_f + \theta_i C^i_{fz}\cos\epsilon_f + \phi_i C^i_{fz}\sin\epsilon_f) F^{i-1}_{ry} - \phi_i d_{fi} F^{i-1}_{rz} \\ &\quad - \phi_i C^i_{rz} F^i_{rx} - (d_{ri} + \theta_i C^i_{rz}) F^i_{ry} - \phi_i d_{ri} F^i_{rz} \\ &\quad - (\theta_i\cos\epsilon_f + \phi_i\sin\epsilon_f) M^{i-1}_{rx} + (-\theta_i\sin\epsilon_f + \phi_i\cos\epsilon_f) M^{i-1}_{ry} - M^{i-1}_{rz} \\ &\quad + M^i_{rz} + \theta_i M^i_{rx} - \phi_i M^i_{ry} + \tilde{M}^i_{sz} \end{aligned}$$

There is a very useful aspect of these dynamic equations: All the governing equations are linear functions in terms of accelerations of general coordinates and the constraint forces. If the constraint forces are not necessarily to be solved, by applying linear operations to the equations of motion, all the constraint forces can be eliminated. Then, we obtain the differential equations in terms of selected general coordinates only.

4.7 Simple Control Model

In the simplified control model, only the planar translational motion and the yaw motion of tractor and the yaw motion of each trailing units are considered. The natural

way of deriving simple model should be the simplification of the complex model by setting certain modes (general coordinate) to zero. All the simple models available in the literature are derived in this way. In this section, a general practical method of deriving a simple model is presented. Using this method, the motion equations can be written without deriving the complex model.

If we ignore the roll, pitch and bouncing motions of each unit of HDV, the system has N + 2 degrees of freedom: two degree of freedom for planar motion, N degrees of freedom for yaw motions. The translational motion of the tractor, i.e. v_x and v_y, and the yaw rate of each unit, i.e. $\dot{\epsilon}_i$, are a possible set of generalized coordinates. In section 4.4 we have shown that all the trailers' velocities and accelerations can be determined in terms of v_x and v_y and $\dot{\epsilon}_i$s. Then, by applying the newton's second law to the system, two differential equations can be easily obtained. The equations of motion in U_1-frame are:

$$\begin{aligned} F_{xu1}^{total} &= \left(\sum_{i=1}^{n} M_i\right)(\dot{v}_x - \dot{\epsilon}_1 v_y) \\ &+ \sum_{i=2}^{n}\left(\sum_{j=i}^{n} M_j\right)\{d_{r(i-1)}\left[\ddot{\epsilon}_{i-1}\sin(\epsilon_{i-1}-\epsilon_1) + \dot{\epsilon}_{i-1}^2\cos(\epsilon_{i-1}-\epsilon_1)\right] \\ &+ d_{fi}\left[\ddot{\epsilon}_i\sin(\epsilon_i-\epsilon_1) + \dot{\epsilon}_i^2\cos(\epsilon_i-\epsilon_1)\right]\} \end{aligned}$$

$$\begin{aligned} F_{yu1}^{total} &= \left(\sum_{i=1}^{n} M_i\right)(\dot{v}_y + \dot{\epsilon}_1 v_x) \\ &+ \sum_{i=2}^{n}\left(\sum_{j=i}^{n} M_j\right)\{d_{r(i-1)}\left[-\ddot{\epsilon}_{i-1}\cos(\epsilon_{i-1}-\epsilon_1) + \dot{\epsilon}_{i-1}^2\sin(\epsilon_{i-1}-\epsilon_1)\right] \\ &+ d_{fi}\left[-\ddot{\epsilon}_i\cos(\epsilon_i-\epsilon_1) + \dot{\epsilon}_i^2\sin(\epsilon_i-\epsilon_1)\right]\} \end{aligned} \tag{122}$$

where, F_{xu1}^{total} is the total external force in the x direction of U_1-frame, and F_{yu1}^{total} is the total external force in the y direction of U_1-frame. They are the sum of all the tire forces in the each direction and are given by: ,

$$\begin{aligned} F_{xu1}^{total} &= \sum_{i=1}^{n}\left[\left(\sum_{j=1}^{4} F_{txj}^{i}\right)\cos(\epsilon_i-\epsilon_1) - \left(\sum_{j=1}^{4} F_{tyj}^{i}\right)\sin(\epsilon_i-\epsilon_1)\right] \\ F_{yu1}^{total} &= \sum_{i=1}^{n}\left[\left(\sum_{j=1}^{4} F_{txj}^{i}\right)\sin(\epsilon_i-\epsilon_1) + \left(\sum_{j=1}^{4} F_{tyj}^{i}\right)\cos(\epsilon_i-\epsilon_1)\right] \end{aligned} \tag{123}$$

where, F_{txj}^{i}s and F_{tyj}^{i}s are defined as shown in Fig. 26.

In considering dynamic equations related to the yaw motion, there are relative motions between each adjacent units. In order to account for each unit's yaw motion, the units consisting the HDV system have to be considered individually. If we apply

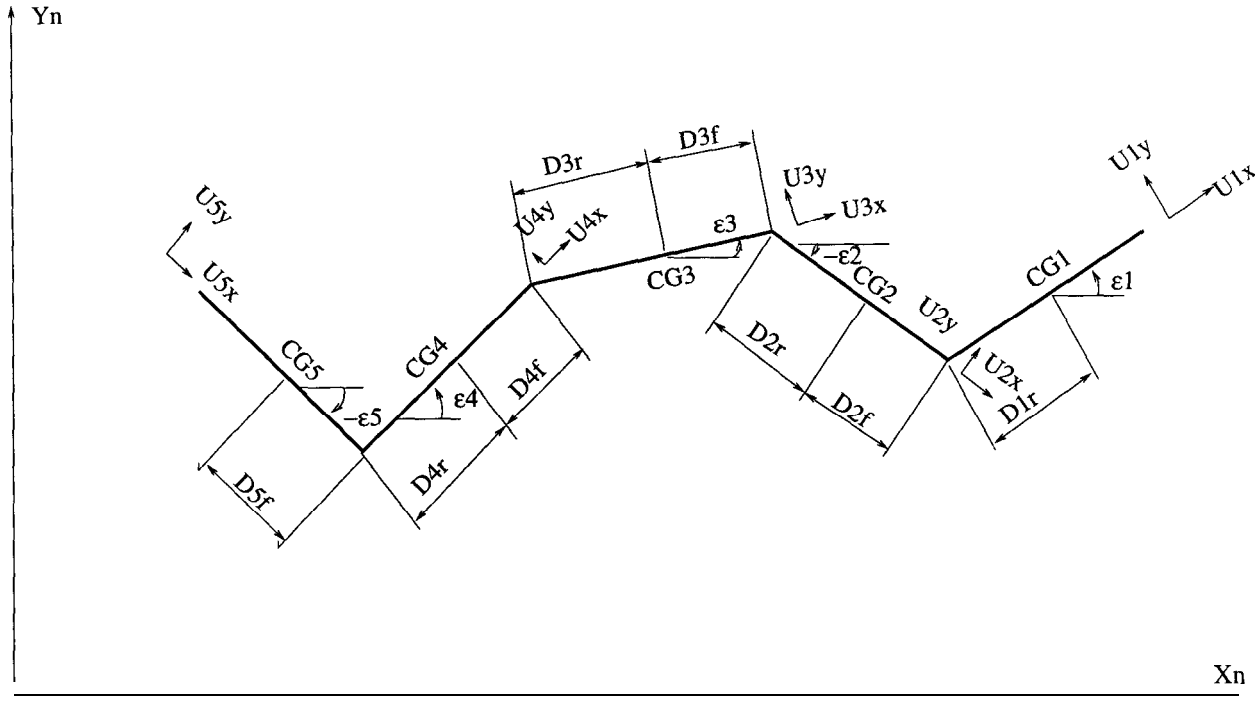

Figure 26: Simple Heavy Duty Vehicle System

Euler's rotational motion equations to each unit, we have to consider the constraint forces and constraint moments. For applications, however, an explicit expressions of differential equations is desired. This means that we need to cancel all the unknown constraint forces from the equations of motion. Although, the constraint forces appear linearly in equations, it requires considerable algebra to write down analytic simple model. Is there any way that we can directly write down the equations as we do for the planar motion? There are three facts which call our attention:

- In the Lagrangian mechanics, we do not have to consider the constraint forces.
- The velocity and acceleration of the i^{th} unit are dependent on the tractor's translational motion$(\dot{x}_u, \dot{y}_u)$ and only on the yaw motions of its preceding units and current unit $(\epsilon_j$, for $j \leq$ i).
- The potential energy is constant.

Keeping these in mind, we use Lagrangian method to derive the equations of yaw motions.

The Lagrangian equation is:

$$\frac{d}{dt}\left(\frac{\partial L}{\partial \dot{q}_i}\right) - \frac{\partial L}{\partial \epsilon_i} = F_{q_i} \tag{124}$$

where, the q_is are generalized coordinates, $\boldsymbol{L}$ is the Lagrangian and F_{q_i} is the generalized force associated with generalized coordinate q_i.

For HDV,

$$\begin{gathered}\boldsymbol{L} = \sum_{i=1}^{N} T_i \\ T_i(\dot{\epsilon}_1, \epsilon_1, \dot{\epsilon}_2, \epsilon_2, \ldots \dot{\epsilon}_{i-1}, \epsilon_{i-1}, \dot{\epsilon}_i, \epsilon_i) = \tfrac{1}{2} M_i [\vec{v}_i]_{ui} \cdot [\vec{v}_i]_{ui}\end{gathered} \tag{125}$$

The velocity is given in section 4.4. Then, the Lagrangian equation for ϵ_i is:

$$\sum_{i=1}^{n} \left[\frac{d}{dt}\left(\frac{\partial L_i}{\partial \dot{\epsilon}_j}\right) - \frac{\partial L_i}{\partial \epsilon_j}\right] = F_{\epsilon_j} \tag{126}$$

We define,

$$\begin{gathered}\bar{L}_j^i := \frac{d}{dt}\left(\frac{\partial L_i}{\partial \dot{\epsilon}_j}\right) \\ \tilde{L}_j^i := \frac{\partial L_i}{\partial \epsilon_j}\end{gathered} \tag{127}$$

The $\bar{L}_j^i$ can be expressed as the following:

For $j = 1$,

$$\bar{L}_1^1 = I_{zz}^1 \ddot{\epsilon}_1$$

$$\bar{L}_1^2 = -M_2 d_{r1}\{\dot{v}_y - d_{r1}\ddot{\epsilon}_1 - d_{f2}\ddot{\epsilon}_2 \cos(\epsilon_2 - \epsilon_1) + d_{f2}(\dot{\epsilon}_2 - \dot{\epsilon}_1)\dot{\epsilon}_2 \sin(\epsilon_2 - \epsilon_1)\}$$

$$\begin{aligned}\bar{L}_1^i = {} & -M_i d_{r1}\{\dot{v}_y - d_{r1}\ddot{\epsilon}_1 - \textstyle\sum_{j=2}^{i-1}[(d_{fj} + d_{rj})\ddot{\epsilon}_j \cos(\epsilon_j - \epsilon_1)] - d_{fi}\ddot{\epsilon}_i \cos(\epsilon_i - \epsilon_1)\} \\ & -M_i d_{r1}\{\textstyle\sum_{j=2}^{i-1}[(d_{fj} + d_{rj})\dot{\epsilon}_j(\dot{\epsilon}_j - \dot{\epsilon}_1)\sin(\epsilon_j - \epsilon_1)] + d_{fi}\dot{\epsilon}_i(\dot{\epsilon}_i - \dot{\epsilon}_1)\sin(\epsilon_i - \epsilon_1)\}\end{aligned} \tag{128}$$

From equation (125), we can conclude that $\bar{L}_j^i = 0$ for $j > i$.

For $i \geq j$ and $j \geq 2$, $\bar{L}_j^i$s are:

$$\begin{aligned}\bar{L}_2^2 = {} & M_2 d_{f2}\{[\dot{v}_x \sin(\epsilon_2 - \epsilon_1) - \dot{v}_y \cos(\epsilon_2 - \epsilon_1)] + d_{r1}\ddot{\epsilon}_1 \cos(\epsilon_1 - \epsilon_2) + d_{f2}\ddot{\epsilon}_2 \\ & + (\dot{\epsilon}_2 - \dot{\epsilon}_1)[v_x \cos(\epsilon_2 - \epsilon_1) + v_y \sin(\epsilon_2 - \epsilon_1) + d_{r1}\dot{\epsilon}_1 \sin(\epsilon_1 - \epsilon_2)]\} + I_{zz}^2 \ddot{\epsilon}_2\end{aligned} \tag{129}$$

and, for $i \geq k \geq 2$

$$\begin{aligned}
\bar{L}^i_k \;=\; & M_i(d_{fk} + d_{rk}(1-\delta_{ik}))\{[\ddot{v}_x \sin(\epsilon_k - \epsilon_1) - \dot{v}_y \cos(\epsilon_k - \epsilon_1)] + d_{r1}\ddot{\epsilon}_1 \cos(\epsilon_1 - \epsilon_k) \\
& + \textstyle\sum_{j=2}^{i-1}[(d_{fj} + d_{rj})\ddot{\epsilon}_j \cos(\epsilon_j - \epsilon_k)] + d_{fi}\ddot{\epsilon}_i \cos(\epsilon_i - \epsilon_k) \\
& + \textstyle\sum_{j=2}^{i-1}[(d_{fj} + d_{rj})\dot{\epsilon}_j(\dot{\epsilon}_j - \dot{\epsilon}_1)\sin(\epsilon_k - \epsilon_j)] + d_{fi}(\dot{\epsilon}_i - \dot{\epsilon}_1)\sin(\epsilon_k - \epsilon_i) \\
& + (\dot{\epsilon}_k - \dot{\epsilon}_1)[v_x \cos(\epsilon_k - \epsilon_1) + v_y \sin(\epsilon_k - \epsilon_1) + d_{r1}\dot{\epsilon}_1 \sin(\epsilon_1 - \epsilon_k)] \qquad (130) \\
& + (\dot{\epsilon}_k - \dot{\epsilon}_1)\left[\textstyle\sum_{j=2}^{i-1}(d_{fj} + d_{rj})\dot{\epsilon}_j \sin(\epsilon_j - \epsilon_k) + d_{fi}\dot{\epsilon}_i \sin(\epsilon_i - \epsilon_k)\right]\} \\
& + I^i_{zz}\ddot{\epsilon}_i\delta_{ik}
\end{aligned}$$

where, $\delta_{ik} = 1$ for $i = k$, else $\delta_{ik} = 0$

$\tilde{L}^i_j$ are given by,

$$\begin{aligned}
\tfrac{\partial L_1}{\partial \epsilon_1} &= 0 \\
\tfrac{\partial L_2}{\partial \epsilon_1} &= M_2 d_{r1}\dot{\epsilon}_1 v_x - M_2 d_{f2}\dot{\epsilon}_2([v_{u2x}]_{u2} - [v_{u1x}]_{u2}) \\
\tfrac{\partial L_i}{\partial \epsilon_1} &= M_i d_{r1}\dot{\epsilon}_1 v_x - \textstyle\sum_{j=2}^{i-1}(d_{fj} + d_{rj})\dot{\epsilon}_j([v_{uix}]_{uj} - [v_{u1x}]_{uj}) \\
&\quad - d_{fi}\dot{\epsilon}_i([v_{uix}]_{ui} - [v_{u1x}]_{ui}), \quad (i \geq 3) \qquad (131) \\
\tfrac{\partial L_2}{\partial \epsilon_2} &= M_2 d_{f2}\dot{\epsilon}_2 [v_{u2x}]_{u2} \\
\tfrac{\partial L_i}{\partial \epsilon_j} &= M_i(d_{fj} + d_{rj})\dot{\epsilon}_j [v_{uix}]_{uj}, \quad (N \geq i \geq j \geq 2) \\
\tfrac{\partial L_n}{\partial \epsilon_n} &= M_n d_{fn}\dot{\epsilon}_n [v_{unx}]_{un}
\end{aligned}$$

where, $[v_{uix}]_{uj}$ is the velocity of i^{th} unit in x direction of U_j-frame and $[v_{uiy}]_{uj}$ is the velocity of i^{th} unit in y direction of U_j-frame.

The generalized forces are given by,

$$F_{g\epsilon_j} = \textstyle\sum_{i=1}^{n}\sum_{k=1}^{4} \frac{\partial \vec{r}_{ik}}{\partial \epsilon_j} \cdot \vec{F}_{ik} \qquad (132)$$

where, $\frac{\partial \vec{r}_{ik}}{\partial \epsilon_j}$s are given by:

for $i=1$ and $j=1$,

$$\frac{\partial \vec{r}_{11}}{\partial \epsilon_1} = \begin{bmatrix} -\frac{Twf1}{2} \\ l_{f1} \end{bmatrix}_{u1}, \qquad \frac{\partial \vec{r}_{12}}{\partial \epsilon_1} = \begin{bmatrix} \frac{Twf1}{2} \\ l_{f1} \end{bmatrix}_{u1}$$

$$\frac{\partial \vec{r}_{13}}{\partial \epsilon_1} = \begin{bmatrix} -\frac{Twr1}{2} \\ -l_{r1} \end{bmatrix}_{u1}, \qquad \frac{\partial \vec{r}_{14}}{\partial \epsilon_1} = \begin{bmatrix} \frac{Twr1}{2} \\ -l_{r1} \end{bmatrix}_{u1} \tag{133}$$

for $i = 2$,

$$\frac{\partial \vec{r}_{2j}}{\partial \epsilon_1} = \begin{bmatrix} -d_{r1}\sin(\epsilon_2 - \epsilon_1) \\ -d_{r1}\cos(\epsilon_2 - \epsilon_1) \end{bmatrix}_{u2}, \quad for \quad j = 1, \cdots, 4 \tag{134}$$

$$\frac{\partial \vec{r}_{21}}{\partial \epsilon_2} = \begin{bmatrix} -\frac{Twf2}{2} \\ -d_{f2} + l_{f2} \end{bmatrix}_{u2}, \qquad \frac{\partial \vec{r}_{22}}{\partial \epsilon_2} = \begin{bmatrix} \frac{Twf2}{2} \\ -d_{f2} + l_{f2} \end{bmatrix}_{u2}$$

$$\frac{\partial \vec{r}_{23}}{\partial \epsilon_2} = \begin{bmatrix} -\frac{Twr2}{2} \\ -d_{f2} - l_{r2} \end{bmatrix}_{u2}, \qquad \frac{\partial \vec{r}_{24}}{\partial \epsilon_2} = \begin{bmatrix} \frac{Twr2}{2} \\ -d_{f2} - l_{r2} \end{bmatrix}_{u2} \tag{135}$$

for $i \geq 3, k = 1$,

$$\frac{\partial \vec{r}_{ij}}{\partial \epsilon_1} = \begin{bmatrix} -d_{r1}\sin(\epsilon_i - \epsilon_1) \\ -d_{r1}\cos(\epsilon_i - \epsilon_1) \end{bmatrix}_{ui}, \quad for \quad j = 1, \cdots, 4 \tag{136}$$

for $i \geq 3$, $\boldsymbol{k} = 2, \cdots, (i-1)$,

$$\frac{\partial \vec{r}_{ij}}{\partial \epsilon_k} = \begin{bmatrix} -(d_{fi} + d_{ri})\sin(\epsilon_i - \epsilon_k) \\ -(d_{fi} + d_{ri})\cos(\epsilon_i - \epsilon_k) \end{bmatrix}_{ui}, \text{ f o r } j = 1, \cdots, 4, \tag{137}$$

for $i \geq 3$, $\boldsymbol{k} = i$,

$$\frac{\partial \vec{r}_{i1}}{\partial \epsilon_i} = \begin{bmatrix} -\frac{Twfi}{2} \\ -d_{fi} + l_{fi} \end{bmatrix}_{ui}, \qquad \frac{\partial \vec{r}_{i2}}{\partial \epsilon_i} = \begin{bmatrix} \frac{Twfi}{2} \\ -d_{fi} + l_{fi} \end{bmatrix}_{ui}$$

$$\frac{\partial \vec{r}_{i3}}{\partial \epsilon_i} = \begin{bmatrix} -\frac{Twri}{2} \\ -d_{fi} - l_{ri} \end{bmatrix}_{ui}, \qquad \frac{\partial \vec{r}_{i4}}{\partial \epsilon_i} = \begin{bmatrix} \frac{Twri}{2} \\ -d_{fi} - l_{ri} \end{bmatrix}_{ui} \tag{138}$$

From the above discussion, we can establish three tables which can be resorted when deriving simple models of heavy duty vehicle system of N units. Table one is for $\bar{L}^i_j$, table two is for $\tilde{L}^i_j$ and table three is for $\frac{\partial \vec{r}_{ik}}{\partial \epsilon_j}$, where $\boldsymbol{k} = 1, 2, 3$ or $\boldsymbol{k} = 4$. Because of the characteristic of L^i and $\vec{r}_{ik}, \bar{L}^i_j, \tilde{L}^i_j$ and $\frac{\partial \vec{r}_{ik}}{\partial \epsilon_j}$ are equal to zeros for all $j > i$. So, the three tables take upper triangular form as shown below:

Table one:

$$\left[\bar{L}^i_j\right] = \left[\frac{d}{dt}\frac{\partial L_i}{\partial \dot{\epsilon}_j}\right] = \begin{vmatrix} \bar{L}^1_1 & \bar{L}^2_1 & \bar{L}^3_1 & \bar{L}^4_1 & \cdots & \bar{L}^n_1 \\ & \bar{L}^2_2 & \bar{L}^3_2 & \bar{L}^4_2 & \cdots & \bar{L}^n_2 \\ & & \bar{L}^3_3 & \bar{L}^4_3 & \cdots & \bar{L}^n_2 \\ & & & \ddots & & \\ & & & & \bar{L}^{n-1}_{n-1} & \bar{L}^n_{n-1} \\ & & & & & \bar{L}^n_n \end{vmatrix} \tag{139}$$

Table two:

$$\left[\tilde{L}^i_j\right] = \left[\frac{\partial L_i}{\partial \epsilon_j}\right] = \begin{vmatrix} \tilde{L}^1_1 & \tilde{L}^2_1 & \tilde{L}^3_1 & \tilde{L}^4_1 & \cdots & \tilde{L}^n_1 \\ & \tilde{L}^2_2 & \tilde{L}^3_2 & \tilde{L}^4_2 & \cdots & \tilde{L}^n_2 \\ & & \tilde{L}^3_3 & \tilde{L}^4_3 & \cdots & \tilde{L}^n_3 \\ & & & \ddots & & \\ & & & & \tilde{L}^{n-1}_{n-1} & \tilde{L}^n_{n-1} \\ & & & & & \tilde{L}^n_n \end{vmatrix} \tag{140}$$

Table three:

$$\left[\frac{\partial \vec{r}_{ik}}{\partial \epsilon_j}\right] = \begin{vmatrix} \frac{\partial \vec{r}_{1k}}{\partial \epsilon_1} & \frac{\partial \vec{r}_{2k}}{\partial \epsilon_1} & \frac{\partial \vec{r}_{3k}}{\partial \epsilon_1} & \frac{\partial \vec{r}_{4k}}{\partial \epsilon_1} & \cdots & \frac{\partial \vec{r}_{nk}}{\partial \epsilon_1} \\ & \frac{\partial \vec{r}_{2k}}{\partial \epsilon_2} & \frac{\partial \vec{r}_{3k}}{\partial \epsilon_2} & \frac{\partial \vec{r}_{4k}}{\partial \epsilon_2} & \cdots & \frac{\partial \vec{r}_{nk}}{\partial \epsilon_2} \\ & & \frac{\partial \vec{r}_{3k}}{\partial \epsilon_3} & \frac{\partial \vec{r}_{4k}}{\partial \epsilon_3} & \cdots & \frac{\partial \vec{r}_{nk}}{\partial \epsilon_3} \\ & & & \ddots & \vdots & \vdots \\ & & & & \frac{\partial \vec{r}_{(n-1)k}}{\partial \epsilon_{n-1}} & \frac{\partial \vec{r}_{nk}}{\partial \epsilon_{n-1}} \\ & & & & & \frac{\partial \vec{r}_{nk}}{\partial \epsilon_n} \end{vmatrix} \tag{141}$$

Then, the Lagrangian equaition for generalized coordinate ϵ_i can be obtained by applying equation (126) to the i^{th} rows of each table.

4.8 Example: Simple Model of Tractor Semi-trailer

This section presents non-linear simplified model of tractor-semitrailer as a special case of the method described in section 4.7. For the tractor semi-trailer dynamical system, the only external forces come from the tire forces. In simplified model, we assume the linear tire model.

4.8.1 Dynamics of Tractor Semi-trailer

Tractor Semitrailer system is a two unit system, therefore, $n = 2$. Consequently, the simplified model has 4 degrees of freedom: Longitudinal and lateral motion, yaw motion of the tractor and yaw motion of the semi-trailer. By expanding equation (122) for $n = 2$, the longitudinal and lateral dynamics equation is obtained as follows:

$$\begin{aligned} F_{xu1}^{total} &= (M_1 + M_2)(\dot{v}_x - \dot{\epsilon}_1 v_y) \\ &\quad + M_2 \{ d_{r1}[\dot{\epsilon}_1^2] + d_{f2}[\ddot{\epsilon}_2 \sin(\epsilon_2 - \epsilon_1) + \dot{\epsilon}_2^2 \cos(\epsilon_2 - \epsilon_1)] \} \end{aligned}$$

$$\begin{aligned} F_{yu1}^{total} &= (M_1 + M_2)(\dot{v}_y + \dot{\epsilon}_1 v_x) \\ &\quad + M_2 \{ d_{r1}[-\ddot{\epsilon}_1] + d_{f2}[-\ddot{\epsilon}_2 \cos(\epsilon_2 - \epsilon_1) + \dot{\epsilon}_2^2 \sin(\epsilon_2 - \epsilon_1)] \} \end{aligned} \quad (142)$$

where,

$$F_{xu1}^{total} = \sum_{j=1}^{4} F_{txj}^1 + \left(\sum_{j=1}^{4} F_{txj}^2\right) \cos(\epsilon_2 - \epsilon_1) - \left(\sum_{j=1}^{4} F_{tyj}^2\right) \sin(\epsilon_2 - \epsilon_1)$$

$$F_{yu1}^{total} = \sum_{j=1}^{4} F_{tyj}^1 + \left(\sum_{j=1}^{4} F_{txj}^2\right) \sin(\epsilon_2 - \epsilon_1) + \left(\sum_{j=1}^{4} F_{tyj}^2\right) \cos(\epsilon_2 - \epsilon_1) \quad (143)$$

From equation (142) and equation (143), and by rearranging the terms, we get:

$$\begin{aligned} &(M_1 + M_2)\dot{v}_y - m_2 d_{r1} \ddot{\epsilon}_1 - M_2 d_{f2} \cos(\epsilon_2 - \epsilon_1)\ddot{\epsilon}_2 \\ &+ (M_1 + M_2)\dot{\epsilon}_1 v_x + M_2 d_{f2} \dot{\epsilon}_2^2 \sin(\epsilon_2 - \epsilon_1) \\ = \; &\sum_{j=1}^{4} F_{tyj}^1 + \left(\sum_{j=1}^{4} F_{txj}^2\right) \sin(\epsilon_2 - \epsilon_1) + \left(\sum_{j=1}^{4} F_{tyj}^2\right) \cos(\epsilon_2 - \epsilon_1) \end{aligned} \quad \textbf{(144)}$$

In deriving yaw motion equations, let the generalized coordinates $[q_1, q_2]^T$ be $[\epsilon_1, \epsilon_2]^T$. The tractor yaw motion equations is given by:

$$(\tilde{L}_1^1 + \tilde{L}_1^2) - (\tilde{L}_1^1 + \tilde{L}_1^2) = \left(\sum_{k=1}^{4} \frac{\partial \vec{r}_{1k}}{\partial \epsilon_1} \vec{F}_{ik}\right) + \left(\sum_{k=1}^{4} \frac{\partial \vec{r}_{2k}}{\partial \epsilon_1} \vec{F}_{2k}\right) \quad (145)$$

where,

$$\begin{aligned}
\tilde{L}_1^1 &= I_{zz}^1 \ddot{\epsilon}_1 \\
\tilde{L}_1^2 &= -M_2 d_{r1}\{\dot{v}_y - d_{r1}\ddot{\epsilon}_1 - d_{f2}\ddot{\epsilon}_2 \cos(\epsilon_2 - \epsilon_1) + d_{f2}(\dot{\epsilon}_2 - \dot{\epsilon}_1)\dot{\epsilon}_2 \sin(\epsilon_2 - \epsilon_1)\} \\
\tilde{L}_1^1 &= 0 \\
\tilde{L}_1^2 &= M_2 d_{r1}\dot{\epsilon}_1 \ [v_x + d_{f2}\dot{\epsilon}_2 \sin(\epsilon_2 - \epsilon_1)]
\end{aligned} \tag{146}$$

and,

$$\begin{aligned}
\textstyle\sum_{k=1}^4 \frac{\partial \vec{r}_{1k}}{\partial \epsilon_1}\vec{F}_{1k} &= \tfrac{T_{wf1}}{2}(F_{tx2}^1 - F_{tx1}^1) + \tfrac{T_{wr1}}{2}(F_{tx4}^1 - F_{tx3}^1) \\
&\quad + l_{f1}(F_{ty1}^1 + F_{ty2}^2) - l_{r1}(F_{ty3}^1 + F_{ty4}^1)
\end{aligned} \tag{147}$$

$$\begin{aligned}
\textstyle\sum_{k=1}^4 \frac{\partial \vec{r}_{2k}}{\partial \epsilon_1}\vec{F}_{2k} &= -d_{r1}\sin(\epsilon_2 - \epsilon_1)(F_{tx1}^2 + F_{tx2}^2 + F_{tx3}^3 + F_{tx4}^4) \\
&\quad - d_{r1}\cos(\epsilon_2 - \epsilon_1)(F_{ty1}^2 + F_{ty2}^2 + F_{ty3}^2 + F_{ty4}^4)
\end{aligned}$$

From equations (145), (146) and (147), and by rearranging terms, we have the equation of motion for tractor as follows:

$$\begin{aligned}
&-M_2 d_{r1}\dot{v}_y + (M_2 d_{r1}^2 + I_{zz}^1)\ddot{\epsilon}_1 + M_2 d_{r1} d_{f2}\ddot{\epsilon}_2 \cos(\epsilon_2 - \epsilon_1) \\
&-M_2 d_{r1} d_{f2}\dot{\epsilon}_2^2 \sin(\epsilon_2 - \epsilon_1) - M_2 d_{r1}\dot{\epsilon}_1 v_x \\
= \ &\tfrac{T_{wf1}}{2}(F_{tx2}^1 - F_{tx1}^1) + \tfrac{T_{wr1}}{2}(F_{tx4}^1 - F_{tx3}^1) + l_{f1}(F_{ty1}^1 + F_{ty2}^1) - l_{r1}(F_{ty3}^1 + F_{ty4}^1) \\
&-d_{r1}\sin(\epsilon_2 - \epsilon_1)(F_{tx1}^2 + F_{tx2}^2 + F_{tx3}^2 + F_{tx4}^2) \\
&-d_{r1}\cos(\epsilon_2 - \epsilon_1)(F_{ty1}^2 + F_{ty2}^2 + F_{ty3}^2 + F_{ty4}^2)
\end{aligned} \tag{148}$$

The semi-trailer yaw motion equation is given by:

$$\bar{L}_2^2 - \tilde{L}_2^2 = \textstyle\sum_{k=1}^4 \frac{\partial \vec{r}_{2k}}{\partial \epsilon_2}\vec{F}_{2k} \tag{149}$$

where,

$$\begin{aligned}
\bar{L}_2^2 &= M_2 d_{f2}\{\dot{v}_x \sin(\epsilon_2 - \epsilon_1) - \dot{v}_y \cos(\epsilon_2 - \epsilon_1) + d_{r1}\ddot{\epsilon}_1 \cos(\epsilon_2 - \epsilon_1) + d_{f2}\ddot{\epsilon}_2 \\
&\quad + (\dot{\epsilon}_2 - \dot{\epsilon}_1)[v_x \cos(\epsilon_2 - \epsilon_1) + v_y \sin(\epsilon_2 - \epsilon_1) - d_{r1}\dot{\epsilon}_1 \sin(\epsilon_2 - \epsilon_1)]\} + I_{zz}^2 \ddot{\epsilon}_2 \\
\tilde{L}_2^2 &= M_2 d_{f2}\dot{\epsilon}_2\{v_x \cos(\epsilon_2 - \epsilon_1) + v_y \sin(\epsilon_2 - \epsilon_1) - d_{r1}\dot{\epsilon}_1 \sin(\epsilon_2 - \epsilon_1)\}
\end{aligned} \tag{150}$$

and,

$$\begin{aligned}
\textstyle\sum_{k=1}^4 \frac{\partial \vec{r}_{2k}}{\partial \epsilon_2}\vec{F}_{2k} &= \tfrac{T_{wf2}}{2}(F_{tx2}^2 - F_{tx1}^2) + \tfrac{T_{wr2}}{2}(F_{tx4}^2 - F_{tx3}^2) \\
&\quad + (l_{f2} - d_{f2})(F_{ty1}^2 + F_{ty2}^2) - (l_{r2} + d_{f2})(F_{ty3}^2 + F_{ty4}^2)
\end{aligned} \tag{151}$$

From equations (149), (150) and (151), and by rearranging the terms, we have the yaw motion equation of the semitrailer as follows:

$$\begin{aligned} & M_2 d_{f2}\dot{v}_x \sin(\epsilon_2-\epsilon_1) - M_2 d_{f2}\cos(\epsilon_2-\epsilon_1)\dot{v}_y \\ & + M_2 d_{r1} d_{f2}\ddot{\epsilon}_1 \cos(\epsilon_2-\epsilon_1) + (M_2 d_{f2}^2 + I_{zz}^2)\ddot{\epsilon}_2 \\ & - M_2 d_{f2}\dot{\epsilon}_1[v_x \cos(\epsilon_2-\epsilon_1) + v_y \sin(\epsilon_2-\epsilon_1)] + M_2 d_{r1} d_{f2}\sin(\epsilon_2-\epsilon_1)\dot{\epsilon}_1^2 \\ = \; & \tfrac{T_{wf2}}{2}(F_{tx2}^2 - F_{tx1}^2) + \tfrac{T_{wr2}}{2}(F_{tx4}^2 - F_{tx3}^2) \\ & + (l_{f2} - d_{f2})(F_{ty1}^2 + F_{ty2}^2) - (l_{r2} + d_{f2})(F_{ty3}^2 + F_{ty4}^2) \end{aligned} \tag{152}$$

4.8.2 Linear Tire Model

In the simplified model, we assume tire model is linear and the steering angles of front wheel of each unit, the relative articulation yaw angle are small. The longitudinal and lateral forces of the i^{th} unit tires are:

$$\begin{aligned} F_{ak}^i &= C_{sf}^i \lambda_{sf}^i \\ F_{bk}^i &= C_{\alpha if}\alpha_{if} \end{aligned} \tag{153}$$

for the front wheels ($k = 1, 2$), and

$$\begin{aligned} F_{ak}^i &= C_{sr}^i \lambda_{sr}^i \\ F_{bk}^i &= C_{\alpha ir}\alpha_{ir} \end{aligned} \tag{154}$$

for the rear wheels ($k = 3, 4$), where, C_{sf}^i and C_{sr}^i are longitudinal stiffness of the front tires and rear tires of the i^{th} unit respectively, and $C_{\alpha if}$ and $C_{\alpha ir}$ are the cornering stiffness of the front tires and the rear tires of the i^{th} unit respectively. From Fig. 27, by applying the coordinate transformation to the front wheel forces, we have:

$$\begin{aligned} F_{txk}^i &= F_{ak}^i \cos\delta_i - F_{bk}^i \sin\delta_i \\ F_{tyk}^i &= F_{ak}^i \sin\delta_i + F_{bk}^i \cos\delta_i \end{aligned} \tag{155}$$

for $k = 1, 2$. and by re-labeling the rear tire forces, we have:

$$\begin{aligned} F_{txk}^i &= F_{ak}^i \\ F_{tyk}^i &= F_{bk}^i \end{aligned} \tag{156}$$

for $k = 3, 4$.

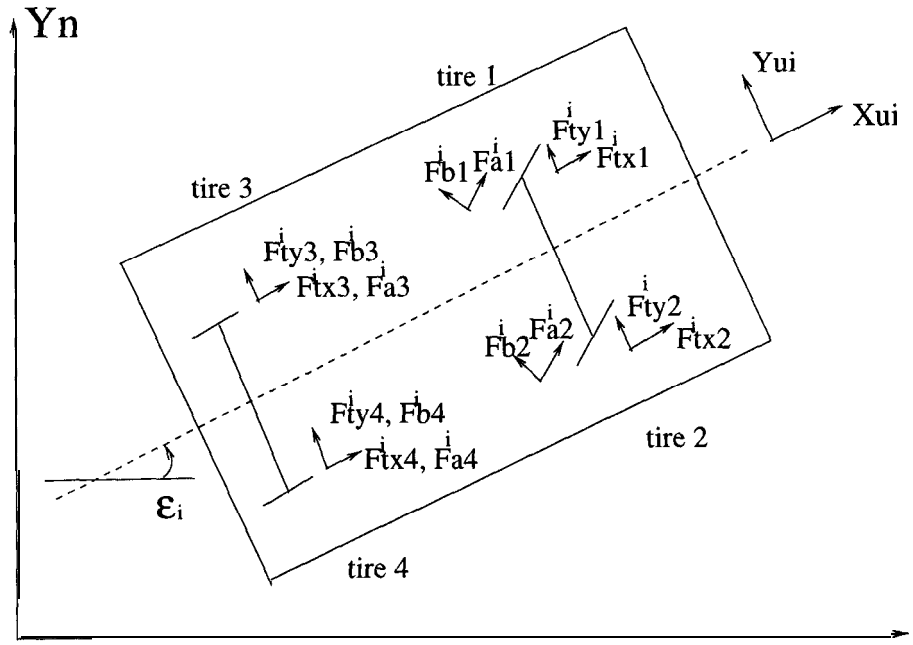

Figure 27: Linear Tire Foreces

The tire slip angles are defined as:

$$\alpha_{if} = \delta_i - \arctan\left(\frac{[v_{ify}]_{ui}}{[v_{ifx}]_{ui}}\right) \tag{157}$$

for the front wheels of the i^{th} unit, where, $[v_{ifx}]_{ui}$ and $[v_{ify}]_{ui}$ are the front wheel velocity components in x and y direction of the U_i-frame respectively, and

$$\alpha_{ir} = -\arctan\left(\frac{[v_{iry}]_{ui}}{[v_{irx}]_{ui}}\right) \tag{158}$$

for the rear wheels of the i^{th} unit, where, $[v_{irx}]_{ui}$ and $[v_{iry}]_{ui}$ are the rear wheel velocity components in the x and y direction of the U_i-frame respectively. Referring to Fig. 27, the velocity components are given by:

$$\begin{aligned}
[v_{ifx}]_{u1} &= [v_{uix}]_{ui} \pm \tfrac{T_{wf1}}{2}\dot{\epsilon}_1 \\
[v_{irx}]_{u1} &= [v_{uix}]_{ui} \pm \tfrac{T_{wr1}}{2}\dot{\epsilon}_1 \\
[v_{ify}]_{u1} &= [v_{uiy}]_{ui} + l_{f1}\dot{\epsilon}_1 \\
[v_{iry}]_{u1} &= [v_{uiy}]_{ui} - l_{r1}\dot{\epsilon}_1
\end{aligned} \tag{159}$$

where, $[v_{uix}]_{ui}$ and $[v_{uiy}]_{ui}$ are the U_i-frame velocity components in the x and y directions of the U_i coordinate system. They are given in section 4.4.

For the linear tire model, we make the following assumptions.

- If we do not consider the traction or braking force, the tire longitudinal force is small compared to the lateral force, so let $F_{ak}^{i} = 0, \quad for\ k = 1, 2, 3, 4.$
- The relative yaw angle between units are small.
- the steering angles and the slip angles are small.
- Ignore quadratic and higher order terms.
- The longitudinal velocity of each wheel are approximately equal to v_x.

Under these assumptions, the tire forces for the tractor are:

$$\begin{aligned} F_{tx1}^{1} &= F_{tx2}^{1} = -N_f^1 C_{\alpha 1 f} \frac{v_y + \dot{\epsilon}_1 l_{f1}}{v_x} \delta_1 \\ F_{tx3}^{1} &= F_{tx4}^{1} = 0 \\ F_{ty1}^{1} &= F_{ty2}^{1} = N_f^1 C_{\alpha 1 f} (\delta_1 - \frac{v_y + \dot{\epsilon}_1 l_{f1}}{v_x}) \\ F_{ty3}^{1} &= F_{ty4}^{1} = N_r^1 C_{\alpha 1 r} (-\frac{v_y - \dot{\epsilon}_1 l_{r1}}{v_x}) \end{aligned} \tag{160}$$

similarly, the tire forces for the semitrailer are:

$$\begin{aligned} F_{tx1}^{2} &= F_{tx2}^{2} = -N_f^2 C_{\alpha 2 f} \frac{v_y - d_{r1}\dot{\epsilon}_1 l_{f1} - (d_{f2} - l_{f2})\dot{\epsilon}_2 - v_x(\epsilon_2 - \epsilon_1)}{v_x} \delta_2 \\ F_{tx3}^{2} &= F_{tx4}^{2} = 0 \\ F_{ty1}^{2} &= F_{ty2}^{2} = N_f^2 C_{\alpha 2 f} (\delta_2 - \frac{v_y - d_{r1}\dot{\epsilon}_1 - (d_{f2} - l_{f2})\dot{\epsilon}_2 - v_x(\epsilon_2 - \epsilon_1)}{v_x}) \\ F_{ty3}^{2} &= F_{ty4}^{2} = N_r^2 C_{\alpha 2 r} (-\frac{v_y - d_{r1}\dot{\epsilon}_1 - (d_{f2} + l_{r2})\dot{\epsilon}_2 - v_x(\epsilon_2 - \epsilon_1)}{v_x}) \end{aligned} \tag{161}$$

4.8.3 Simple Model

In lateral vehicle control, we assume that the vehicle has constant longitudinal velocity. Thus, by substituting equation (160) and (161) into the second equation of (144), and

ignoring the second order terms,

$$
\begin{aligned}
F_{yt1}^{total} &= 2N_f^1\delta_1 + 2N_f^2 C_{\alpha 1f}\cos(\epsilon_2-\epsilon_1)\delta_2 \\
&\quad -\tfrac{2}{v_x}\{(N_f^1 C_{\alpha 1f} + N_r^1 C_{\alpha 1r}) + (N_f^2 C_{\alpha 2f} + N_r^2 C_{\alpha 2r})\cos(\epsilon_2-\epsilon_1)\}v_y \\
&\quad -\tfrac{2}{v_x}\{(N_f^1 C_{\alpha 1f} l_{f1} - N_r^1 C_{\alpha 1r} l_{r1}) - (N_f^2 C_{\alpha 2f} + N_r^2 C_{\alpha 2r}) d_{r1}\cos(\epsilon_2-\epsilon_1)\}\dot{\epsilon}_1 \\
&\quad -\tfrac{2}{v_x}\{-(N_f^2 C_{\alpha 2f} + N_r^2 C_{\alpha 2r}) d_{f2}\cos(\epsilon_2-\epsilon_1) \\
&\quad +(N_f^2 C_{\alpha 2f} l_{f2} - N_r^2 C_{\alpha 2r} l_{r2})\cos(\epsilon_2-\epsilon_1)\}\dot{\epsilon}_2 \\
&\quad +2(N_f^2 C_{\alpha 2f} + N_r^2 C_{\alpha 2r})\cos(\epsilon_2-\epsilon_1)(\epsilon_2-\epsilon_1)
\end{aligned}
\tag{162}
$$

By substituting equation (160) and (161) into equation (147), and ignoring the second order terms,

$$
\begin{aligned}
F_{g\epsilon_1} &= 2N_f^1 C_{\alpha 1f} l_{f1}\delta_1 - 2N_f^2 C_{\alpha 2f} d_{r1}\cos(\epsilon_2-\epsilon_1)\delta_2 \\
&\quad -\tfrac{2}{v_x}\{(N_f^1 C_{\alpha 1f} l_{f1} - N_r^1 C_{\alpha 1r} l_{r1}) - (N_f^2 C_{\alpha 2f} + N_r^2 C_{\alpha 2r}) d_{r1}\cos(\epsilon_2-\epsilon_1)\}v_y \\
&\quad -\tfrac{2}{v_x}\{(N_f^1 C_{\alpha 1f} l_{f1}^2 + N_r^1 C_{\alpha 11r} l_{r1}^2) + (N_f^2 C_{\alpha 2f} + N_r^2 C_{\alpha 2r}) d_{r1}^2\cos(\epsilon_2-\epsilon_1)\}v_y \\
&\quad -\tfrac{2}{v_x}\{(N_f^1 C_{\alpha 1f} l_{f1}^2 + N_r^1 C_{\alpha 1r} l_{r1}^2) + (N_f^2 C_{\alpha 2f} + N_r^2 C_{\alpha 2r}) d_{r1}^2\cos(\epsilon_2-\epsilon_1)\}\dot{\epsilon}_1 \\
&\quad -\{(N_f^2 C_{\alpha 2f} + N_r^2 C_{\alpha 2r}) d_{f2} d_{r1}\cos(\epsilon_2-\epsilon_1) \\
&\quad +(-N_f^2 C_{\alpha 2f} l_{f2} + N_r^2 C_{\alpha 2r} l_{r2}) d_{r1}\cos(\epsilon_2-\epsilon_1)\}\dot{\epsilon}_2 \\
&\quad -2d_{r1}(N_f^2 C_{\alpha 2f} + N_r^2 C_{\alpha 2r})\cos(\epsilon_2-\epsilon_1)(\epsilon_2-\epsilon_1)
\end{aligned}
\tag{163}
$$

By substituting equations (160) and (161) into equation (151),

$$
\begin{aligned}
F_{g\epsilon_2} &= 2N_f^2 C_{\alpha 2f}(l_{f2} - df2) \\
&\quad -\tfrac{2}{v_x}\{N_f^2 C_{\alpha 2f}(l_{f2} - d_{f2}) - N_r^2 C_{\alpha 2r}(l_r 2 + d_{f2})\}v_y \\
&\quad -\tfrac{2}{v_x}\{-N_f^2 C_{\alpha 2f}(l_{f2} - d_{r2}) + N_r^2 C_{\alpha 2r}(l_{r2} + d_{f2})\}d_r 1\dot{\epsilon}_1 \\
&\quad -\tfrac{2}{v_x}\{[-N_f^2 C_{\alpha 2f}(l_{f2} - d_{f2}) + N_r^2 C_{\alpha 2r}(l_{r2} + d_{f2})]d_{f2} \\
&\quad +\left[N_f^2 C_{\alpha 2f}(l_{f2} - d_{f2}) l_{f2} + N_r^2 C_{\alpha 2r}(l_{r2} + d_{f2}) l_{r2}\right]\}\dot{\epsilon}_2 \\
&\quad +2N_f^2 C_{\alpha 2f}(l_{f2} - d_{f2})(\epsilon_2-\epsilon_1) - 2N_r^2 C_{\alpha 2r}(l_{r2} + d_{f2})(\epsilon_2-\epsilon_1)
\end{aligned}
\tag{164}
$$

Combining equation pairs (144) and (162), (148) and (163), (152) and (152), and rewriting them into the matrix form, we get:

$$
M(q,\dot{q})\ddot{q} + C(q,\dot{q}) + \tfrac{2}{v_x}D(q) + K(q) = \Delta(q)\begin{bmatrix}\delta_1\\ \delta_2\end{bmatrix}
\tag{165}
$$

where, $q = [v_y, \quad \dot{\epsilon}_1, \quad \dot{\epsilon}_2]^T$ and,

$$M(q,\dot{q}) = \begin{pmatrix} M_1 + M_2 & -M_2 d_{r1} & -M_2 d_{f2}\cos(\epsilon_2 - \epsilon_1) \\ -M_2 d_{r1} & I_{zz}^1 + M_2 d_{r1}^2 & M_2 d_{r1} d_{f2}\cos(\epsilon_2 - \epsilon_1) \\ -M_2 d_{f2}\cos(\epsilon_2 - \epsilon_1) & M_2 d_{r1} d_{f2}\cos(\epsilon_2 - \epsilon_1) & I_{zz}^2 + M_2 d_{f2}^2 \end{pmatrix}$$

$$C(q,\dot{q}) = \begin{pmatrix} (\boldsymbol{M_1} + M_2)\dot{\epsilon}_1 v_x + M_2 d_{f2}\dot{\epsilon}_2^2 \sin(\epsilon_2 - \epsilon_1) \\ -M_2 d_{r1} v_x \dot{\epsilon}_1 - M_2 d_{r1} d_{f2}\sin(\epsilon_2 - \epsilon_1)\dot{\epsilon}_2^2 \\ -M_2 d_{f2}\dot{\epsilon}_1 v_x \cos(\epsilon_2 - \epsilon_1) - (M_2 d_{f2}\dot{\epsilon}_1 v_y - M_2 d_{f2} d_{r1}\dot{\epsilon}_1^2)\sin(\epsilon_2 - \epsilon_1) \end{pmatrix}$$

$$\begin{aligned}
D(1,1) &= (N_f^1 C_{\alpha 1f} + N_r^1 C_{\alpha 1r}) + (N_f^2 C_{\alpha 2f} + N_r^2 C_{\alpha 2r}\cos(\epsilon_2 - \epsilon_1)) \\
D(1,2) &= (N_f^1 C_{\alpha 1f} l_{f1} - N_r^1 C_{\alpha 1r} l_{r1}) - (N_f^2 C_{\alpha 2f} + N_r^2 C_{\alpha 2r}) d_{r1}\cos(\epsilon_2 - \epsilon_1) \\
D(1,3) &= -(N_f^2 C_{\alpha 2f} + N_r^2 C_{\alpha 2r}) d_{f2}\cos(\epsilon_2 - \epsilon_1) \\
&\quad + (N_f^2 C_{\alpha 2f} l_{f2} - N_r^2 C_{\alpha 2f} l_{f2} - N_r^2 C_{\alpha 2r} l_{r2})\cos(\epsilon_2 - \epsilon_1) \\
D(2,1) &= (N_f^1 C_{\alpha 1f} l_{f1} - N_r^1 C_{\alpha 1r} l_{r1}) - (N_f^2 C_{\alpha 2f} + N_r^2 C_{\alpha 2r}) d_{r1}\cos(\epsilon_2 - \epsilon_1) \\
D(2,2) &= (N_f^1 C_{\alpha 1f} l_{f1}^2 + N_r^1 C_{\alpha 1r} l_{r1}^2) + (N_f^2 C_{\alpha 2f} + N_r^2 C_{\alpha 2r}) d_{r1}^2\cos(\epsilon_2 - \epsilon_1) \\
D(2,3) &= (N_f^2 C_{\alpha 2f} + N_r^2 C_{\alpha 2r}) d_{r1} d_{f2}\cos(\epsilon_2 - \epsilon_1) \\
&\quad + (-N_f^2 C_{\alpha 2f} l_{f2} + N_r^2 C_{\alpha 2r} l_{r2}) d_{r1}\cos(\epsilon_2 - \epsilon_1) \\
D(3,1) &= N_f^2 C_{\alpha 2f}(l_{f2} - d_{r2}) - N_r^2 C_{\alpha 2r}(l_{r2} + d_{f2}) \\
D(3,2) &= [-N_f^2 C_{\alpha 2f}(l_{f2} - d_{f2}) + N_r^2 C_{\alpha 2r}(l_{r2} + d_{f2})] d_{r1} \\
D(3,3) &= [-N_f^2 C_{\alpha 2f}(l_{f2} - d_{f2}) + N_r^2 C_{\alpha 2r}(l_{r2} + d_{f2})] d_{f2} \\
&\quad + [N_f^2 C_{\alpha 2f}(l_{r2} - d_{f2}) d_{f2} + N_r^2 C_{\alpha 2r}(l_{r2} + d_{f2}) l_{r2}]
\end{aligned}$$

$$K(q) = \begin{pmatrix} 0 & -2(N_f^2 C_{\alpha 2f} + N_r^2 C_{\alpha 2r})\cos(\epsilon_2 - \epsilon_1) & 2(N_f^2 C_{\alpha 2f} + N_r^2 C_{\alpha 2r})\cos(\epsilon_2 - \epsilon_1) \\ 0 & 2(N_f^2 C_{\alpha 2f} + N_r^2 C_{\alpha 2r}) d_{r1}\cos(\epsilon_2 - \epsilon_1) & 2(N_f^2 C_{\alpha 2f} + N_r^2 C_{\alpha 2r}) d_{r1}\cos(\epsilon_2 - \epsilon_1) \\ 0 & -2N_f^2 C_{\alpha 2f}(l_{f2} - d_{f2}) + 2N_r^2 C_{\alpha 2r}(l_{r2} + d_{f2}) & 2N_f^2 C_{\alpha 2f}(l_{f2} - d_{f2}) - 2N_r^2 C_{\alpha 2r}(l_{r2} + d_{f2}) \end{pmatrix}$$

$$\Delta(q) = \begin{pmatrix} 2N_f^1 C_{\alpha 1f} & 2N_f^2 C_{\alpha 2f}\cos(\epsilon_2 - \epsilon_1) \\ 2N_f^1 C_{\alpha 1f} l_{f1} & -2N_f^2 C_{\alpha 2f} d_{r1}\cos(\epsilon_2 - \epsilon_1) \\ 0 & 2N_f^2 C_{\alpha 2f}(l_{f2} - d_{f2}) \end{pmatrix}$$

If we denote:

$$
\begin{aligned}
C_{\alpha f} &= N_f^1 C_{\alpha 1 f} \\
C_{\alpha r} &= N_r^1 C_{\alpha 1 r} \\
C_{\alpha t} &= N_r^2 C_{\alpha 2 r} \\
N_f^2 &= 0 \\
\delta_2 &= 0
\end{aligned}
\tag{166}
$$

then, the D(q) and A(q) matrix can be rewritten as follows:

$$
\begin{aligned}
D_1(1,1) &= C_{\alpha f} + C_{\alpha r} + C_{\alpha t}\cos(\epsilon_2 - \epsilon_1) \\
D_1(1,2) &= C_{\alpha f} l_{f1} - C_{\alpha r} l_{r1} - C_{\alpha t} d_{r1}\cos(\epsilon_2 - \epsilon_1) \\
D_1(1,3) &= -C_{\alpha t}(d_{f2} + l_{r2})\cos(\epsilon_2 - \epsilon_1) \\
D_1(2,1) &= C_{\alpha f} l_{f1} - C_{\alpha r} l_{r1} - C_{\alpha t} d_{r1}\cos(\epsilon_2 - \epsilon_1) \\
D_1(2,2) &= C_{\alpha f} l_{f1}^2 + C_{\alpha r} l_{r1}^2 + C_{\alpha t} d_{r1}^2\cos(\epsilon_2 - \epsilon_1) \\
D_1(2,3) &= C_{\alpha t} d_{r1} d_{f2}\cos(\epsilon_2 - \epsilon_1) + C_{\alpha t} l_{r2} d_{r1}\cos(\epsilon_2 - \epsilon_1) \\
D_1(3,1) &= -C_{\alpha t}(l_{r2} + d_{f2}) \\
D_1(3,2) &= C_{\alpha t}(l_{r2} + d_{f2}) d_{r1} \\
D_1(3,3) &= C_{\alpha t}(l_{r2} + d_{f2})^2
\end{aligned}
\tag{167}
$$

$$
K_1(q) = \begin{pmatrix} 0 & 2C_{\alpha t} & -2C_{\alpha t} \\ 0 & -2C_{\alpha t} d_{r1} & 2C_{\alpha t} d_{r1} \\ 0 & -2C_{\alpha t}(l_{r2} + d_{f2}) & 2C_{\alpha t}(l_{r2} + d_{f2}) \end{pmatrix}
$$

$$
\Delta_1(q) = \begin{pmatrix} 2C_{\alpha f} & 0 \\ 2C_{\alpha f} l_{f1} & 0 \\ 0 & 0 \end{pmatrix}
$$

If we further redefine dimensional parameters as follows:

$$
\begin{aligned}
d_1 &= d_{r1} & d_3 &= d_{f2} \\
l_1 &= l_{f1} & l_2 &= l_{r1} \\
l_3 &= d_{f2} + l_{r2}
\end{aligned}
\tag{168}
$$

and, let:

$$\begin{aligned} \epsilon_f &= \epsilon_2 - \epsilon_1 \\ \cos(\epsilon_2 - \epsilon_1) &\approx 1 \end{aligned} \tag{169}$$

then, equation (165) becomes identical with the simplified model equation derived in (Chen, 1996), which is the same as the eqution (1) of section 2 of this report.

5 Conclusions

This report presents the accomplishments under MOU 289, "Lateral Control of Heavy Duty Vehicles for Automated Highway Systems", during the funding year 1996-97. A linear analysis of tractor semitrailer model was presented. This analysis was followed by the design of a simple linear controller for lane following. This controller is *a* baseline controller in terms of performance of other linear and nonlinear controllers. Offtracking analysis was presented for a single unit vehicle and tractor semitrailer. This analysis is independent of the control design. Therefore, any control design can incorporate the offtracking information to center the vehicle in the lane. Finally, modeling of multi-unit articulated vehicles was presented. Any road train combination with tractor followed by trailers, semitrailers and appropriate dollies can be modeled by the proposed method. Both the complex simulation model and the simplified control design model were derived for the general road train. As an example, the simplified model of a tractor-semitrailer was presented and compared with the previous model. The experimenal study based on the anallysis presented in this report will be continued under MOU 313.

References

[1] Adams, W.J.P., and Spence, D.R., "Practical Aspects of Testing antilock Systems on Commercial Vehicles", *Conference on Braking of Road Vehicles,* Lougborough, 1976, Proc. Inst. of Mech. Engrs., London 1977, pp.125-134.

[2] Bernard, J.E., Winkler, C,B., and Fancher, P.S., "A Computer Based Mathematical Method for Predicting the Directional Response of Truck and Tractor-Trailers", Phase Two Technical Report, Rept. No. UM-HSRI-PF-73-1, Highway Saf. Res. Inst., Univ. of Mic higan, Ann Arbor 1973.

[3] Bernard, J. E. and Vanderploeg, M., 1981, "Static and Dynamic Offtracking of Articulated Vehicles," SAE Technical paper no. 800151, pp 936-943.

[4] Bishel, R.A., "dual Mode truck: Automated and Manual Operation", SAE Technical Paper series, number 931837, August 1993.

[5] Blosseville, J .M., Blondeel, F., and Graton, M., "Towards an Automated Highway System Applied to Freight Transport in France: First Considerations", Proceedings of University of California/PATH-France Workshop, 24-25 October, 1995, California PATH, Richmond, CA.

[6] Chen, C. and Tomizuka, M., "Dynamic Modeling for Articulated Vehicles for Automated Highway Systems", Proceedings of the American Control Conference, Seattle, 1995, pp. 953-657.

[7] Chen, C., 1996, "Backstepping Design of Nonlinear Systems and Its Application to Vehicle Lateral Control in Automated Highway Systems", PhD Thesis, UC Berkeley, CA.

[8] Chieh Chen and M. Tomizuka, *"Steering and Independent Braking Control of Tractor-Semitrailer Vehicles in Automated Highway Systems", Proc. of IEEE Conference on Decision and Control",* New Orleans, 1995.

[9] Yanakiev, D., and Kanellakopoulos, I., " Analysis, Design and Evaluation of AVCS for Heavy Duty Vehicles: Phase I report" California PATH working paper UCB-ITS-PWP-95-12, August 1995.

[10] Dugoff, H., "On the Influence of Aerodynamic Forces and Moments on the Lateral Stability of Articulated Highway Vehicles", Proceedings of the 1st International Conference on Vehicle Mechanics, Detroit, 1968, pp.215-245.

[11] Ellis, J.R., and Read, P.L., "A Study of the Response of a Double Bottom Vehicle to Steering and Braking, Vehicle System Dynamics", Vo1.5, No.4, 1976, pp.205-219.

[12] Ervin, R.D. et al., "The Yaw Stability of Tractor-Semitrailers During Cornering", Report No. UM-HSRI-79-21-2, DOT-HS-805 141, Highway Saf. Res. Inst., Univ. of Michgan, 1979.

[13] Ervin, R.D., "IVHS and the truckmaker: Identifying the Need for Research", UMTRI Final Report, number UMTRI-92-34, September 1992.

[14] Eshleman, R.L., and DeSai, S., and Hanify, D.W., "Analytical-Experimental Response of Articulated Vehicles", SAE Paper 730674, 1973.

[15] Favre, B., "The Position of Truck Manufacturer Regarding Intelligent transportation Systems Advanced Technologies", Proceedings of University of California/PATH-France Workshop, 24-25 October, 1995, California PATH, Richmond, CA.

[16] Fenton, R.E. and Mayhan, R.J., "Automated Highway Studies at Ohio State University-An overview", IEEE transactions on Vehicular Technology, vol. VT-40, no, 1, Feb. 1991, pp. 100-113.

[17] J. Guldner, H.S. Tan and S. Patwardhan, *"A general Framework for Automatic Steering Control:System Analysis"*, Proc. of the American Control Conf., Albuquerque, New Mexico, 1997, pp. 1598-1602.

[18] "Highway Statistics", 49th Edition, Washington, DC: Federal Highway Administration, 1994.

[19] Hingwe, P. and Tomizuka, M., 1997, "Experimental Evaluation of a Chatter Free Sliding Mode Control for Lateral Control in AHS", Proceedings of the American Control Conference, Albuquerque, New Mexico, pp. 3365-3369.

[20] Hingwe, P., Tomizuka, M., "Experimental Study of Chatter Free Sliding Mode Control for Lateral Control of Commuter Buses in AHS", PATH research report no. UCB-ITS-PRR-96-31, California PATH, Richmond CA, 1996.

[21] Kanellakopoulos, I., and Tomizuka, M., "Commercial Trucks and Buses in Automated Highway Systems" to appear in Automated Highway Systems, edited by P. Iannou, Plenum Publishing Corporation, 1996.

[22] Keller, A.T., "Jackknife Control for Tractor-Trailer", SAE Paper 730643, 1973.

[23] Kemp, R.N., Chinn, B.P. and Brock, G., "Articulated Vehicle Roll Stability:Method of Assessment Effects of Vehilce Characteristics", TRRL Report 788, Transport and Road Research Laboratory, Crowthorne, Berkshire, 1978.

[24] Lam, C.P., Guntur, R.R., and Wong, J.Y., "Evaluation of the Braking Performance of a Tractor-Semitrailer Equiped with Two Different Types of Anti-Lock System", SAE Paper 791046, 1979.

[25] Mikulcik, E.C., "The Dynamics of Tractor-Semitrailer Vehicles: The Jackkinfing Problem", Ph.D. Thesis, Cornell University, Ithaca, N.Y., 1968.

[26] "Motor Vehicles Facts and Figures", American Automobile Manufacturers' Association, 1993.

[27] North, M.R., and Oliver, S.J., "Transient Load Transfer in An Articlulated Vehicle Under Braking Conditions", MIRA Report No.1967/7, Motor Industry Research Association, 1967.

[28] Patwardhan, S, Tan, H.S., Guldner, J., 1997 "A general framework for Automated Steering Control: System Analysis", Proceedings of the American Control Conference, Albuquerque, New Mexico, pp. 1598-1602.

[29] Peng, H. and Tomizuka, M., 1993, "Preview Control for Vehicle Lateral Guidance in Highway Automation," *ASME Journal of Dynamic Systems, Measurement and Control,* Vol. 115, No. 4, pp. 678-686.

[30] Rakheja, S., Vallurupalli, R.K., and Woodrooffe, J. (1995) " Influence of articulation damping on the yaw and lateral dynamic response of the vehicle," *Heavy Vehicle System,* Special Series, *Int. J. of Vehicle Design,* Vol. 2, No. 2, pp. 105-123.

[31] 1964 SAE Handbook, Society of Automotive Engineers, Warrendale, PA, 1964.

[32] Segel, L., "Discussion of The Forced Lateral Oscillations of Trailers, Transcations of the ASME Journal of Applied Mechanics", Vo1.25, 1958, pp.308-

[33] Shladover, S. et al., "Automatic Vehicle Control Development in PATH Program", IEEE Transactions on Vehicular Technology, VT-40, no, 1, Feb. 1991, pp. 114-130.

[34] Susemihl, E.A., and Krauter, A.I., "Jackknifing of Tractor-semitrailer Trucks: Detection and Corrective Action", Trans. of the ASME J. of Dynamic System, Measurement and Control, Vo1.96, No.2, 1974, pp.244-252.

[35] X. Tong, B. Tabarrok and M. El-Gindy, (1995) " Computer Simulation Analysis of Canadian Logging Trucks", Technical Report, CSTT-HWV-TR-004, National Research Council Canada.

[36] Walsh, R.E., and Cicchetti, G.E., "Use of Simplified Jackknife Restaint Device Significantly Reduces the Hazard of Jackknifing", SAE Paper 730642, 1973.

[37] Winker, C.B., Nisonger, R.L., and Ervin, R.D., "Testing the Michigan Double Bottom Tanker", SAE Paper 781066, 1978.

[38] Zimmermann, T.A., Fuchs, U. Franke and B. Klingenberg, "VECOTR - A Vision Enhanced/ Controlled Truck for Operational Research", SAE Technical paper series, number 942284, November 1994.

[39] *"Report of the Subcommittee on Truck Size and Weight of the AASHTO Joint Committee on Domestic Freight Policy"* American Association of State Highway and Transportation Officials, June, 1995.